Lithofacies, Cyclicity and Diagenetic Characteristics of the Mississippian Mission Canyon Formation, Southeast Saskatchewan

A Thesis
Submitted to the Faculty of Graduate Studies and Research

In partial Fulfillment of the Requirements
For the Degree of
Master of Science
In Geology
University of Regina

by

Congwei Ji
Regina, Saskatchewan, Canada

March, 2016

UNIVERSITY OF REGINA

FACULTY OF GRADUATE STUDIES AND RESEARCH

SUPERVISORY AND EXAMINING COMMITTEE

Congwei Ji, candidate for the degree of Master of Science in Geology**,** has presented a thesis titled, ***Lithofacies, Cyclicity and Diagenetic Characteristics of the Mississippian Mission Canyon Formation, Southeast Saskatchewan,*** in an oral examination held on December 15, 2015. The following committee members have found the thesis acceptable in form and content, and that the candidate demonstrated satisfactory knowledge of the subject material.

External Examiner:	Melinda Yurkowski, Saskatchewan Geological Survey
Supervisor:	Dr. Osman Salad Hersi, Department of Geology
Committee Member:	Dr. Hairuo Qing, Department of Geology
Chair of Defense:	Dr. Hussameldin Ibrahim, Industrial Systems Engineering

Abstract

In southeastern Saskatchewan, the Mississippian Mission Canyon Formation was deposited in the northern platform margin of the Williston Basin and includes, from bottom to top, Tilston Beds, Alida Beds, Kisbey interval and Frobisher Beds. The formation is dominated by carbonate lithofacies, subordinate evaporites and economically important sandstone lithofacies (Kisbey interval) also occur within the formation.

Cores, cuttings, wireline logs and petrographic studies of these strata in the research area have allowed identification of lithologic attributes, cyclicity and diagenetic features of the strata. Eight lithofacies have been identified: i) oolitic and bioclastic packstone/ grainstone (Facies PG), ii) oncolitic rudstone (Facies RD,) iii) bioclastic & oolitic mudstone/wackestone (Facies MW), iv) dolomudstone (Facies DS), v) sandstone/ siltstone (Facies SS), vi) sandy dolomudstone (Facies SD), vii) sandy packstone/ grainstone (Facies SP) and viii) anhydrite (Facies AH). The overall depositional setting can be summarized as shallow-marine environment characterized by bioclastic and oolitic carbonate subtidal sand shoals with a landward lagoonal to tidal mud-flat system. The sandstone lithofacies of the Kisbey interval suggests a connection between tidal creeks that cut a carbonate-dominated shallow platform and a possibly fluvial system that brought the detrital grains into the basin.

The temporal lithofacies arrangement of the studied stratigraphic interval shows clear vertically-stacked rhythmic units defined by shallowing-upward cycles of basal subtidal lithofacies (PG, RD,SP, MW) grading to restricted lagoonal / tidal mudflat deposits (MW, DS, SD, SS & AH). Fischer Plot analysis of these rhythmic units suggests higher (4th to 5th) order Milankovitch cycles that can be grouped into six, possibly 3rd-

order depositional cycles. These 3rd-order cycles appear to correlate well with the Mississippian cyclothems, and thus attributable to eustatic sea level changes.

The diagenetic products, their paragenetic sequence and effects on the reservoir quality of the strata have been discerned. The diagenetic products and their paragenetic sequence are as follows: micritization and micrite envelope, fibrous calcite cement, bladed calcite cement, fine crystalline dolomite (dolomite event 1), dissolution event 1, compaction, fracture, equant calcite cement, fine to medium crystalline dolomite (dolomite event II), anhydrite cement 1, dissolution event II, and anhydrite cement II. Four major diagenetic processes profoundly affected porosity development of the Mission Canyon Formation. Cementation, compaction, dolomitization and dissolution were active throughout the evolution of the formation.

Besides these diagenetic features, primary and secondary porosities that define the reservoir qualities of the sections were identified. They include, interparticle, intraparticle, intercrystalline, fenestral, fracture, vuggy and moldic porosities. Different degrees of porosity-destroying and porosity-enhancing features result in porosity and permeability differences among the lithofacies units of the Mission Canyon Formation. The Tilston Beds and Kisbey interval show good porosity (Tilston: average 19.7%; Kisbey: average 18.2%) and permeability (Tilston: average 33.7 millidarcies; Kisbey: average 199.3 millidarcies) while the Alida Beds and Frobisher Beds exhibit moderate porosity (Alida: average 14.5%; Frobisher: 11.3%) and permeability (Alida: average 11.0 millidarcies; Frobisher: average 45.5 millidarcies), the permeability correlates positively with the porosity. The tidal channel and carbonate sand shoal show good porosity and permeability.

Acknowledgements

I would like to thank my supervisor, Dr. Osman Salad Hersi, for his support, encouragement and patience throughout the study. Critical reviews of the thesis by Melinda Yurkowski and Dr. Hairuo Qing are greatly appreciated. Dr. Donald Kent and Mr. John Lake are gratefully acknowledged for their expert advice and suggestions.

This project is financially supported by the Government of Saskatchewan through the Saskatchewan Geological Survey. The author extends her gratitude to the staff of the Saskatchewan Ministry of Economy’s Subsurface Geological Laboratory for providing free access to the core facility, as well as providing me with pertinent data and materials. I also thank the staff of the core facility for their core handling and support.

Furthermore, I express my gratitude to the faculty, staff and my colleagues in the Department of Geology, University of Regina.

Table of Contents

List of Tables

List of Figures

1.0 Introduction

1.1 General Introduction

The Mississippian stratigraphic succession of southeastern Saskatchewan is dominated by carbonate rocks with subordinate siliciclastic and evaporitic intervals. The strata have produced 2.4 billion barrels of oil from 1953 to 2013 in southeastern Saskatchewan (Yurkowski, 2014). These strata accumulated on the northern flanks of the Williston Basin, a subcircular basin with a depocentre in North Dakota (Figure 1.1). The present-day structural Williston Basin has an area of approximately 250 000 km^2, with its structural centre located near the town of Williston, North Dakota (Kent and Christopher, 1994). The basin occupied a large area of the western North American craton during the Mississippian (Bjorlie and Anderson, 1978; Lake, 1991). Mississippian strata subcrop at the sub-Mesozoic unconformity maintaining northwest-southeast subcrop trends, along which many of the Mississippian hydrocarbon reservoirs occur in southern Saskatchewan, North Dakota and Montana (Figure 1.1; Fuzesy, 1960; Kent, 1987; Kent et al., 1988; Nickel and Yang, 2011). In southern Saskatchewan, the Mississippian strata are represented by the siliciclastic rocks of the upper part of the Bakken Formation and conformably overlying carbonate-dominated Madison Group followed by siliciclastic rocks of the Big Snowy Group (Nickel and Yang, 2011; Marsh, 2006). The Mississippian strata of southern Saskatchewan and adjacent states south of the border are prolific in hydrocarbons and the geologic study of the Mississippian stratigraphic interval has been active since the discovery of hydrocarbons in these strata (Yurkowski, 2014). These studies mainly dealt with the siliciclastic strata (e.g., the Bakken Fm, Halabura et al., 2007; Angulo and Buatois, 2011; Imam et al., 2011) and the carbonate strata (i.e., Madison Group) of the region. The Madison Group consist of three formations that are, in ascending order, Lodgepole, Mission Canyon and Charles. Oil accumulations occur stratigraphically below the pre-Mesozoic unconformity where porous limestone and subordinate sandstone units of the Mission Canyon Formation have been truncated and sealed, and also occur in the permeable units of the Mission Canyon Formation in downdip areas. Understanding the lateral and vertical facies distribution, their reservoir qualities and factors affecting the porosity and permeability of the strata is essential for better exploitation of the hydrocarbons preserved in the strata. The Mission Canyon Formation of Southeastern Saskatchewan has been stratigraphically subdivided into Tilston Beds, Alida Beds, Kisbey interval and Frobisher Beds (Figure 1.2). Kent (2004, 2007) endorsed a mixed eolian-shallow marine depositional setting while Halabura (2006) envisaged a fluvio-marine system for the mixed carbonate-clastic-evaporite succession of the Mission Canyon Formation. Within the Kisbey Sandstone, Howard (2000) recognized three sedimentary environments: wave influenced sandstone shoals, storm transported sand deposits in an open marine environment, and tidal channel sands.

1.2 Purpose of study

Previous studies used lithostratigraphic principles to describe and interpret the depositional setting of the various units of the Mission Canyon Formation (Fuzesy, 1960; Kent, 1987; Kent et al., 1988; Nickel and Yang, 2011; Howard, 2000). The cyclicity and sequence stratigraphic approach was applied in deciphering and interpreting the depositional setting and their stratigraphic cyclicity (e.g., Lake, 1991). The main objectives of this thesis are to deal with a detailed lithofacies description of the Mississippian Mission Canyon Formation, interpret their depositional environments, and determine the nature of lithofacies cyclicity and its eustatic significance. Drill cores and wireline logs available at the Saskatchewan Geological Survey (Subsurface Lab) were used to accomplish this study. The study also addresses the diagenetic evolution of the Mission Canyon Formation and interprets their impact on the reservoir quality of the strata. The study area is confined within Townships 1 to 8 and Ranges 30W1 to 6W2 in southeastern Saskatchewan (Figure 1.1).

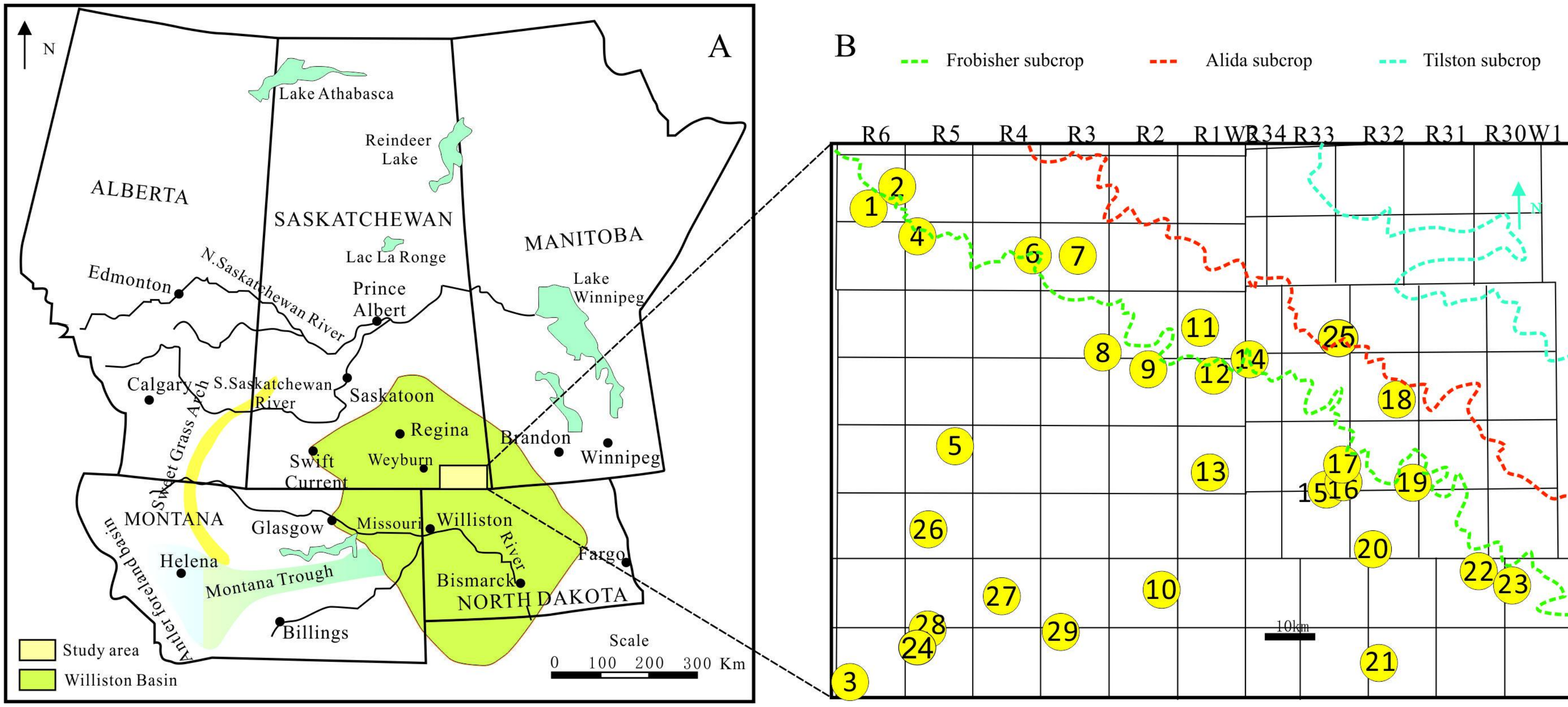

Figure 1.1 A: Location map showing the study area in southeastern Saskatchewan, configuration of the Williston Basin, and the location of Sweetgrass Arch, Montana Trough and Antler foreland basin (modified from Nimegeers, 2006). B: map showing the distribution of studied wells in the study area as identified in table 1.1.

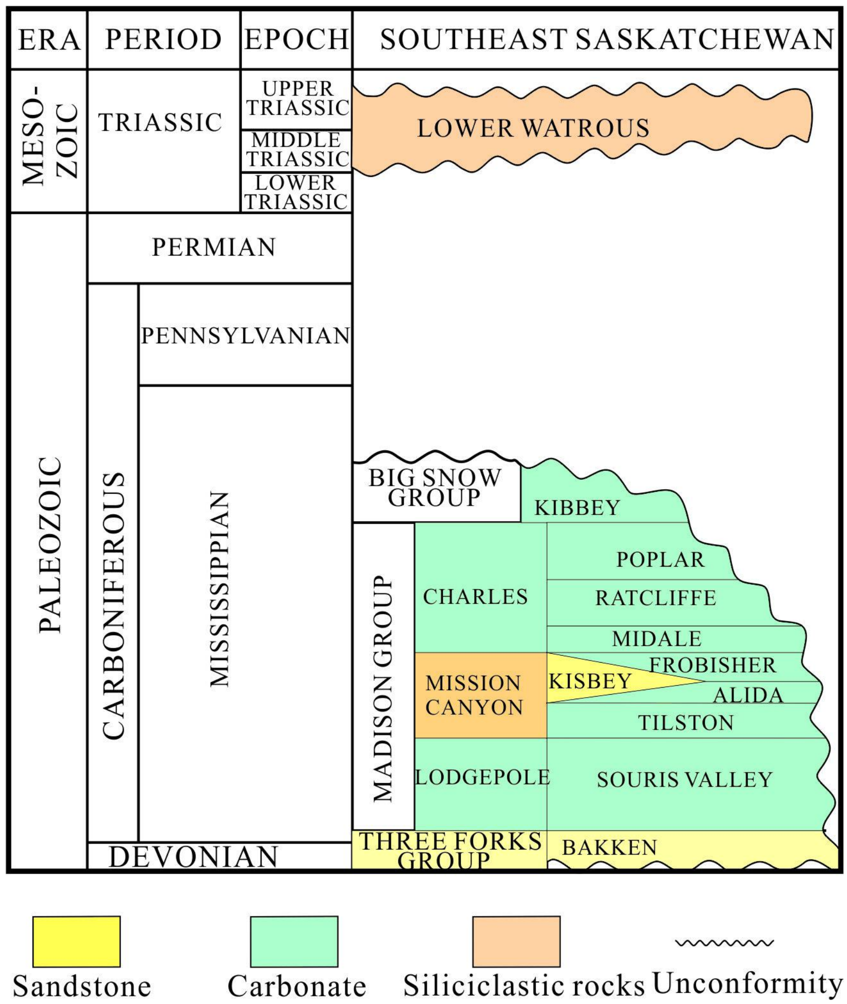

Figure 1.2 Stratigraphic column showing Mississippian units along subcrop in southeastern Saskatchewan. Units within each formation are referred to as 'Beds'. The regional Mississippian (sub-Mesozoic) unconformity separates the units from the overlying Triassic Lower Watrous Member of the Watrous Formation (modified from Saskatchewan Geological Survey, 2013).

1.3 Methodology

In order to accomplish this study, core data, wireline log data, petrographic data and permeability-porosity data were collected, integrated and interpreted. The data includes:

Core data: Twenty-five cores and drill cuttings from four wells containing the Mission Canyon Formation have been examined (Figure 1.1, Table 1.1). All of these cores penetrate through Frobisher and Kisbey intervals, fifteen cores penetrate Alida Beds and only two wells penetrate Tilston Beds.

Petrographic data: Eighty-five thin sections from nine of the examined cores and other 300 thin sections scattered in different stratigraphic intervals of the other wells have been petrographically studied and their microfacies and diagenetic properties identified.

Wireline log data: More than 200 well logs have been studied (Figure 1.3) and incorporated with the other types of data.

Porosity and permeability data: All of the porosity and permeability values were taken from GeoScout (June 2014). The data are confined with the Mission Canyon Formation stratigraphic interval.

Table 1.1 List of 29 studied wells in southeastern Saskatchewan, of which twenty five contain cores (1-25) and 4 have only drill cuttings (26-29).

Well number	Well ID	Licence number	Cored interval (m)	Cutting interval checked (m)	Numbers of thin sections
1	01/04-09-008-06W2	67B002	1228.0-1243.6		
2	11/13-13-008-06W2	87I040	1181.0-1199.0		17
3	01/03-08-001-06W2	57D025	1759.8-1891.0		
4	21/03-32-007-05W2	84A107	1224.0-1241.4		
5	01/03-26-004-05W2	55J092	1374.0-1483.2		1
6	41/03-24-007-04W2	93H085	1208.0-1226.8		2
7	41/04-22-007-03W2	08J439	1195.0-1213.3		
8	01/06-01-006-03W2	62L012	1220.7-1246.8		
9	01/07-34-005-02W2	85G245	1227.0-1245.0		
10	01/09-23-002-02W2	56J006	1371.0-1440.1 1475.2-1490.2		
11	01/05-20-006-01W2	00F231	1190.0-1208.2		
12	01/02-27-005-01W2	85K115	1183.0-1202.3		
13	41/10-09-004-01W2	08C362	1238.5-1256.8		
14	41/09-33-005-34W1	87K208	1152.0-1154.8 1155.0-1173.0		
15	31/06-02-004-33W1	97G141	1173.5-1192.8		
16	01/04-12-004-33W1	96I248	1164.6-1182.6 1183.0-1201.0		33
17	11/06-12-004-33W1	96K245	1164.0-1199.0		4
18	01/16-10-005-32W1	55C028	1074.4-1116.5		7
19	01/08-01-004-32W1	67F004	1091.2-1106.5		
20	21/16-05-003-32W1	98F112	1192.8-1211.2		
21	11/15-18-001-32W1	90G125	1281.5-1300.5		8
22	02/16-27-002-31W1	56K120	1100.5-1127.2		
23	50/11-19-002-30W1	72L015	1075.0-1092.8		
24	01/01-11-006-33W1	86J054	1133.0-1177.2		10
25	01/12-29-001-05W2	54D007	1859.3-1889.8		3
26	41/13-16-003-05W2	08G476		1595-1615	
27	41/15-16-002-04W2	08J206		1602-1620	
28	91/16-32-001-05W2	08H550		1720-1735	
29	41/09-32-001-03W2	08C328		1623-1635	

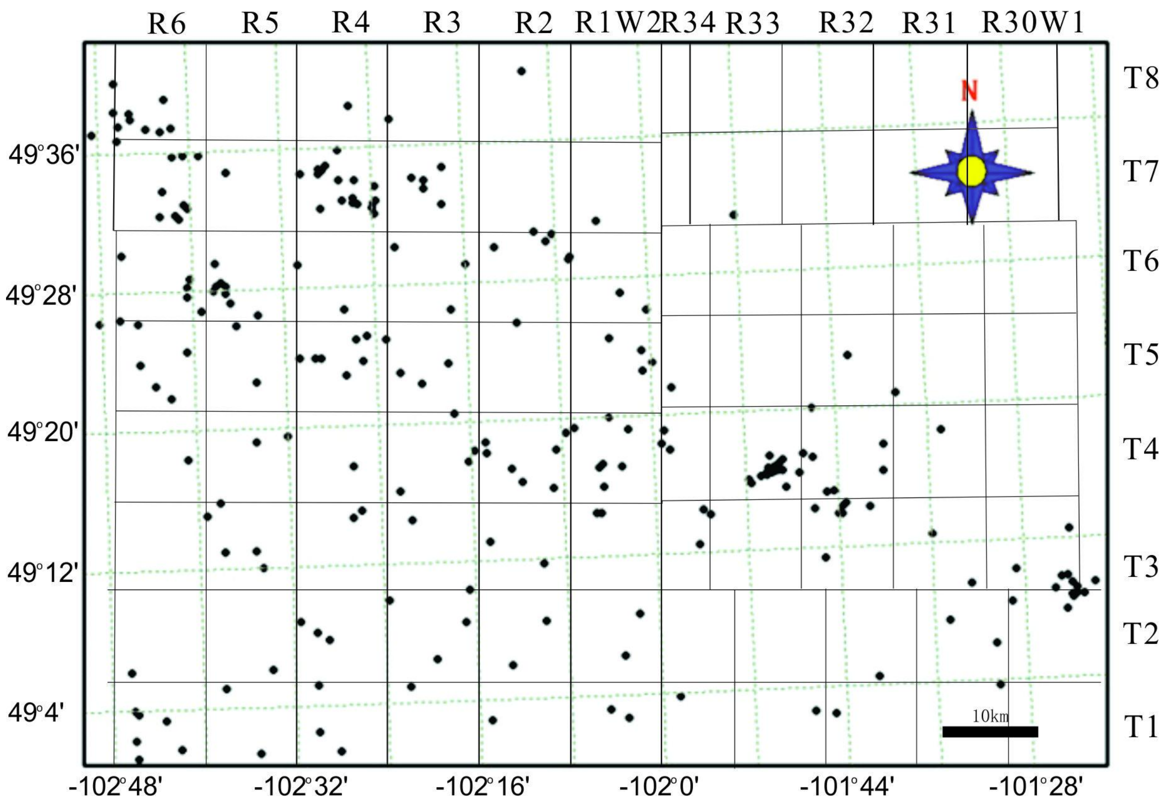

Figure 1.3 Map showing the distribution of studied well logs in the study area.

1.4 Previous work

The Mississippian Mission Canyon Formation of Williston Basin comprises a mixed carbonate-siliciclastic-evaporitic succession (Figure 1.2). Carbonate lithology prevails in these rocks in both regions north and south of the Canada-USA border. Thinner, laterally extensive siliciclastic (e.g., MC-2, K-3, Kisbey Sandstone and K-1 units, Table 1.2) and evaporite strata are also present. The stratigraphic nomenclature and interpretation of the depositional environments of these strata have been addressed by different researchers in the past (e.g., Thomas, 1954; Porter, 1955; Fuller, 1956; Edie, 1958; Fuzesy, 1960; Legault, 1999; Kent, 2004, 2007; Halabura, 2006; Table 1.2). Presence of clastic rocks within the Mississippian strata of southeastern and south-central Saskatchewan, as well as in the adjacent states of Montana and North Dakota played a significant role in influencing the stratigraphic subdivision of the strata. The Mission Canyon Formation of Southeastern and south-central Saskatchewan has been stratigraphically subdivided based on different approaches (e.g., lithostratigraphy, sequence stratigraphy, marker-defined facies and wireline logs). The nomenclatural evolution of the clastic-bearing interval has been addressed by Kent (2007). Prior to Kent's (2007) work, Carlson and Lefever (1987) have discussed the nomenclature dilemma to subdivide the Mission Canyon Formation of the Williston Basin. Thomas (1954) first recognized a discrete sandstone/siltstone interval in the Mission Canyon Formation of southeastern Saskatchewan and named it MC_4 (Table 1.2). This sandstone interval was later called Kisbey Sandstone by Fuller (1956). More sandstone intervals were recognized by Edie (1958) and Fuzesy (1960). Edie (1958) identified two sandstone/siltstone intervals separated by a carbonate unit and named the clastic units as

1st Kisbey and 2nd Kisbey intervals. The former is quite extensive and correlative with Fuller's (1956) Kisbey Sandstone (equivalent to MC4 of Thomas, 1954) but 2nd Kisbey sandstone is laterally limited to the southeastern corner of the Province. More clastic intervals were identified by Legault (1999) and adopted the terms K1, K2 and K3 marker beds, following marker-bed terminology used in the Mission Canyon Formation of North Dakota (e.g., Harris et al., 1966; Carlson and Lefever, (1987). The K2 interval of Legault (1999) correlates with Kisbey Sandstone of Fuller (1956) and 1st Kisbey unit of Edie (1958). Consideration of Fuller's (1956) Kisbey Sandstone as a marker bed separating underlying Alida Beds from overlying Frobisher Beds (e.g., Legault, 1999) puts other clastic units (e.g., K1 and K3) into the Alida and Frobisher Beds, respectively. Halabura (2006) took a sequence stratigraphic approach adopting allostratigraphic subdivision of the Mission Canyon Formation (e.g., Alida Alloformation, Kisbey Alloformation, etc). Kent (2007, p.3) employed a different stratigraphic scheme, where he lumped "all beds containing quartz sand or silt" under the name "Kisbey interval" (Table 1.2).

The interpretation of the origin and depositional setting of the siliciclastic-carbonate strata of the Mission Canyon Formation of southeast Saskatchewan has been discussed in different papers (Howard, 2000; Kent, 2004, 2007; Halabura, 2006, Halabura and Costa, 2005, and Ji and Salad Hersi, 2013a). Many researchers have indicated that the strata of the Mission Canyon Formation are part of an overall shallowing-upward trend in the Mississippian (e.g., Kent, 1984; Waters and Sando, 1987) and that cyclicity can be identified on several scales (e.g., Elliot, 1982; Hoff, 1987; Lake, 1991).

Table 1.2 Nomenclatures of Mississippian Mission Canyon Formation in Southeast Saskatchewan.

<table>
<tr><th>Thomas (1954)</th><th>Fuller (1956)</th><th>Edie (1958)</th><th>Fuzesy (1960)</th><th>Legault (1999)</th><th>Halabura (2006)</th><th>Kent (2007) This paper</th><th></th></tr>
<tr><td>–</td><td>Midale beds</td><td>Midale beds</td><td rowspan="2">Midale beds</td><td></td><td></td><td rowspan="2">Midale beds</td><td rowspan="2"></td></tr>
<tr><td>–</td><td>Frobisher evaporite</td><td>Frobisher evaporite</td><td></td><td></td></tr>
<tr><td rowspan="3">MC_5</td><td rowspan="3">Hasting-Frobisher beds</td><td rowspan="3">MC_5</td><td rowspan="3">Frobisher Beds</td><td>Sherwood Sub-Interval</td><td rowspan="3">Frobisher Alloformation</td><td>Frobisher Beds</td><td rowspan="9">Mission Canyon Formation</td></tr>
<tr><td>K1</td><td rowspan="5">Kisbey interval</td></tr>
<tr><td>Mohall Sub-Interval</td></tr>
<tr><td>MC_4</td><td>Kisbey sandstone</td><td>1st Kisbey</td><td>Kisbey sandstone</td><td>K2</td><td>Kisbey Alloformation</td></tr>
<tr><td rowspan="3">MC_3</td><td rowspan="3">Forget-Nottingham ls.</td><td></td><td rowspan="3">Alida Beds</td><td>Glenburn Sub-Interval</td><td rowspan="3">Alida Alloformation</td></tr>
<tr><td>2nd Kisbey</td><td>K3</td></tr>
<tr><td></td><td>Landa-Wayne Sub-Interval</td><td>Alida Beds</td></tr>
<tr><td>MC_2</td><td>MC_2 beds</td><td>MC_2</td><td rowspan="2">Tilston Beds</td><td></td><td rowspan="2">Tilston interval</td><td rowspan="2">Tilston Beds</td></tr>
<tr><td>MC_1</td><td>MC_1limestone</td><td>MC_1</td><td></td></tr>
</table>

2.0 Geological Background

2.1 Stratigraphic Framework

There are no outcrops of Mississippian rocks in southeastern Saskatchewan. The Mississippian rocks are overlain by some 1210 m-thick Mesozoic and Cenozoic clastic rocks and underlain by about 1000 m of Paleozoic rocks in southeast Saskatchewan. The Mississippian rocks are unconformably overlain by the Triassic Watrous Formation. Post-Bakken Mississippian rocks in Saskatchewan have been subdivided into two groups: Madison Group and the overlying, erosionally-reduced Big Snowy Group (Figure 1.2). The Madison Group of the Williston Basin contains a 400 to 700 m thick section of mainly carbonate succession and minor evaporite and sandstone sediments (Kent, 1984). The sedimentation pattern of the group is typical of a major upward shoaling sequence, deposited as a thick basin-ward migrating wedge of sediments. Superimposed on this system are individual cycles of transgressive-regressive pulses, which are interpreted as the result of sea level fluctuations (Wilson, 1975). The Madison Group forms the bulk of the Mississippian succession and consists of the Lodgepole, Mission Canyon and Charles formations, in ascending order (Figure 1.2). The Mission Canyon Formation of southeastern Saskatchewan consists of four stratigraphic units: Tilston, Alida, Kisbey and Frobisher, in ascending stratigraphic order (Nickel and Yang, 2011; Marsh, 2006; Ji and Salad Hersi, 2014; Figure 1.2).

In this thesis, the nomenclature established by Kent (2007) has been adopted

(Table 1.2). The Alida-Kisbey boundary is put at the base of the first appearance of sandstone or sandy/silty carbonate beds and the top of Kisbey is put at the top of the youngest (highest) bed of sandstone or sandy / silty carbonate (Ji and Salad Hersi, 2013b). The lower and upper contacts of the Kisbey interval are characterized by a relative higher gamma ray response and lower photoelectric curve than the underlying Alida Beds and the overlying Frobisher Beds (Figure 2.1). In areas where no quartz grains are present, the Kisbey interval is composed predominantly of argillaceous dolomudstone which is characterized by a higher gamma ray response.

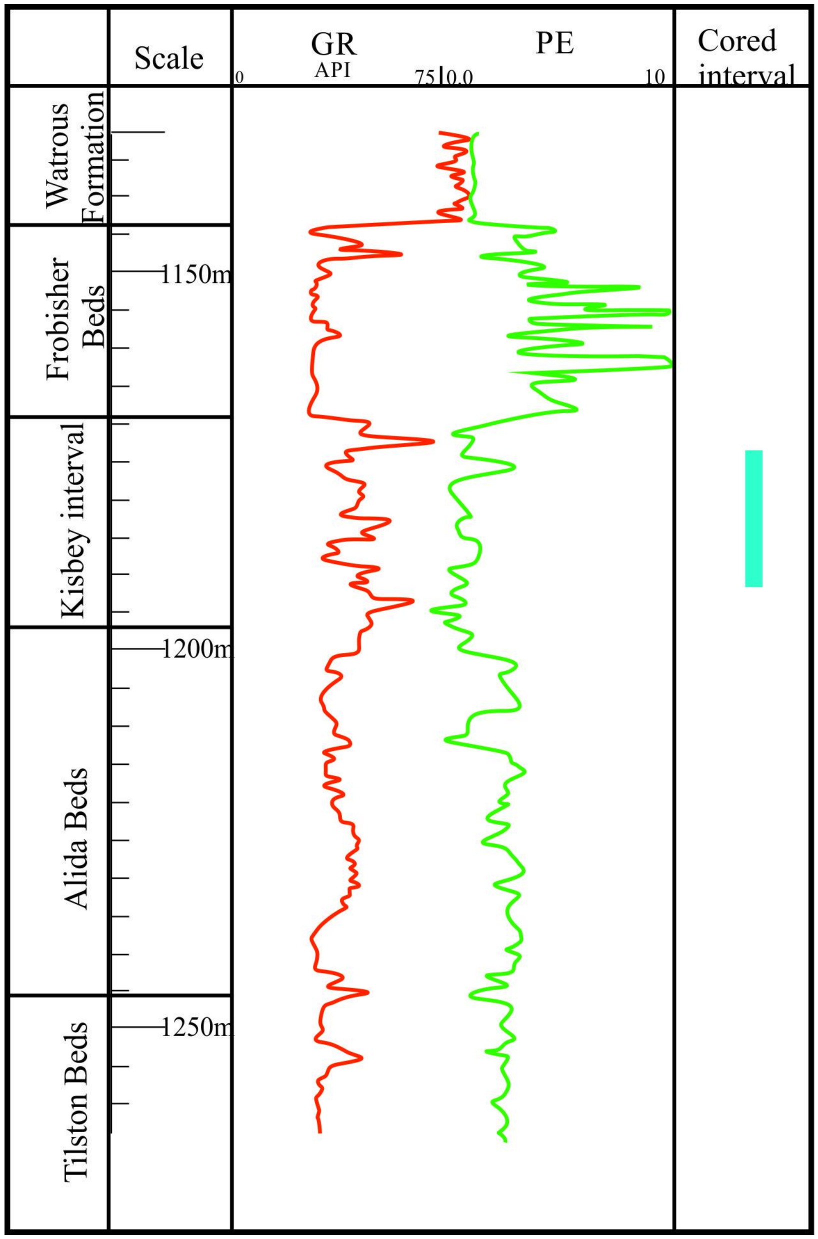

Figure 2.1 Typical Gamma Ray (GR) and Photoelectric (PE) curves of Mission Canyon Formation in southeast Saskatchewan. Well 31/6-2-4-33W1, 97G141.

2.2 Tectonic framework

The paleogeography of Williston Basin during the Mississippian Epoch was influenced by western North American continental margin tectonic evolution and basement tectonic movement within the basin. The basin occupied a large area of the western North American craton during the Mississippian Epoch (Bjorlie and Anderson, 1978; Lake, 1991). During the late Devonian to early Mississippian time, the major tectonic elements were the Antler Orogenic Belt, the Antler Foreland Basin, the Prophet Trough, and the Central Montana Trough (Figure 1.1, 2.2). Uplift of the Sweetgrass Arch during this time interval caused an isolation of the Williston Basin and its disconnection from the large Western Canada Sedimentary Basin. However, the basin was connected to the Pacific Ocean via the Montana Trough (Gerhard et al., 1991; Reid and Dorobek, 1993) (Figures 1.1, 2.2). Mississippian sediments were deposited in a tectonically stable environment (Richards, 1989; Rott and Qing, 2005) and their lateral and vertical (temporal) distribution suggests that they evolved as a transgressive-regressive cycle equivalent to the upper part of Sloss's (1963) Kaskaskia Supersequence. Porter et al. (1982) stated that the development of the basin was caused by uplifting and erosion of the cratonic arches surrounding the basin in periods between the transgressive-regressive cycles, as a result of differential subsidence of the basin during the cycles. Four major transgression and regression events have occurred across the basin from the Cambrian to the Jurassic Periods. Due to a lull in orogenic movement in the early Mississippian Epoch, the Williston Basin became relatively stable, with reduced siliciclastic input and the establishment of a carbonate platform, represented by the Lodgepole Formation/Souris

Valley Beds (Figure 1.2) (LeFever et al., 1991). Carbonate accumulation persisted throughout the deposition of the Madison Group. However, evaporite and sandstone intercalations in the upper part of the Madison Group (Figure 1.2; Nimegeers, 2006) indicate intermittent sea level fluctuations, restriction of the depositional environment, and episodic siliciclastic progradations during deposition of the Mississippian Madison Group. Sediments in the Mississippian Mission Canyon Formation were deposited in a relatively stable, broad, and shallow epicontinental sea in a periodically restricted condition (Richards, 1989; Rott and Qing, 2005). The Watrous Formation, unconformity overlying the Mississippian strata, is dominated by siliciclastic rocks deposited in shallow marine environment (Gerhard, *et al*, 1982).

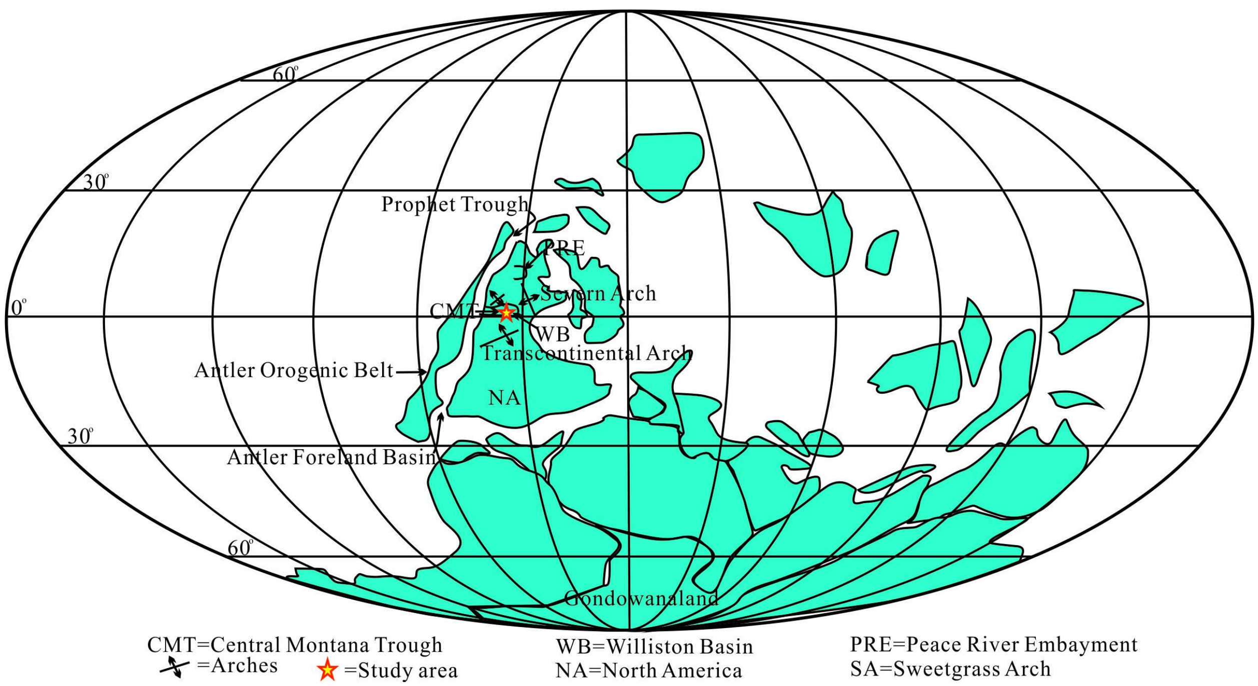

Figure 2.2 Paleo-tectonic element of the early Carboniferous (modified from Howard, 2000).

3.0 Lithofacies Description and Interpretation

3.1 General description

The Tilston Beds are composed of carbonate rocks with subordinate anhydrite and are overlain by Alida Beds (Kent, 2014). Alida Beds consist of limestone and minor dolostone and anhydrite interbeds (Fuzesy, L.M., 1960; Rott and Qing, 2006; 2013), and are overlain by the Kisbey interval which consists of interbeds of limestone, dolostone, siltstone/sandstone, and sandy carbonates (Kent, 2007). The Frobisher Beds are dominated by limestone and dolostone lithofacies (Fuzesy, L.M., 1960; Marsh, 2006) and succeed the uppermost sandstone or sandy carbonate bed of the Kisbey interval. The top of the Mississippian succession in southeastern Saskatchewan is marked by an unconformity (Figures 3.1; 3.2).

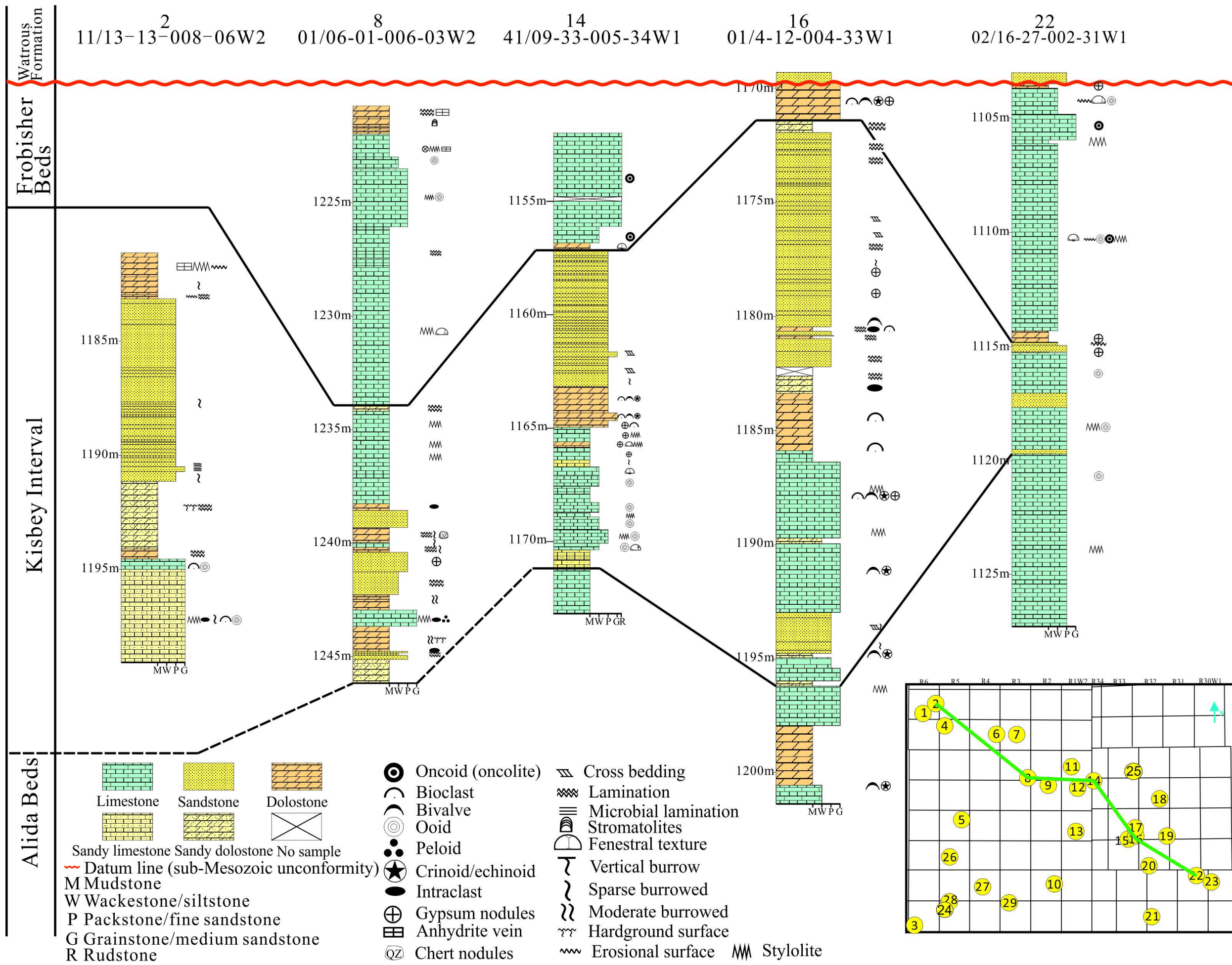

Figure 3.1 Cross section showing the lithologies of Alida Beds, Kisbey interval and Frobisher Beds in cores from five wells in the study area. Datum is the sub-Mesozoic unconformity surface, the depth of which was determined on wireline logs for the three wells in which this contact is not cored. Dashed lines indicate the top of the Alida as inferred from wireline logs.

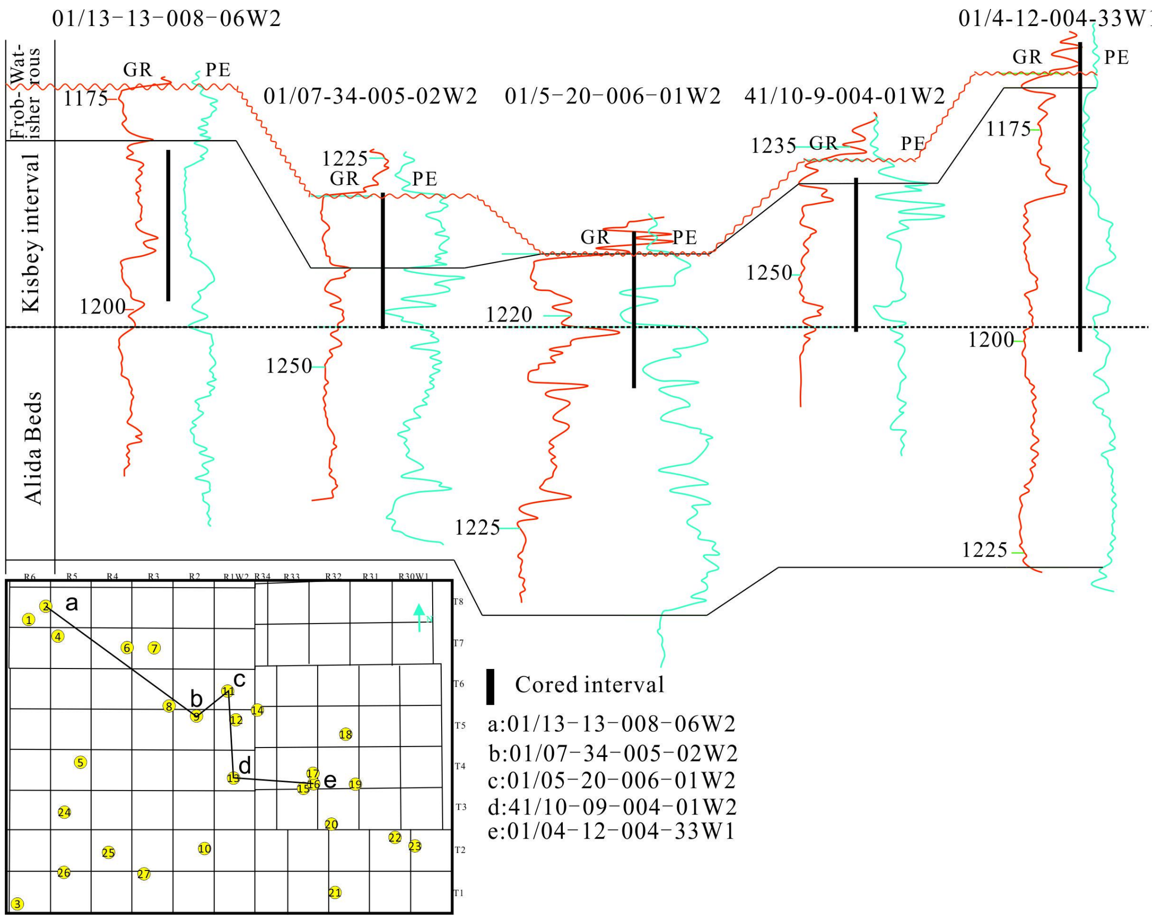

Figure 3.2 Cross section showing the Gamma Ray (GR) and Photo Electronic (PE) curve of Alida Beds, Kisbey interval and Frobisher Beds from five wells in the study area; the well location are showing in inset map.

3.2 Lithofacies properties

The various lithofacies identified in the Mission Canyon Formation in the study area are based on the study of 25 cored wells (Figure 1.1), wireline logs and 85 thin sections from the Mission Canyon Formation (Table 1.1). Petrographic analysis of the studied strata allows identification of eight lithofacies which include: i) oolitic, bioclastic packstone to grainstone (Facies PG), ii) oncolitic rudstone (Facies RD), iii) oolitic, bioclastic mudstone to wackestone (Facies MW), iv) dolomudstone (Facies DS), v) siltstone to sandstone (Facies SS), vi) sandy dolomudstone (Facies SD), vii) sandy packstone to grainstone (Facies SP) and viii) anhydrite (Facies AH) (Table 3.1). The characteristics of these eight lithofacies are described below.

Table 3.1 Lithofacies description of the studied strata and their inferred depositional environments.

Facies	Lithofacies	Description	Sedimentary structures	Distribution	Depositional Environment
PG	Packstone / grainstone	Light to dark grey packstone, grainstone and rudstone	Fenestral, structure and microbial laminations	Tilston, Alida, Frobisher Beds and locally in Kisbey interval	Shoal/open marine
RD	Rudstone	Grey rudstone	Fenestral structure and microbial lamination	Frobisher Beds	Subtidal to intertidal
MW	Mudstone / wackestone	Light to dark grey mudstone / wackstone	Fenestral structure, microbial laminations	Tilston, Alida, Kisbey and Frobisher intervals	Lagoon to intertidal
DS	Dolomudstone	Pale grey to grey dolomudstone	Fenestral structure, mudcracks and microbial laminations (including domal stromatolites)	Tilston, Alida, Kisbey and Frobisher intervals	Intertidal to supratidal
SS	Sandstone / siltstone	Yellowish grey to dark grey fine sandstone/silt-stone to quartz arenite	Massive, bioturbated, tabular and trough cross laminations and horizontal laminations	Kisbey interval	Tidal channel
SD	Sandy dolomudstone	Pale to dark grey sandy dolomudstone	Massive	Kisbey interval	Intertidal to supratidal
SP	Sandy packstone / grainstone	Grey sandy packstone / grainstone	Fenestral structure / cross lamiantion	Kisbey interval	Subtidal
AH	Anhydrite	White and red anhydrite Massive and nodular	Massive and nodular	Tilston, Alida and Frobisher Beds	Supratidal

3.2.1 Packstone to grainstone lithofacies (PG)

Description: The packstone to grainstone facies is characterized by thick to medium bedded, light to dark grey limestone. Sedimentary structures in this lithofacies include a fenestral fabric and minor microbial laminations that drape the grainstone layers (Figure 3.3a); stylolites are common. The PG lithofacies has fair to good porosity (e.g., Figure 3.3a, b) and is commonly oil stained. Anhydrite, dolomite and calcite cements locally fill the pore space (Figure 3.3c), and thus reduce the overall porosity of the unit. Although this lithofacies occurs throughout Tilston, Alida, Kisbey and Frobisher units, it occurs most commonly within the upper part of Alida and Frobisher interval. The base of units of this facies is associated with a gradational to sharp contact.

Petrographic analysis reveals that ooids and bioclasts are the most common framework grains (Figure 3.3b, c) of this lithofacies. The bioclasts include crinoids, brachiopods, bivalves, foraminifera, gastropods, bryozoans, and, less commonly, calcareous green algae. The packstone/grainstone lithofacies typically consists of 80% to 90% ooids and bioclasts. Ooids commonly show a poorly preserved internal (cortex) structure due to extensive micritization and, thus, many grains that appear to be peloids may be pervasively micritized ooid grains. This facies is locally dolomitized. The cements of this lithofacies are dominated by anhydrite, dolomite and calcite.

Interpretation: The lithofacies PG accumulated in a high energy, normal marine depositional environment (Edie, 1958; Kent, 1984, Perras, 1990 and Rott and Qing, 2005), representing a carbonate sand shoal. The fact that no exposure surfaces are recognized may suggest that the lithofacies developed in a shallow subtidal setting.

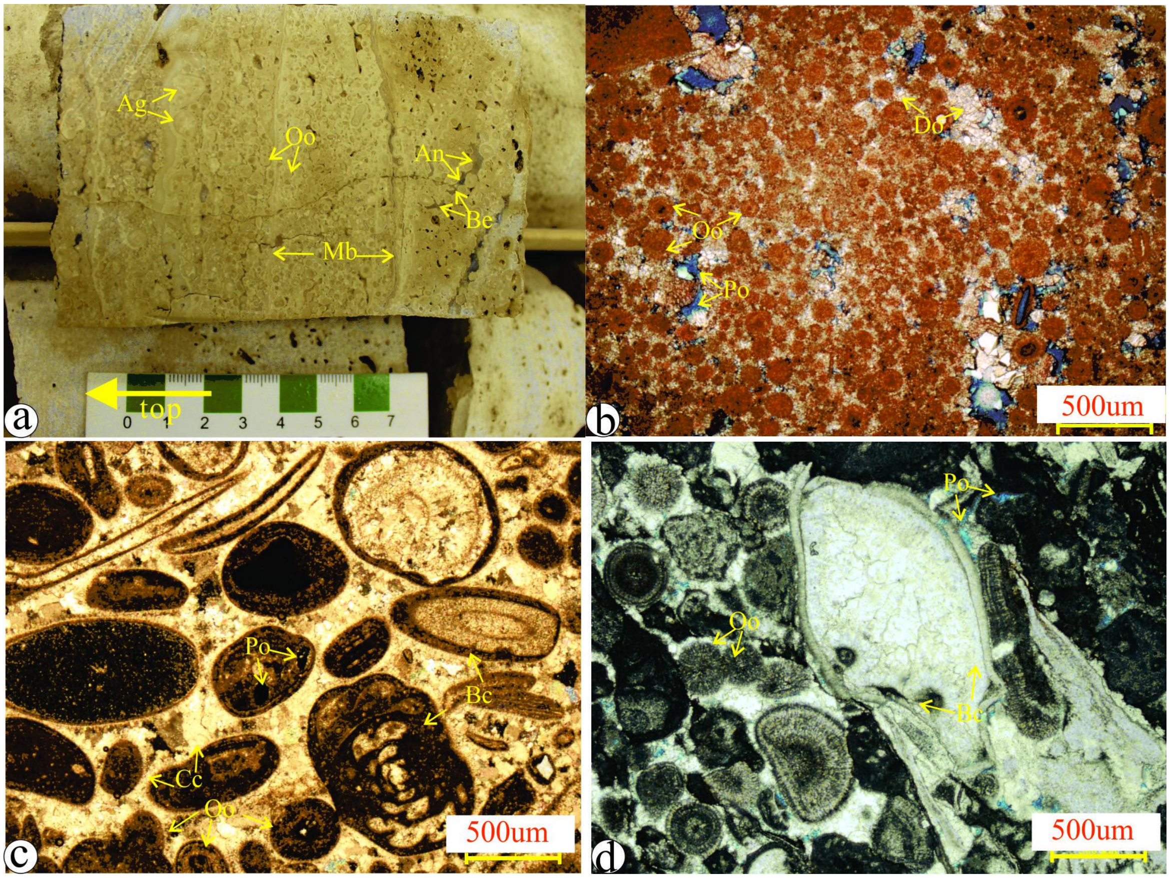

Figure 3.3 a) Core photograph of oolitic grainstone showing microbial lamination (Mb), birdseye structure (Be), aggregate grains (Ag), oolite grains (Oo) and anhydrite cement (An), Frobisher Beds. 1093.5 m, well 01/08-01-004-32W1; 67F004; b) photomicrograph of oolitic grainstone showing oolite grains (Oo), dolomite cement (Do) and pore space (Po, porosity is filled by blue epoxy). The thin section is stained with Alizarin Red. Photo is taken under plane polarized light, Frobisher Beds , 1286.3 m, well 11/15-18-001-32W1; 90G125; c) photomicrograph of oolitic bioclastic grainstone showing oolite grains (Oo), bioclasts (Bc), calcite cement (Cc) and pore space (Po), Photo is taken under X- polarized light. Kisbey interval, 1195.0 m, 11/13-13-008-06W2; 87I040; d) photomicrograph of bioclatic oolitic grainstone showing bioclast (Bc), oolite (Oo) and pore space (Po). Tilston Beds, 1870.6m, 01/12-29-001-5W2; 54D007.

3.2.2 Oncolitic rudstone lithofacies (RD)

Description: The rudstone lithofacies is a grey, medium bedded limestone and has microbial lamination and fenestral structure. The RD lithofacies has good porosity (e.g., Figure 3.4a; b), but the pore spaces are locally filled by anhydrite, dolomite or calcite cements (Figure 3.4), and thus reduce the overall porosity of the unit. This lithofacies is mainly distributed within Frobisher Beds.

The framework grains are dominated by oncoids with subordinate ooids, intraclasts and peloids, although the peloids and intraclasts may have originated as micritized oncoids, ooids or bioclasts. The grain size of the oncoids is granule to pebble size (Figure 3.4).

Interpretation: The textural attributes and sedimentary structures of this lithofacies indicate a moderate-energy depositional environment. The depositional site has been interpreted as an intertidal to subtidal environment (Ueon, et al, 2012).

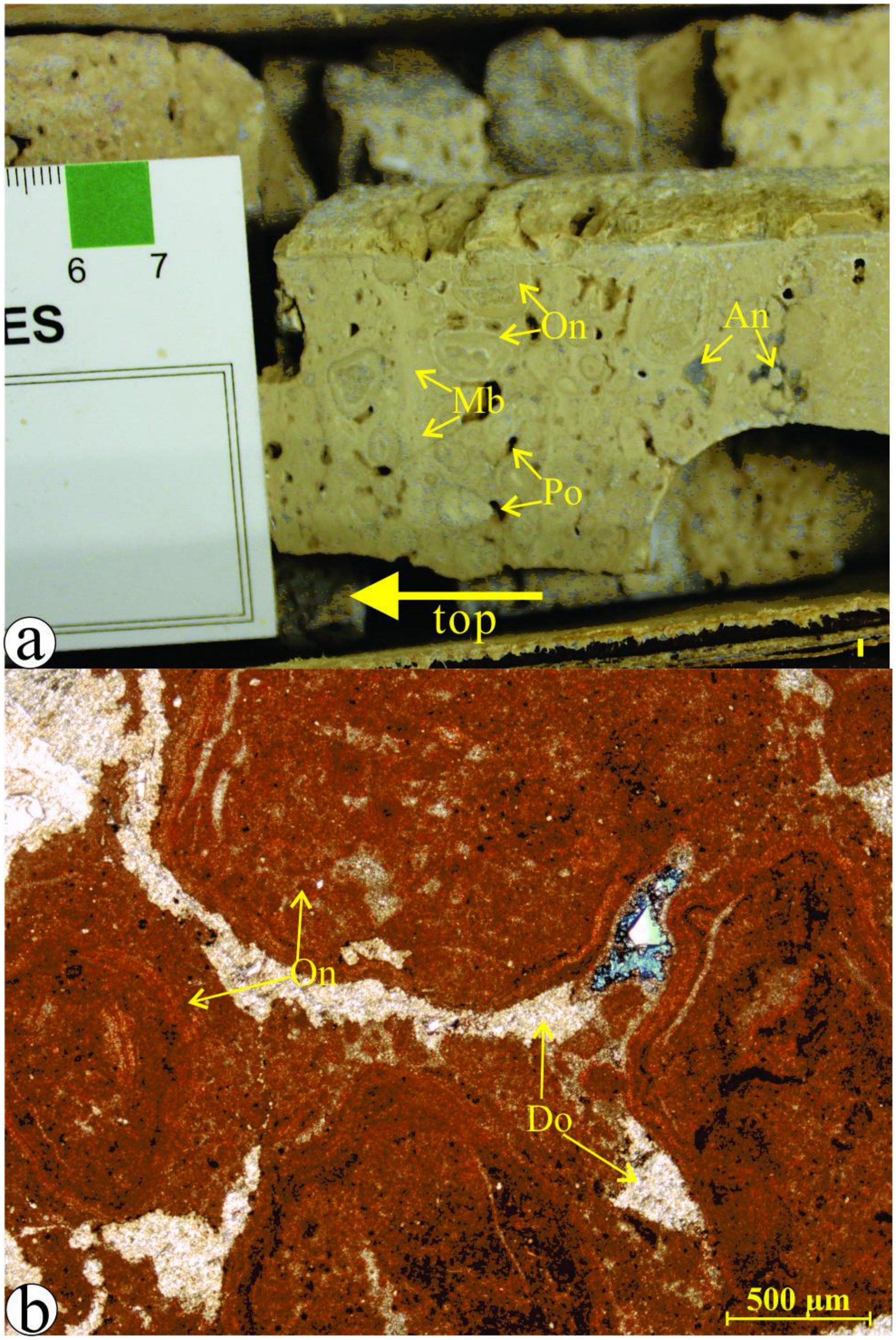

Figure 3.4 a) Core photograph of oncolitic rudstone showing microbial lamination (Mb), oncoids (On), anhydrite cement (An) and pore space (Po). Frobisher Beds, 1154.0 m, 41/09-33-005-34W1; 87K208; b) photomicrograph of oncolitic rudstone showing oncoids grains (On), dolomite cement (Do). The thin section is stained with Alizarin Red. Photo is taken under plane polarized light, Frobisher Beds, 1286.3 m, well 01/05-20-001-32W1; 90G125.

3.2.2 Mudstone to wackestone lithofacies (MW)

Description: The mudstone to wackestone lithofacies consists of laminated to thickly bedded, light to dark grey limestone. Sedimentary structures include microbial laminations and fenestral (birdseye) structure. This lithofacies has 5% to 10% vuggy porosity (Figure 3.5a, b) and subordinate intercrystalline porosity. The lithofacies is typically oil stained. This lithofacies is distributed throughout Tilston, Alida, Kisbey and Frobisher intervals.

Framework grains of Facies MW are dominated by bioclasts, ooids, intraclasts and subordinate oncoids and peloids (Figure 3.5b shows a peloidal, intraclastic wackestone). Oncoids have irregular lamination, a large grain size and appear commonly floating within the micrite matrix. Most oncoid grains are simple, but in many cases, several oncoids are bound together forming a large composite oncoid. The matrix of Facies MW is typically composed of anhedral micrite, partly replaced by very fine crystalline dolomite rhombs. The cement is predominately anhydrite and dolomite.

Interpretation: The textural attributes (high mud content) and sedimentary structures of this lithofacies indicate a low-energy depositional environment, thus, accumulation may have taken place in a protected lagoonal to intertidal mudflat setting (Pratt, 2010; Howard, 2000; Rott and Qing, 2005). The depositional site was probably protected by the carbonate sand shoals of lithofacies PG.

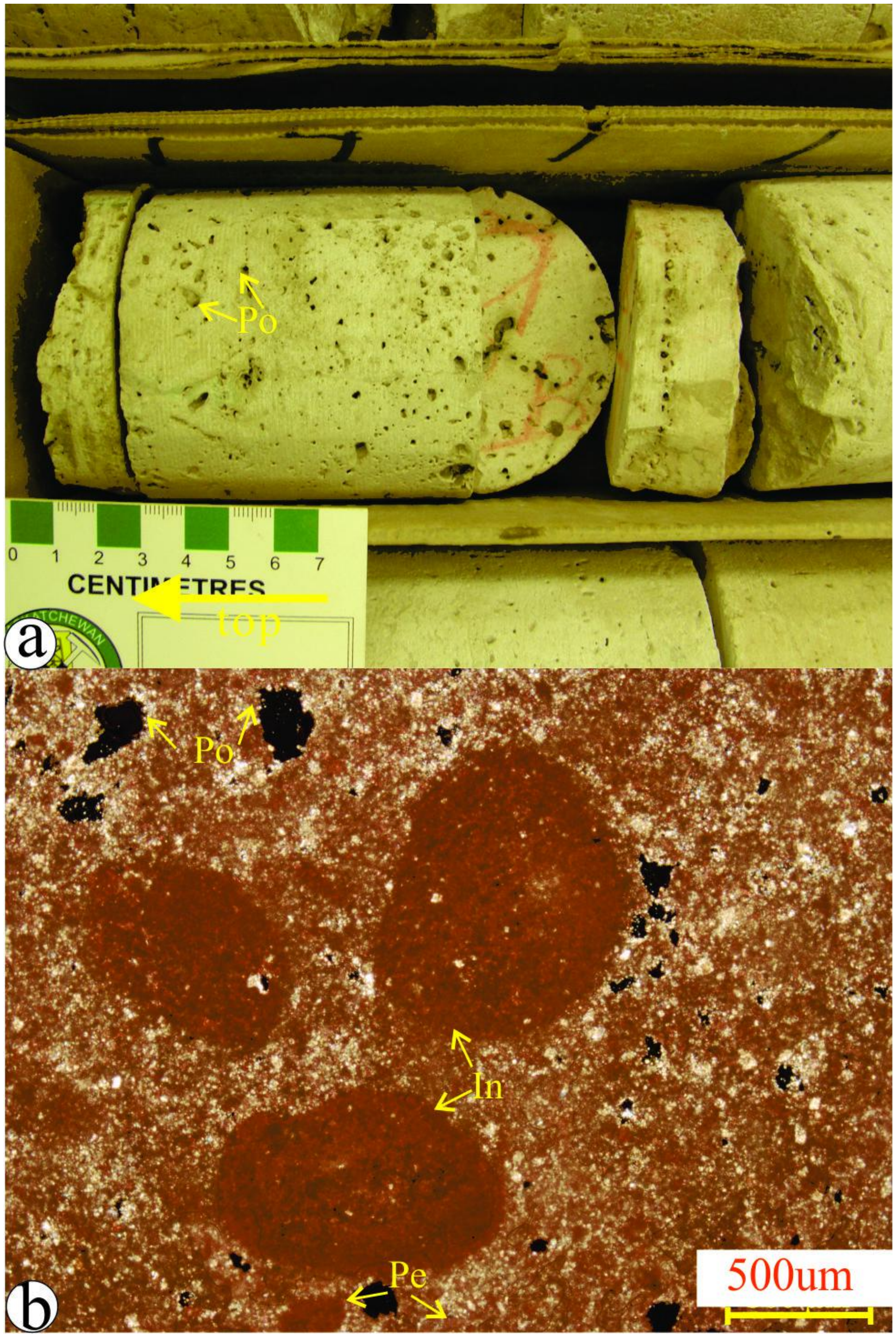

Figure 3.5 a) Core photograph of mudstone with good dissolution porosity (Po). Frobisher Beds, 1185.5m, 01/02-27-005-01W2; 85K115; b) photomicrograph of peloidal intraclastic wackestone with intraclasts (In), peloids (Pe) and pore space (Po); the thin section is stained with Alizarin Red. Photo is taken under X-polarized light. Alida Beds, 1116.1 m, 01/16-10-005-32W1; 55C028.

3.2.3 Dolomudstone lithofacies (DS)

Description: This lithofacies consists of laminated to thinly bedded, pale grey to grey dolomudstone. Fenestral (birdseye) fabric commonly filled by anhydrite, mudcracks and microbial laminations (including domal stromatolites) (Figure 3.6a, b). This lithofacies appears dense with no significant pore space. This lithofacies is always associated with anhydrite. In most cases, the contact with the underlying sandstone lithofacies is gradational. Lithofacies DS is present throughout the Mission Canyon Formation.

Petrographic examination of this lithofacies shows a dolomicrite texture (<4 microns) with a minor amount of fine (around 100 microns) dolomite crystals. Dolomicrite crystals are mainly anhedral, sometimes have relict bioclasts and other possibly peloidal grains. Fine crystalline dolomites appear as euhedral rhombs which usually float in the dolomicrite. The overall dolomudstone lithofacies contains less than 5% anhydrite and dolomite cements.

Interpretation: The dolomudstone texture, relative lack of sedimentary structures and the association with the anhydrite lithofacies suggest deposition within a restricted depositional environment (Kent, 1984). The dolomudstone lithofacies is envisaged as being accumulated in a supratidal to upper intertidal mudflat depositional setting (Shinn, 1983).

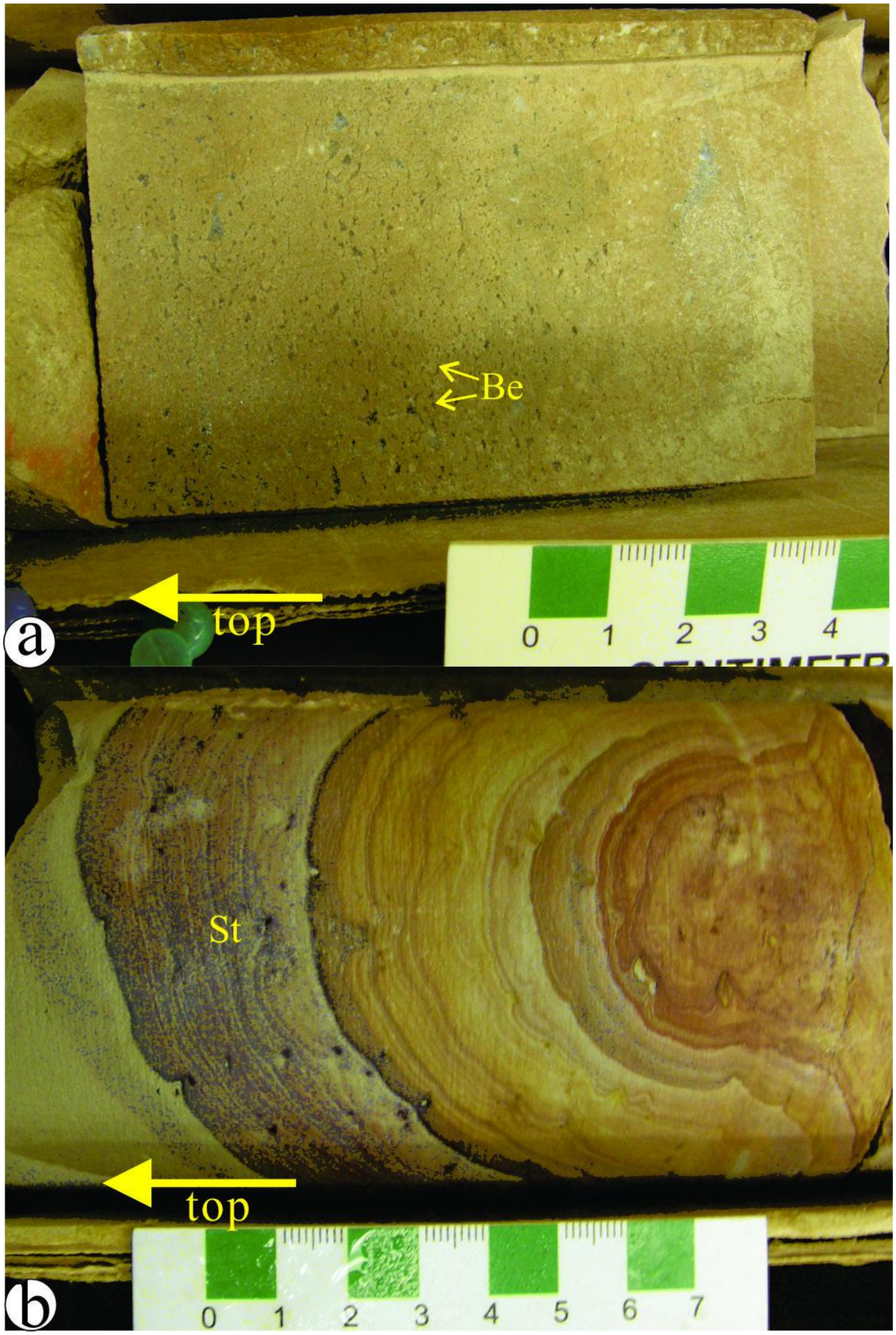

Figure 3.6 a) Dolomudstone lithofacies showing birdseye structure (Be); Frobisher Beds, 1157.1 m, 41/09-33-005-34W1; 87K208; b) Domal stromatolite (St) of fine crystalline dolomudstone, Frobisher Beds. 1221.4 m, 01/06-01-006-03W2; 62L012.

3.2.4 Sandstone (Feldspathic arenite) / siltstone lithofacies (SS)

Description: This lithofacies is a thinly to thickly-bedded, yellowish grey to dark grey siltstone/sandstone. Most of the beds are massive with no internal structures. The unit is commonly interbedded with other carbonate lithofacies but the continuous section of the sandstone lithofacies may locally reach as thick as 20 m (e.g., 01/04-12-004-33W1; 96I248). Some beds do, however, have sedimentary structures including tabular and trough cross-laminations, and horizontal laminations, and may be sparsely to moderately bioturbated (probably *pholadid* and other unidentifiable burrows, Figure 3.7). This facies has moderate porosity and is oil-stained in some cases. The feldspathic arenite/siltstone lithofacies is in contact with a variety of carbonate lithofacies and lower contacts are commonly sharp whereas the upper contacts appear gradational to the carbonate lithofacies. The contact surfaces separating between the beds of sandstone/siltstone lithofacies are sharp to erosional. The sandstone/siltstone lithofacies is confined within the Kisbey interval and is characterized by lateral discontinuity and, thus, it is difficult to correlate from one well to another.

In thin sections, the framework grains are dominated by quartz (>80%), followed by feldspar (~15%) and minor chert grains (<5%) (Figure 3.7b). This facies is generally matrix-free but locally shows a dolomudstone matrix similar to the DS facies. Individual grains of sandstone/siltstone lithofacies are predominantly fine grained (0.1-0.2mm), and are subangular and well sorted (Figure 3.7b). Rare carbonate grains, such as, peloids are locally present within this lithofacies. The cements of this facies are anhydrite, calcite and dolomite.

Interpretation: The feldspathic arenite/siltstone lithofacies shows very few sedimentary structures rendering interpretation difficult. The presence of sharp and erosional contacts, peloids, cross laminations, lack of matrix and vertical burrows suggest a moderate to high energy depositional environment (Campbell, 1967; Allen, 1982). The fact that the unit has a gradational upper contact with the overlying carbonates and is laterally discontinuous (not unequivocally traceable from one well to the next) suggests that it possibly accumulated in confined, intertidal channels that cut through the shallow marine carbonate platform. It is envisaged that the siliciclastic sediments in the tidal channels were fed by intermittent fluvial influx from the north/northeast of the Williston Basin, particularly during relative sea level drop.

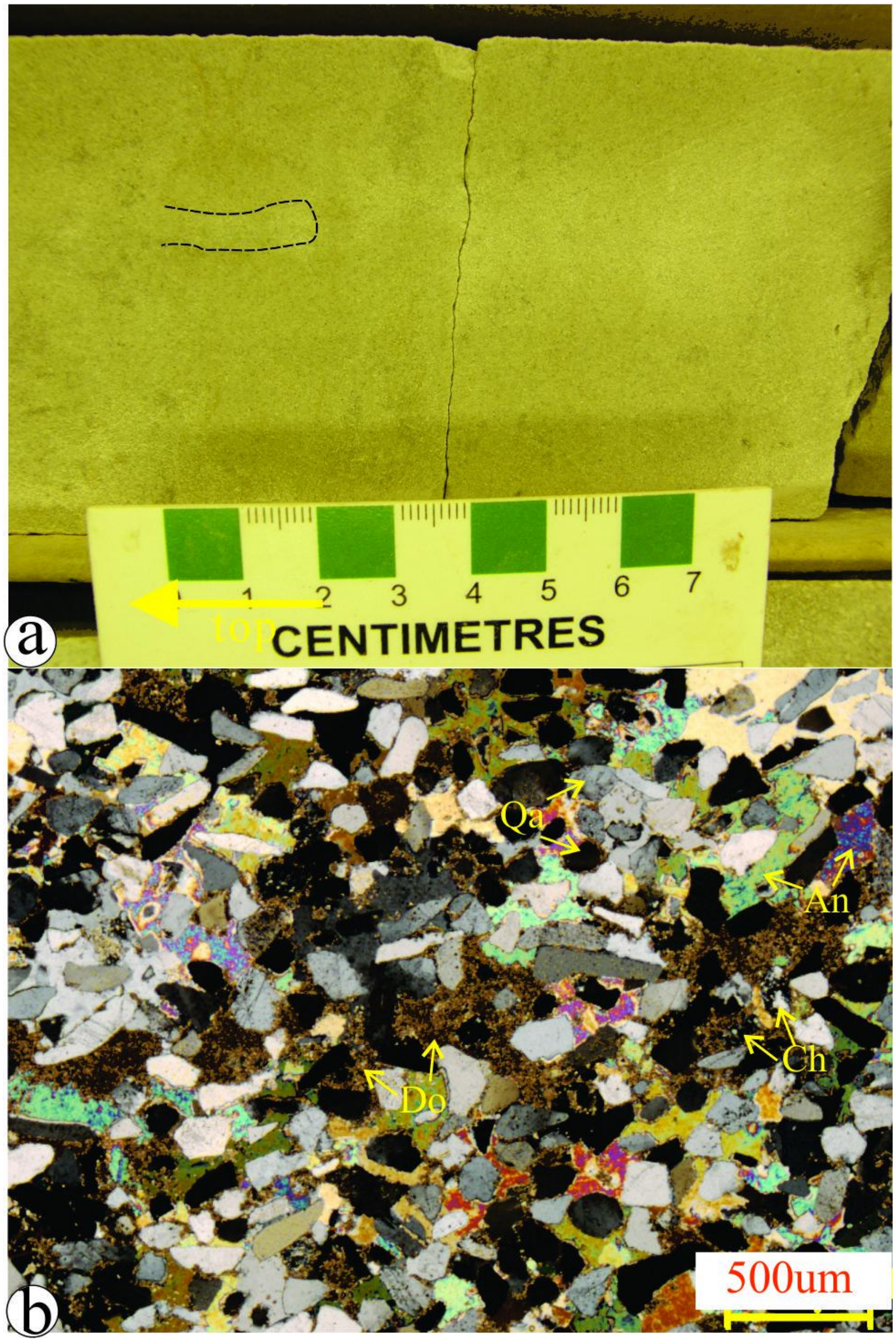

Figure 3.7 a) Core photograph of the sandstone lithofacies (SS) from the Kisbey interval. The unit contains vertical burrows (blake outline, possibly *pholadid burrow*). The photo is taken at 1194.5 m, 01/04-12-004-33W1; 96I248; b) Thin section photomicrograph of the SS facies showing fine to medium grained sandstone dominated by quartz (Qa) and chert (Ch) grains with fine crystalline dolomudstone matrix (Do). The rock is partially cemented by anhydrite (An). Photo is taken under X-polarized light. Kisbey interval, 1194.3 m, 01/04-12-004-33W1; 96I248.

3.2.5 Sandy dolomudstone lithofacies (SD)

Description: This lithofacies is dominated by massive, pale to dark grey sandy to silty dolomudstone that varies in thickness (0.01-4m). It has no visible sedimentary structures. This lithofacies is dense with no significant pore space. In most cases, the lower contact is gradational while the upper contact is sharp or erosional. Lithofacies SD is distributed within the Kisbey interval. It is interbedded with the dolomudstone, sandstone and all other types of limestone lithofacies.

Petrographic examination shows that the sandy dolomudstone lithofacies is composed of dolomicrite, with a minor amount of fine sand to silt size quartz grains (Figure 3.8). Dolomicrite crystals are anhedral. Quartz grains are subangular; they are similar to the grains within the sandstone (SS) lithofacies. The cement of this lithofacies consists of anhydrite and dolomite.

Interpretation: The detrital content of the dolomudstone lithofacies, its microcrystalline texture and relationship with the sandstone and dolomudstone lithofacies suggest a supratidal to upper intertidal mudflat depositional setting for this sandy dolomudstone lithofacies (Pratt, 2010; Carlson and Prospero, 1972; Windom, 1975).

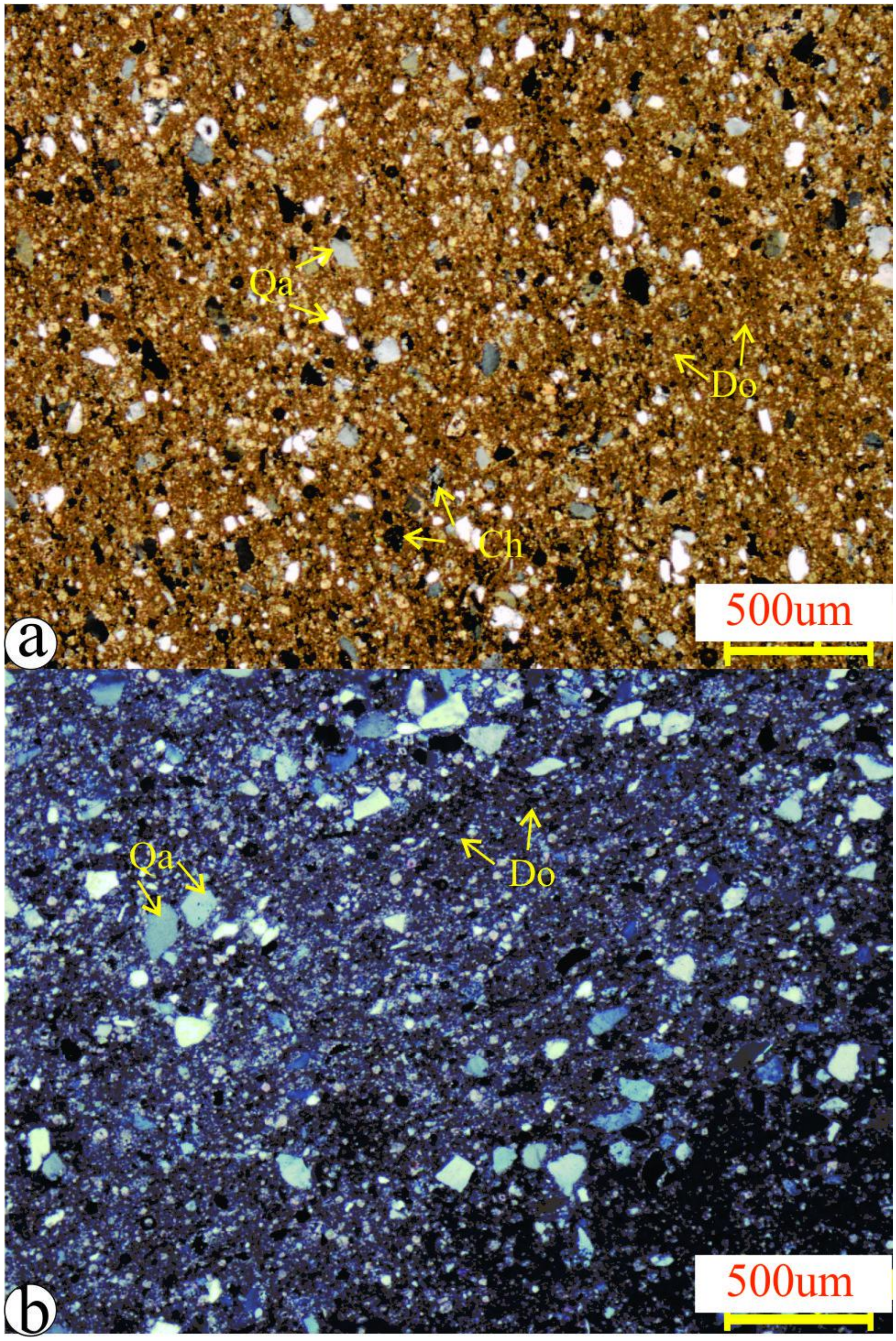

Figure 3.8 a) Photomicrograph of the sandy dolomudstone lithofacies with fine quartz grains (Qa), dolomicrite (Do) and cherts (Ch), Kisbey interval. Photo is taken under X-polarized light, 1183.4 m, well 01/04-12-004-33W1; 96I248; b) photomicrograph of sandy dolomudstone with fine quartz grains (Qa) and dolomicrite (Do). Photo is taken under X-polarized light. Kisbey interval, 1196.6 m, 01/04-12-004-33W1; 96I248.

3.2.6 Sandy packstone / grainstone lithofacies (SP)

Description: The packstone/grainstone facies is characterized by grey sandy packstone/grainstone units that vary in thickness (0.1-5.0m). Sedimentary structures include horizontal and cross lamination. This facies occurs in the Kisbey interval and is associated with the Kisbey sandstone lithofacies (SS) with a gradational to sharp contact.

Microscopic examination reveals that the most common framework grains are fine quartz, ooids and bioclasts (Figure 3.9a, b). The ooids and the bioclasts are partially micritized. The bioclasts include crinoids, brachiopods, bivalves, foraminifera, gastropods, bryozoans, and green algae. The sandy packstone / grainstone lithofacies typically consists an estimated amount of 15% fine quartz and 65% carbonate framework grains (ooids and bioclasts, Figure 3.9). The cements of this lithofacies are anhydrite, dolomite and some calcite.

Interpretation: The lithofacies SP is a sandy version of the packstone to grainstone / rudstone (PG) lithofacies. It is interpreted to represent a high energy, normal marine subtidal depositional environment, possibly well-associated with the subtidal channels that brought sandy components from the shallower, landward portion of the channels and linked to the sandstone lithofacies.

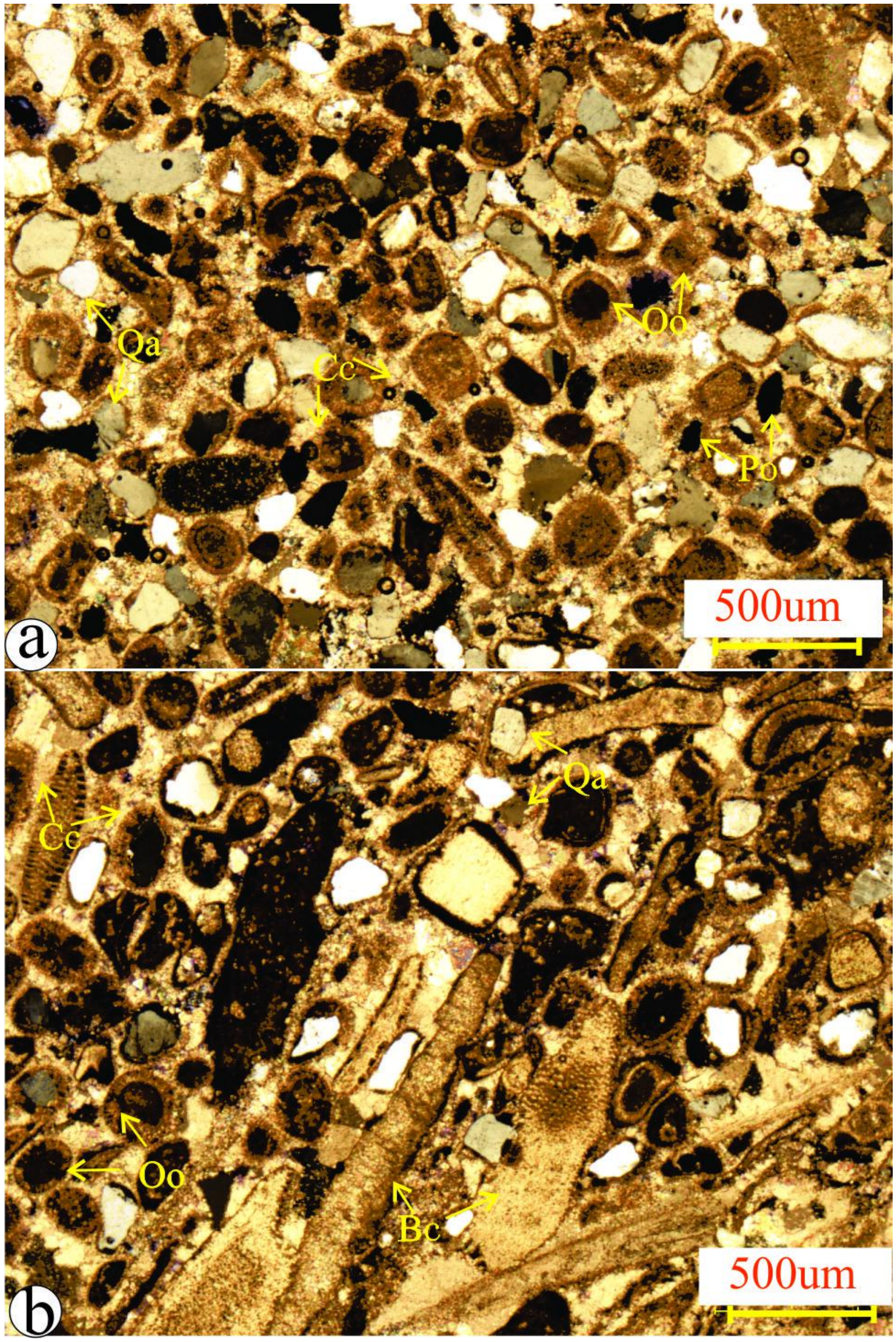

Figure 3.9 a) Photomicrograph of sandy oolitic grainstone with quartz grains (Qa), ooids (Oo) calcite cement (Cc) and pore spaces (Po), Photo is taken under X-polarized light. Kisbey interval, 1198.8 m, 01/13-13-008-06W2; 87I040; b) photomicrograph of sandy bioclastic grainstone with quartz grains (Qa), bioclasts (Bc), ooids (Oo) and calcite cement (Cc). Photo is taken under X-polarized light. Kisbey interval, 1197.1 m, 01/13-13-008-06W2; 87I040.

3.2.7 Anhydrite lithofacies (AH)

Description: This lithofacies is present in Frobisher and Alida beds. In the Frobisher Beds, it consists of laminated to medium-bedded, reddish to whitish coloured anhydrite that does not show any internal structures except subordinate zones with nodular texture. It is locally interbedded with the dolomudstone (DS) lithofacies (Figure 3.10A). In the Alida Beds, lithofacies AH has been recognized from one well (01/16-10-005-32W1; 55C028, well 18 on Figure 1) and is characterized by massive, white-coloured anhydrite (Figure 3.10B). Like the anhydrite layers of the Frobisher beds, the anhydrite facies of the Alida Beds is also associated with the fine crystalline dolostone lithofacies (DS).

Interpretation: Anhydrite indicates deposition within an evaporitic environment (Kent, 1984; Waters and Sando, 1987). The anhydrite lithofacies is interpreted as a supratidal (sabkha) accumulation.

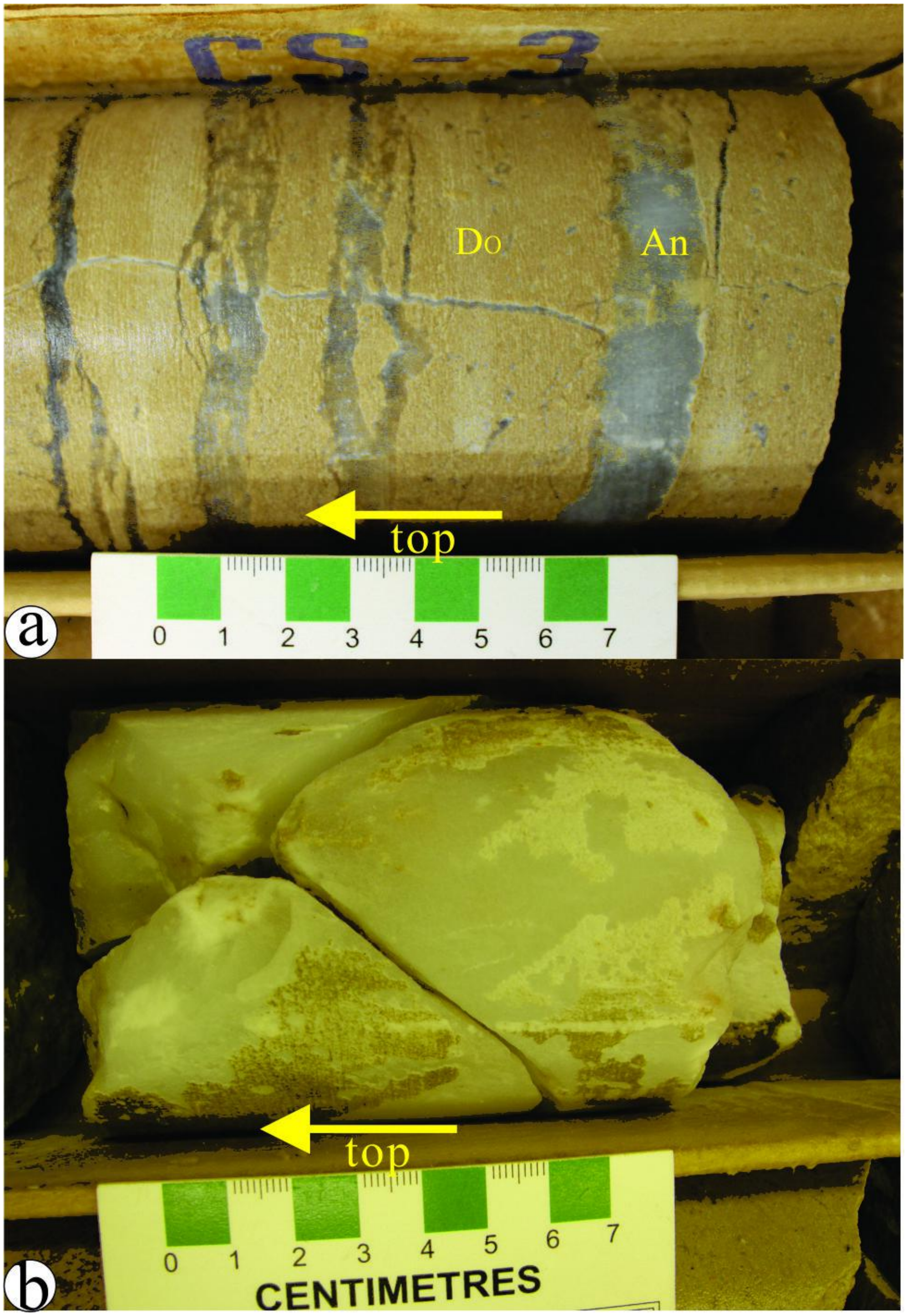

Figure 3.10 a) Interlayered dolomudstone (Do) and anhydrite (An). Frobisher Beds, 1075.5 m, 50/11-19-002-30W1; 72L015; b) massive anhydrite, Gainsborough Evaporite, Alida Beds. 1085.1m, well 01/16-10-005-32W1; 55C028.

3.3 Facies association

The eight lithofacies described above have been grouped into four lithofacies associations (LFA Ⅰ-Ⅳ), based on their lithology, inferred genetical relationship and interpreted depositional environments (Table 3.2).

Lithofacies association Ⅰ consists of packstone/grainstone, sandy packstone/grainstone and rudstone, and usually has a lower sharp to erosional contact with LFA Ⅲ and Ⅳ and upper gradational contact with LFA Ⅲ and Ⅳ. This type of lithofacies association represents high energy subtidal sand shoal and open marine deposition (Edie, 1958; Kent, 1984, Perras, 1990 and Rott and Qing, 2005; Ueon, et al, 2012),

Lithofacies association Ⅱ is composed of sandstone deposition, which usually has lower sharp to erosional contact and upper sharp contact with LFA Ⅳ. Lithofacies association Ⅱ was deposited in a moderate to high energy tidal channel environment (Campbell, 1967; Allen, 1982).

Table 3.2 Summary of facies association for the Mission Canyon Formation

Facies association	Lithofacies	Depositional Environment	Depositional Process
LFA Ⅰ	Packstone/grainstone	Normal marine subtidal sand shoal	High energy
	Sandy packstone/grainstone		
	Rudstone		
LFA Ⅱ	Sandstone	Tidal channel	Moderate to High energy
LFA Ⅲ	Mudstone/wackestone	Lagoon / tidal flat	Low energy
LFA Ⅳ	Dolomudstone	Restricted supratidal flat	Evaporitic
	Sandy dolomudstone		
	Anhydrite		

LFA Ⅲ is composed of mudstones/wackestones and is associated with lower gradational contact and upper sharp to erosional contact with a variety of carbonate lithofacies. This lithofacies association is interpreted as lower energy lagoonal to tidal flat deposition (Pratt, 2010; Howard, 2000; Rott and Qing, 2005).

Dolomudstone, sandy dolomudstone and anhydrite form lithofacies association Ⅳ. This lithofacies association is in contact with a variety of carbonate lithofacies and the lower contacts are commonly gradational. The upper contacts appear sharp to erosional with the carbonate lithofacies. It represents an evaporative tidal, flat environment (Pratt, 2010; Carlson and Prospero, 1972; Windom, 1975; Kent, 1984; Waters and Sando, 1987).

3.4 Depositional environments of the Mission Canyon Formation

3.4.1 Pre-Kisbey depositional system

During the pre-Kisbey deposition period, there is a relative rise in sea level and landward shift of the facies belt, detrital grains was disappeared in the study area. The open marine facies occupied a large area of southern Saskatchewan. The shoal belt (lithofacies packstone/grainstone & sandy packstone/grainstone) developed within the middle part of the study area, whereas the protected tidal flat and lagoon behind the shoal allowed the deposition of the partly dolomitized mudstone/wackestone lithofacies (mudstone/wackestone, sandy dolomudstone & dolomudstone). The supratidal evaporate environment was restricted to the northeast (anhydrite & dolomudstone, Figure 3.11).

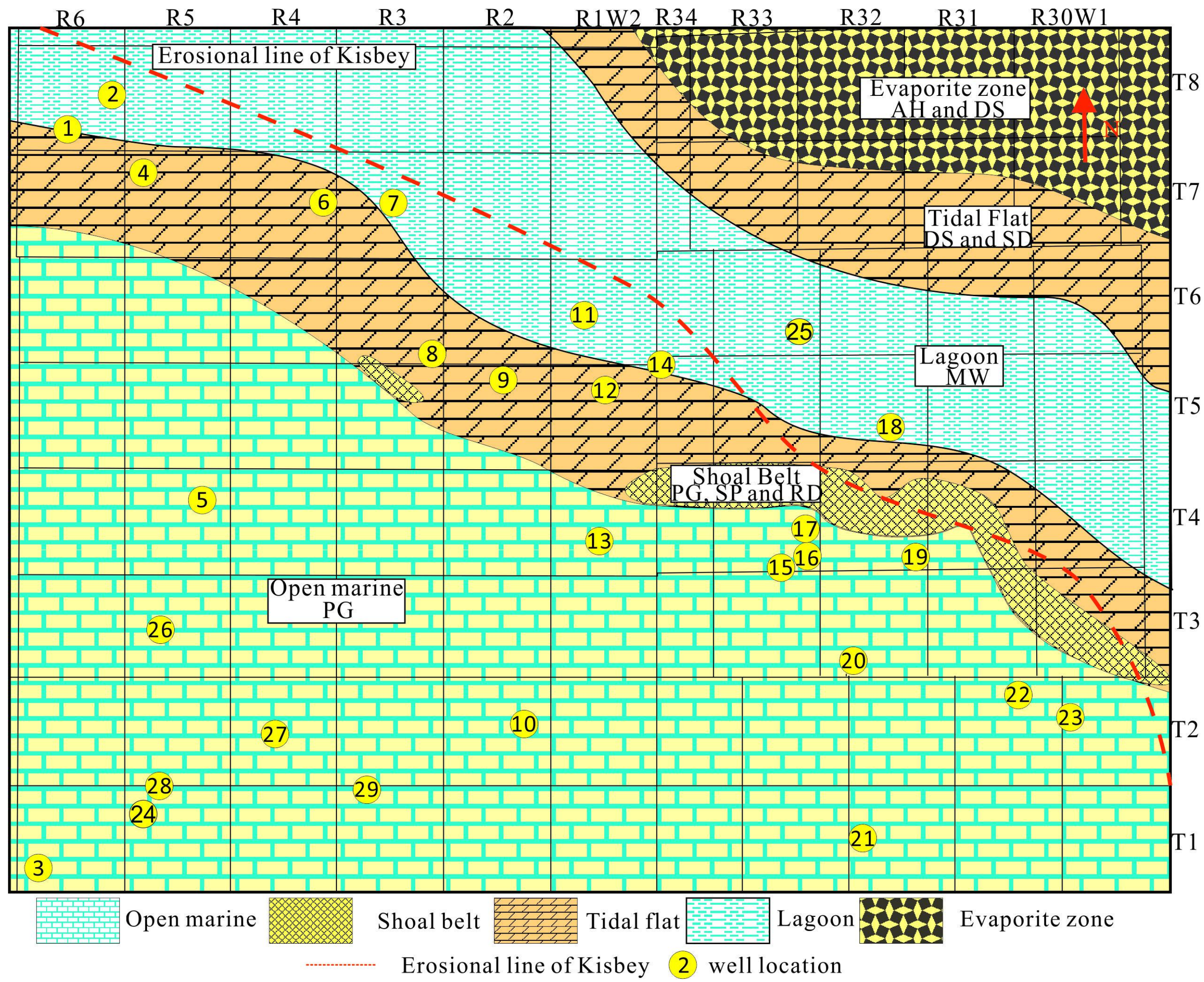

Figure 3.11 Interpreted facies distribution of the pre-Kisbey depositional system in southeast Saskatchewan.

3.4.2 Kisbey depositional system

The sedimentary facies distribution of the Kisbey depositional system is shown in the Figure 3.11. An open marine facies occupied a large area of southern Saskatchewan. The shoal belt (lithofacies packstone/grainstone & sandy packstone/grainstone) developed within the southeastern and middle part of study area. The protected tidal flat and lagoon behind the shoal allowed the deposition of the partly dolomitized mudstone/wackestone lithofacies (mudstone/wackestone, sandy dolomudstone & dolomudstone). The supratidal evaporate environment was restricted to the northeast (anhydrite & dolomudstone, Figure 3.11). During a relative drop in sea level and basin-ward shift of the facies belt, detrital grains were transported into the basin by river-fed tidal channels. Thus, tidal carbonate mudflat deposits and channel-confined sandstone bodies dominate the Kisbey Beds (SS). The sandstone units are laterally discontinuous and difficult to correlate from one section to another. However, correlation using well logs and lithologic comparison, along with data from previous work (Howard, 2000; Kent, 2007) indicates that the tidal channels were oriented NE-SW (Figure 3.12). The Kisbey regression was followed by a transgression, which pushed back the siliciclastic input and allowed reestablishment of the healthy carbonate platform.

3.4.3 Post-Kisbey depositional system

The post-Kisbey deposition system is similar to the pre-Kisbey depositional system (Figure 3.11); the open marine facies developed in a large area of southern Saskatchewan. The shoal belt occupied within the middle part of the study area, whereas the protected tidal flat and lagoon behind the shoal allowed the deposition of the partly dolomitized mudstone/wackestone lithofacies. The supratidal evaporate environment was restricted to the northeast.

In the studied area, the overall depositional setting is interpreted as a peritidal environment characterized by bioclastic and oolitic subtidal shoals (LFA Ⅰ) and associated lagoonal to tidal mudflat system (LFA Ⅲ, Ⅳ). The sandstone lithofacies of the Kisbey interval suggests a connection between tidal creeks in a carbonate-dominated platform and a fluvial system that brought clastic grains into the basin (LFA Ⅱ) (Figure 3.13). The temporal lithofacies arrangement of the studied stratigraphic interval shows clear vertically-stacked rhythmic units defined by shallowing-upward cycles of basal subtidal lithofacies (packstone/grainstone, sandy packstone/grainstone and sandstone) grading to restricted lagoonal/tidal mudflat deposits (mudstone/wackestone, dolomudstone, sandy dolomudstone and anhydrite).

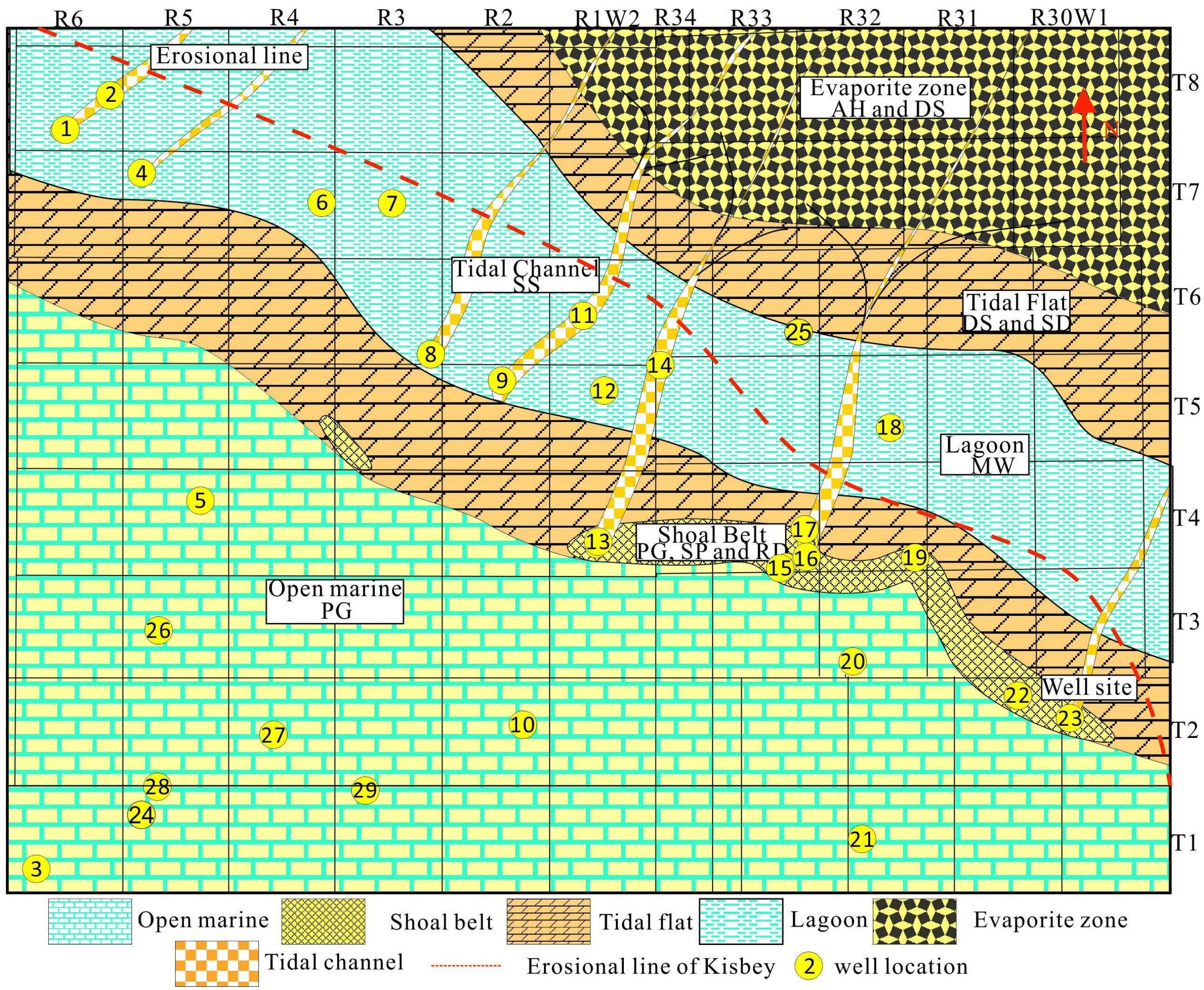

Figure 3.12 Interpreted facies distribution of the Kisbey depositional system in southeast Saskatchewan.

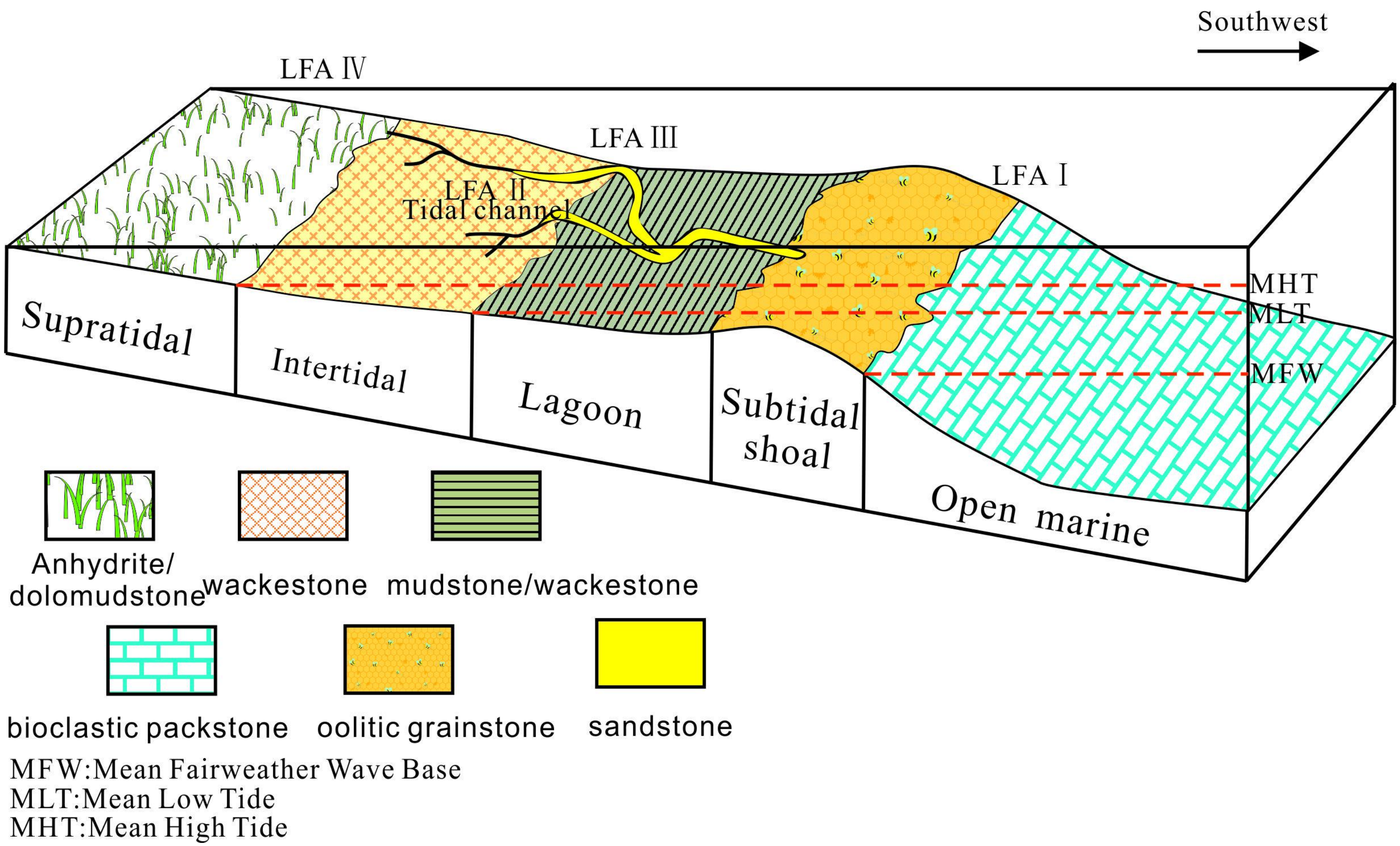

Figure 3.13 Facies model of Mississippian Mission Canyon Formation in the southeast Saskatchewan

3.5 Discussion of sand provenance

The simple mineralogy and limited data makes the provenance analyses of Kisbey sandstone complex and difficult. The possible sources are: older siliciclastic strata in the Williston Basin: Early Mississippian Bakken Formation sandstone, Late Ordovician Stonewall sandstone, Middle Ordovician Winnipeg sandstone, Deadwood sandstone, and Cambrian Precambrian sandstone, any of which may have been exposed at the basin margin during the Mississippian Period.

The sandstone of the Bakken Formation is dominated by siltstone and some fine sandstone, moderately well to well sorted, and has no luminescence when examined under cathodoluminescence. Most quartz grains are monocrystalline with very few polycrystalline grains; quartz overgrowths and orthoclase are common in the rock. Glauconite occurs sparsely in burrows. Rare syntaxial overgrowths of quartz are developed on quartz grains (Pitman, 2001). Bakken sandstone grains are generally finer than Kisbey sandstones (Table 3.3). The Kisbey sandstone grains also have some blue luminescence (Figure 3.14). For the most part, the Bakken Formation sandstone is not the source of Kisbey sandstone.

Stonewall, Winnipeg and Deadwood sandstone are similar to each other (Bitney,1983; McCartney, 1928). The quartz grain size is fine to medium, well rounded to sub-rounded, and only fine quartz grains (<0.1mm) have blue luminescence; frosting and pitting are common in coarse grain whereas the fine grains only show frosting. Pits are quite deep into the large grain and are triangular or roughly horse shoe shaped (Bitney, 1983; McCartney, 1928). The Kisbey sandstone has blue luminescence in large quartz grain (>0.2mm), so the Stonewall, Winnipeg and Deadwood sandstones are not considered as the provenance of Kisbey sandstone.

Precambrian sandstone is fine to medium grained, moderated sorted and well rounded. Some medium quartz grain has blue luminescence (1%) (Figure 3.15; Table 3), and pitting and quartz overgrowths are common. The Kisbey sandstone is finer than the Precambrian sandstone but shows similar blue luminescence, and therefore the Kisbey sandstone is probably sourced from Precambrian sandstone.

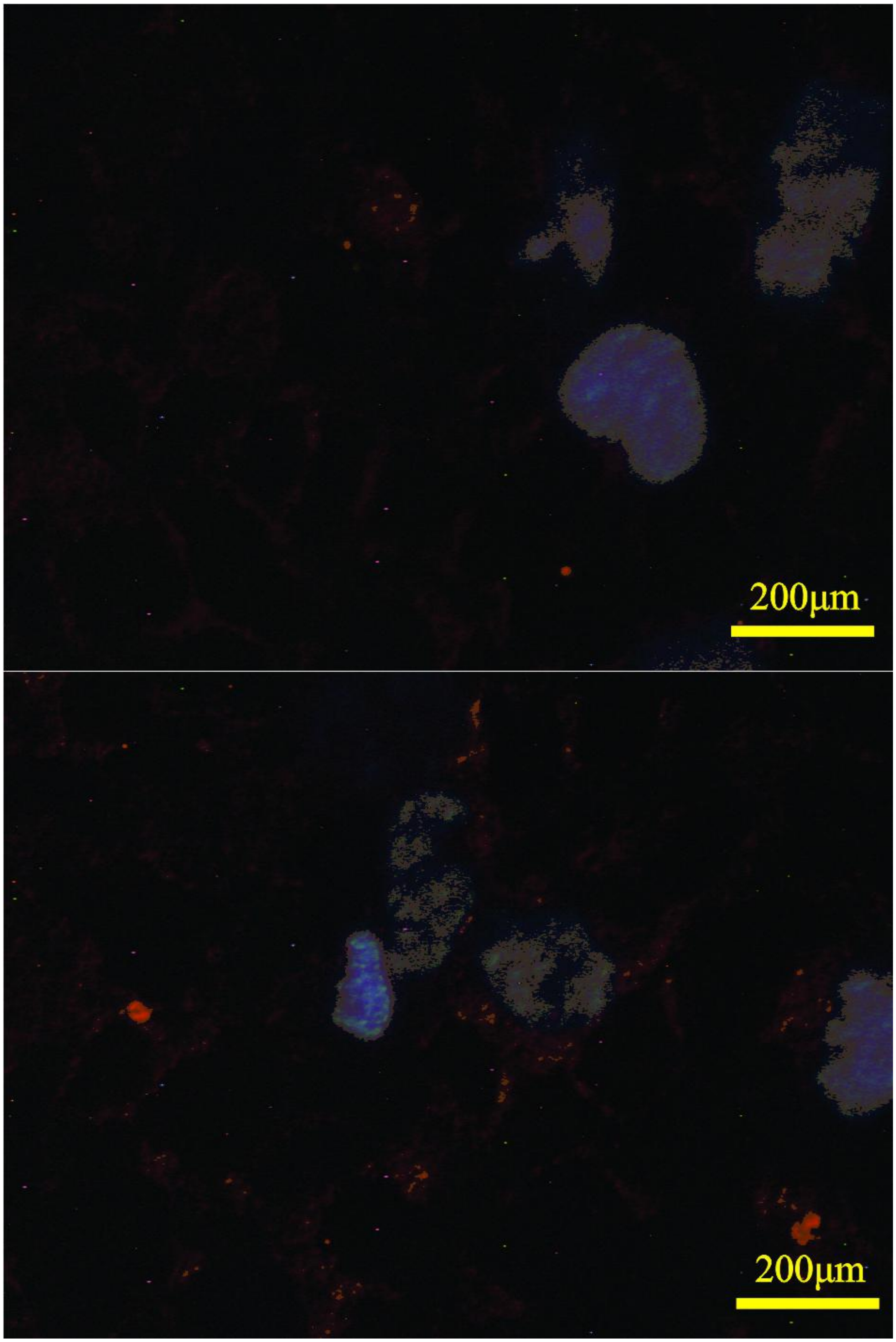

Figure 3.14 Photomicrographs of Kisbey sandstone show blue luminescence in medium quartz grain, Photo is taken under cathodoluminescence. Kisbey interval, 01/14-02-009-07W2, 1204.3m.

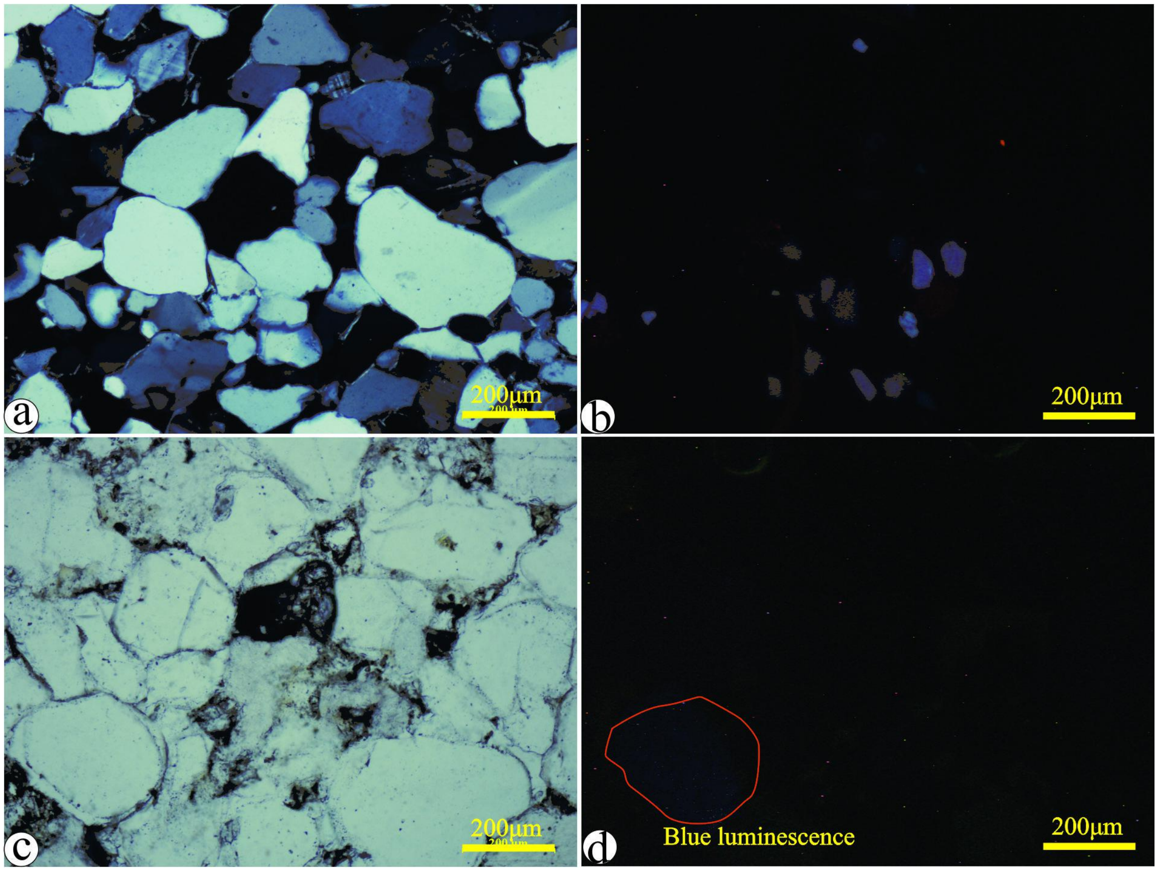

Figure 3.15 a) Photomicrograph of sandstone. Photo is taken under X-polarized light. Deadwood Formation, 1198.8 m, 31/15-32-47-17W2; b) Photomicrograph of Deadwood sandstone show blue luminescence in medium quartz grain, Photo is taken under cathodoluminescence light. Deadwood Formation, 1198.8 m, 31/15-32-47-17W2; c) Photomicrograph of sandstone, Photo is taken under plane polarized light. Precambrian; d) Photomicrograph of Precambrian sandstone show blue luminescent in medium quartz grain, Photo is taken under cathodoluminescent light.

Table 3.3 Summary of Precambrian, Deadwood, Winnipeg, Stonewall and Bakken sandstones characteristics

	Grain size	Sorting	Roundness	CL	Other Characteristic	Heavy mineral
Precambrian sandstone	Fine to medium	Moderate	Well rounded	Some medium quartz grain has blue luminescence	Pitting, monocrystalline, quartz overgrowth are common	Dominated by zircon; staurolite and tourmaline are present.
Deadwood sandstone	Fine to medium	Moderate	Well rounded to subrounded	Only fine quartz grains(<0.1mm) have blue luminescence	Clear, monocrystalline, some quartz overgrowth	No data
Winnipeg sandstone	Fine to medium	Moderate	Well rounded	Similar to Deadwood sandstone (Bitney,1983)	Frosting and pitting in large grain, the small grain just show frosting. Pits are quite deep into the large grain and are triangular or roughly horse shoe shaped.	Dominated by zircon; tourmaline and magnetite are common. Staurolite is present with rare rutile, garnet, and hornblende (McCartney, 1928).
Stonewall sandstone	Fine to medium	Moderate	Well rounded	Similar to Winnipeg sandstone	Similar to Winnipeg sandstone	Similar to Winnipeg sandstone (McCartney, 1928)
Bakken sandstone	Dominated by siltstone, some fine sandstone	Moderate to well sorted	Subangular to subrounded	No luminescence	Most quartz grains are monocrystalline with very few polycrystalline grains, quartz overgrowths, and orthoclase are common in the rock. Glauconite occurs sparsely in burrows. Rare syntaxial overgrowths of quartz are developed on quartz grains. (Pitman, et al., 2001)	Muscovite, biotite, rutile and zircon are found in fine grained units (Ferdous, 2001)
Kisbey sandstone	Silt to medium	Well sorted	Subangular to subrounded	Only some medium quartz grains have blue luminescence	Frosted and pitted, glauconite occurs sparsely. No quartz overgrowths appear.	No data

4.0 Cyclicity of Mississippian Mission Canyon Formation

4.1 Introduction

Carbonate cyclic sedimentation has been the theme of research by many sedimentologists (e.g., Read, et al, 1986; Goldhammer et al., 1990; Schwarzacher, 1999). It consists of repetitions of similar or comparable stratigraphic sections on different scales from millimeters to many hundreds of meters, representing shallowing-upward cycles bounded by marine flooding surfaces (Read, et al, 1986). Punctuated aggradational cycles (PACs) were applied to study episodic stratigraphic accumulation in the Manlius Formation of the Helderberg Group in New York State (Goodwin et al., 1986; Goodwin and Anderson, 1985). Mack and James (1986) analyzed the depositional system and origin of cyclic sedimentation in the Abo-Hueco transitional zone (Lower Permian) at Southwest New Mexico. Koerschner and Read (1989) combined field studies with computer modeling to study carbonate cycles in the Elbrook-Conococheague Formation of Middle to Upper Cambrian in the Appalachians and concluded that the aggraded shelves formed in response to Milankovitch sea level fluctuations. Goldhammer et al. (1990) used examples from Alpine Triassic platform carbonates to illustrate the link between cyclostratigraphy and sequence stratigraphy by understanding composite sea-level changes and the potential for a hierarchy of stratigraphic forcing.

The cyclicity of the Mission Canyon Formation had been studied by several researchers. Lake (1991) recognized two shallowing-upward cycles in the

Alida-Kisbey-Frobisher interval in southeast Saskatchewan. Harris et al (1996) identified six cycles within the same stratigraphic interval of the Mission Canyon Formation in north-central North Dakota. These six cycles include Bluell beds, Sherwood beds, Mohall beds, Glenburn beds, Wayne beds, and Landa beds.

In the study area of southeastern Saskatchewan, the Mission Canyon Formation preserves vertical rhythmicity defined by shallowing-upward cycles. These cyles are defined by basal normal marine subtidal rocks grading to restricted lagoonal/tidal flat deposits. Besides recognizing and describing the nature of this rhythmicity within the formation, this thesis also applies Fischer Plots technique to define the significance of the cycles in terms of sea level changes and to consequently interpret the vertical arrangement of the formation strata by using sequence stratigraphic interpretation.

4.2 Cycle types

The lithofacies and facies association analyses of the strata of the Mission Canyon Formation allow recognition of shallow-marine 62 cycles in this study. These cycles are commonly subtidal limestone lithofacies grading up into intertidal/supratidal carbonates. Based on the dominant lithologic changes in the cycles, three types of shallowing-upward cycles are recognized (Table 4.1).

A) packstone/grainstone to wackestone/mudstone (dolomudstone) cycle: have a base of subtidal packstone to grainstone grading into intertidal to supratidal wackestone / mudstone.

B) wackestone to mudstone (dolomudstone) cycle: the lower part is intertidal wackestone grading up into supratidal mudstone (dolomudstone).

C) packstone/grainstone - wackestone - mudstone (dolomudstone) cycle: the lower subtidal packstone/grainstone grading up into intertidal wackestone and the supratidal mudstone on the top.

These three types of cycles usually have lower sharp to erosional and upper sharp to erosional contacts. The overall depositional setting of Mission Canyon Formation is interpreted as a peritidal environment characterized by carbonate subtidal sand shoals with landward lagoonal to tidal mudflat system (Ji and Salad Hersi, 2013; 2014). The recognized cycles can be divided into thicker, well developed and thinner cycles. Their difference is mainly due to differences in available accommodation spaces. The thicker cycles include subtidal through intertidal to supratidal lithofacies and represent cycles that define higher (deeper) accommodation spaces. The shorter cycles include intertidal to supratidal carbonate lithofacies and represent relatively shallower accommodation spaces. Further details of the subtidal, intertidal and supratidal lithofacies that build-up the three types of cycles are as follows:

Table 4.1 Three types of cycles that constitute the Mission Canyon Formation in Southeastern Saskatchewan

Cycle types	Lithology	Contact	Interpretation
A) 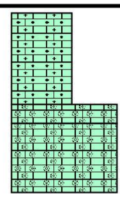	Mudstone (dolomudstone)/ wackestone Bioclastic / oolitic packstone / grainstone	Upper sharp or erosion Gradational contact Lower sharp or erosion	Intertidal/ Supratidal Subtidal
B) 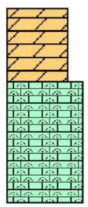	Mudstone (dolomudstone) Bioclastic /oolitic wackestone	Upper sharp or erosion Gradational contact Lower sharp or erosion	Supratidal Intertidal
C) 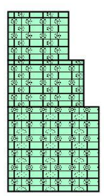	Mudstone(dolomustone) Bioclastic / oolitic wackestone Bioclastic / oolitic packstone / grainstone	Upper sharp or erosion Gradational contact Lower sharp or erosion	Supratidal Intertidal Subtidal

4.2.1 Subtidal deposition

The subtidal lithofacies is composed of packstone/grainstone, sandy packstone/grainstone and rudstone lithologies (Figure 4.1). Sedimentary structures in the subtidal deposits include a fenestral fabric (birdseye) structure, horizontal lamination and microbial laminations (Figure 4.1). The subtidal deposits occur throughout Tilston, Alida, Kisbey and Frobisher intervals. It generally has a lower sharp or erosion contact, commonly over the supratidal sediments of the underlying cycle, and upper gradational contact with intertidal or supratidal deposits.

4.2.2 Intertidal deposition

The intertidal deposition is represented by mudstone to wackestone deposition (Figure 4.2). Microbial laminations, fenestral (birdseye) structure, desiccation cracks and some horizontal laminations are present in the lithofacies of the intertidal deposition. In some cases, the upper part contains few intraclasts that are most likely eroded from the lower unit. The intertidal deposits are distributed through Tilston, Alida, Kisbey and Frobisher intervals. They are associated with a gradational to sharp contact with the lower subtidal units when they occur within a complete cycle of subtidal-intertidal-supratidal, and sharp to erosional contact with lower supratidal contact when they form the basal part of a cycle.

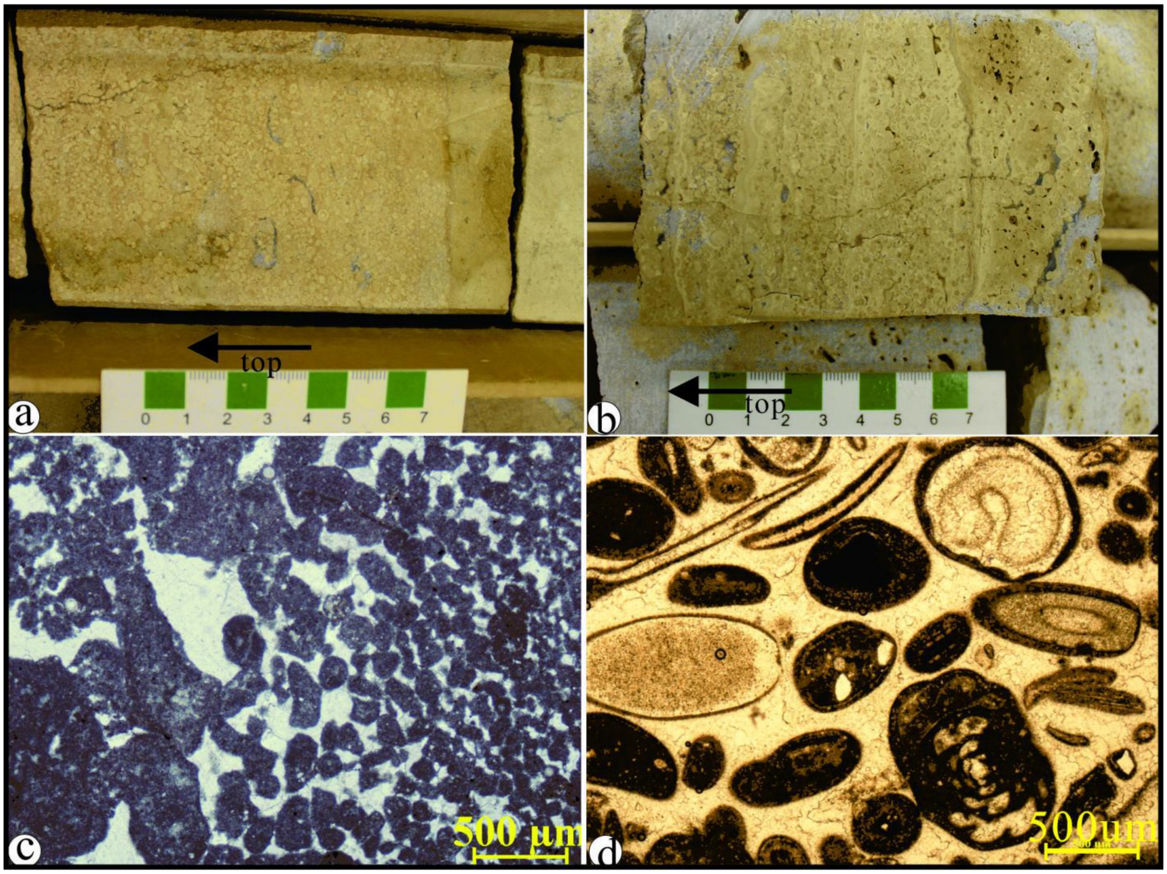

Figure 4.1 a) Core photograph of subtidal oolitic gainstone showing well develop ooid, calcite cement and lower sharp contact with mudstone, 1164.3m, well 41/09-33-005-34W1, 87K208; b) Core photograph of subtidal oolitic gainstone showing microbial lamination and birdseye structure, aggregate, oolite and dolomite cement, 1093.5m, well 01/08-01-004-32W1; 67F004; c) photomicrograph of peloidal grainstone showing peloid grain, intraclasts, dolomite cement, and fenestrate structure, X-polarized light, 1348.7m, well 01/11-28-2-1W2, 58E003; d) Photomicrograph of bioclastic grainstone, some quartz grain, foraminifera, ooid and calcite cement, 1% porosity, single polarized light, 1195.5m, well 01/13-13-008-06W2, 87I040.

Figure 4.2 a) Core photograph of intertidal oolitic wackestone showing birdseye structure, oncoids, ooids, anhydrite filling in the pores in a lime matrix. The uppermost part of photo (a) shows a sharp contact between the darker (upper) unit and the lower (lighter) unit. There seems to be a poorly-developed desiccation crack and the upper part contains few light-colored grains that are most likely eroded from the lower lighter unit. 1155.2m, well 41/09-33-005-34W1; 87K208; b) Core photograph of intertidal oolitic wackestone showing fenestral structure, ooids in a lime matrix, 1838.4m, well 01/03-08-001-06W2; 57D025.

4.2.3 Supratidal

The mudstone, dolomudstone, sandy dolomudstone and anhydrite lithofacies of Mission Canyon Formation form the supratidal deposits of the cycles. Sedimentary structures include fenestral (birdseye) structure, mudcracks and microbial laminations, and domal stromatolites (Figure 4.3). In most cases, the contact with the underlying intertidal/subtidal is gradational and has an upper sharp to erosional contact with the commonly overlying subtidal or intertidal lithofacies of the succeeding cycle.

4.3 Fischer Plot

Fischer plots are a graphical method to define accommodation changes (sea level plus tectonic subsidence) and depositional sequences, on cyclic shallow-marine carbonate strata, by graphing cumulative departure from mean cycle thickness as a function of time. They were proposed by Fischer in 1964 to analyze carbonate cycles by studying the Lofer cyclothems of the Alpine Triassic strata and suggested that there are three megacycles in the Lofer cyclothems caused by subsidence rate change; the horizontal axis was used to represent time and the vertical axis as vertical movements. Goldhammer et al. (1987) revived this type of stratal cyclic analysis to document eustatic fluctuations in sea level within the Milankovitch range of 20 to 100 ka. Read and Goldhammer (1988) used Fischer Plots to define third order sea level curves in Ordovician pertidal cyclic carbonate rocks of the Appalachian Mountains. Sadler et al. (1993) reviewed the use of Fischer Plots and suggested that the vertical axis should be labeled as cumulative departure from mean cycle thickness and the horizontal axis should represent cycle number, to avoid the problem of the poor absolute time control on the

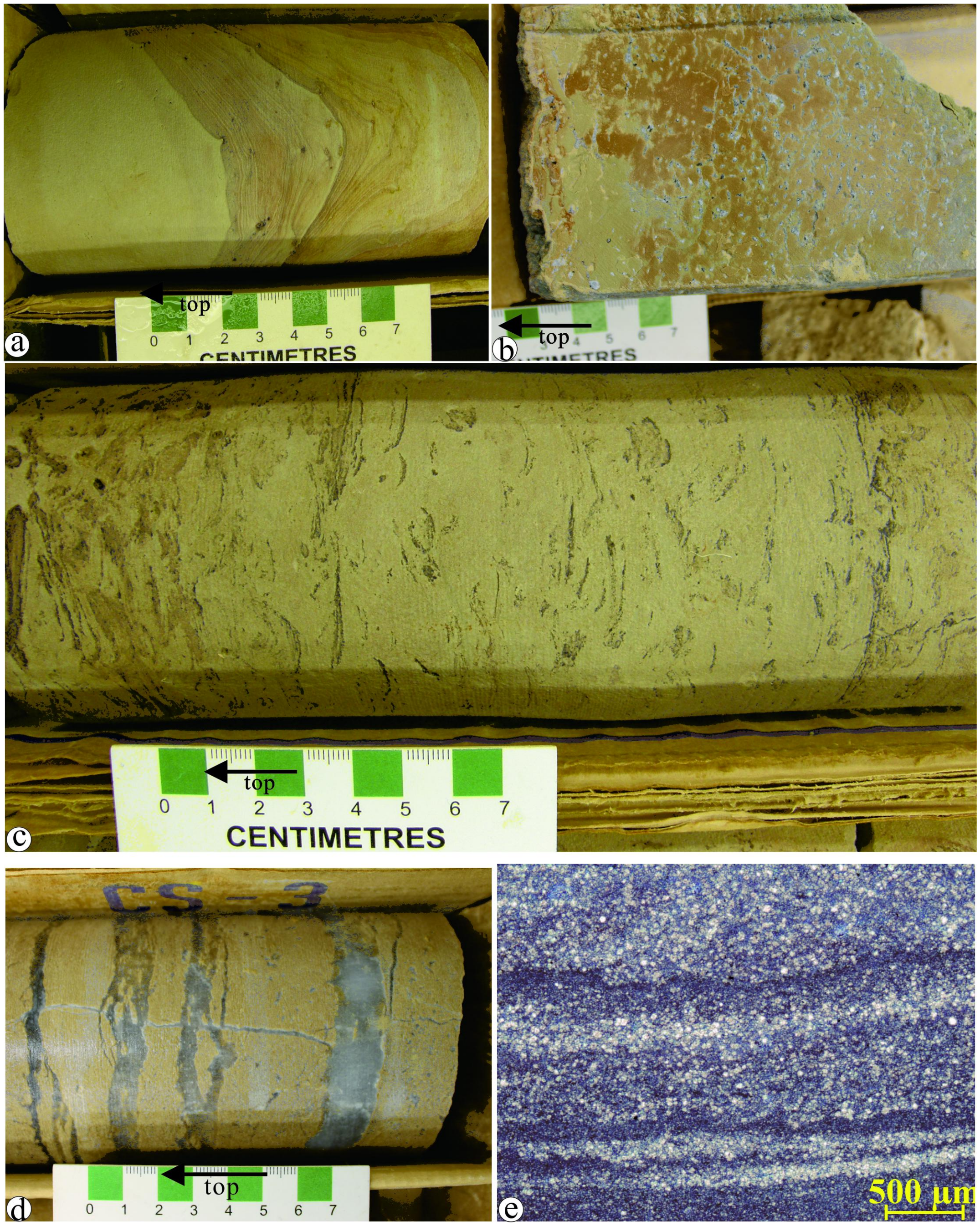

Figure 4.3 a) Core photograph of dolomudstone showing massive dolomite and stromatolite lamination, 1020.0m, well 01/06-01-006-03W2; 62L012; b) Core photograph of dolomudstone showing massive dolomite and birds eye structure, 11165.6m, well 41/09-33-005-34W1; 87K208; c) Core photograph of dolomudstone showing massive dolomite and mudcrack, 1234.6m, well 01/04-09-008-06W2; 67B002; d) Core photograph of dolomudstone showing wispy laminations, 1438.1m, well 01/03-26-004-05W2; 55J092; e) photomicrograph of dolomudstone showing horizontal lamination, more fine crystal dolomite in light lamination, X-polarized light, 1281.7m, well 01/15-34-2-34W1; 00D231.

stratigraphic record (Figure 4.4). Sadler et al. (1993) have also demonstrated that Fischer Plot for peritidal carbonates is more likely to be non-random fluctuations. The horizontal axis is used to represent time, whereas the vertical axis is used to plot cumulative departure from mean cycle thickness. Each cycle had a uniform time period, the individual cyclothems are evenly spaced along it. As the Fischer Plot is based on the mean cycle thickness, it should begin and end at zero elevation (Sadler et al., 1993; Figure 4.4).

Fischer plots illustrate deviations of individual cycle thickness from the average cycle thickness through stratigraphic successions (e.g. Fischer, 1964; Sadler *et al*., 1993; Martin-Chivelet et *al*., 2000). When systematic, cycle thickness deviations can be interpreted in terms of accommodation changes controlled by eustatic fluctuations (Read and Goldhammer, 1988; Montafiez and Osleger, 1993).

The metre-scale, shallowing-upward rhythmic units of the Mission Canyon Formation, is useful for deciphering the relative sea level changes during deposition of the strata. The data considered for the construction of the Fischer Plot cycles are based on the recognition and interpretation of meter-scale peritidal cycles that commonly grade from subtidal to supratidal depositional environments (Pratt, 2010). These shallow marine carbonates may contain erosional surfaces, and the erosional process may cause partial to complete removal of a cycle. Moreover, variations in cycle thicknesses may occur due differences in shelf paleotopography and rate of local carbonate production. Differential compaction may also occur during burial. These differences could result in variations in the number and thicknesses of the cycles within a study area. Therefore, it is very important that one considers these potential pitfalls during data collection and

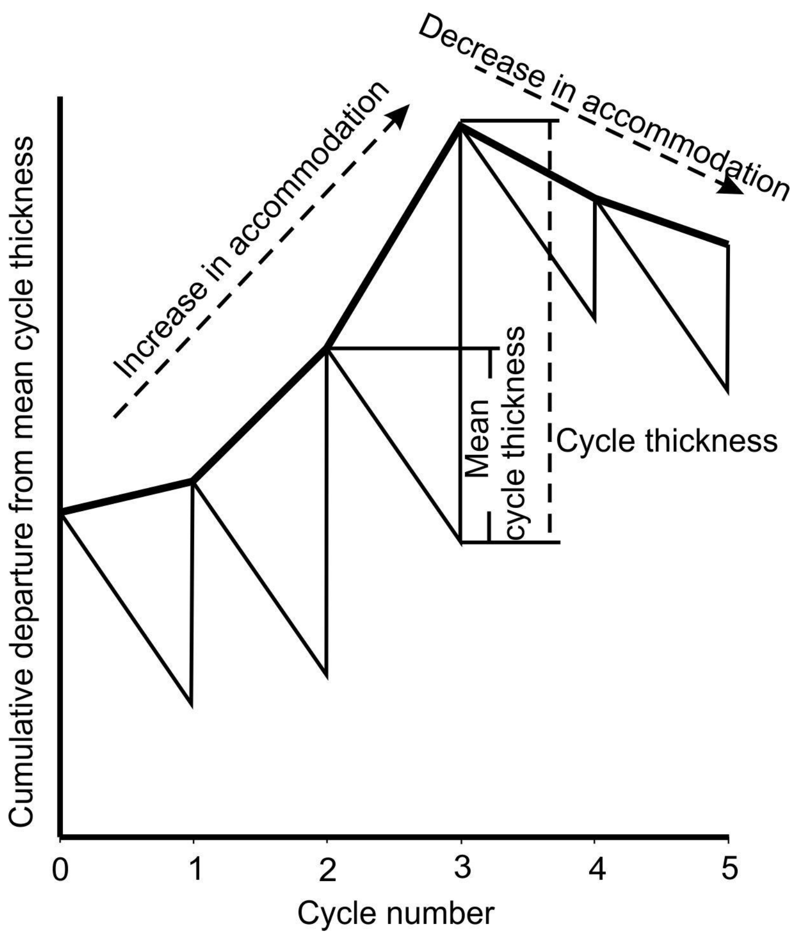

Figure 4.4 Fischer Plot (modified from Sadler et al., 1993).

construction of Fischer Plots.

In order to minimize the effects of the above mentioned potential pitfalls, this study has put emphasis on recognizing and selecting the sections that contain (i) highest number of cycles in each of the four stratigraphic units (i.e, Tilston, Alida, Kisbey and Frobisher), (ii) least erosional surfaces that may indicate significant cycle thickness reductions, (iii) best correlation with the other sections by using lithofacies succession, wireline log analysis, recognition of marker beds and thickness comparison. Besides that, in order to reduce the inherent pitfalls of the Fischer Plot, two different approaches of constructing the curves were applied: 1) construction of the Fischer plot cycles for each of the four stratigraphic unit of the Mission Canyon Formation (each one referenced with its own average thickness and cycles), and 2) consideration of the formation, as a whole, and constructing Fischer Plot cycles for the formation by using an average thickness for the 62 cycles that constitute the formation.

In this study, six measured sections (Figure 1.1) have been chosen for correlation and cyclicity analysis of the Mission Canyon Formation: wells (A) 01/03-08-001-06W2, (B) 01/03-26-004-05W2, (C) 41/04-22-007-03W2, (D) 01/01-11-006-33W1, (E) 01/16-10-005-32W1, and (F) 01/12-29-001-05W2. Wells (A) 01/03-08-001-06W2 and (B) 01/03-26-004-05W2 plots span the Frobisher and Kisbey intervals; the well (C) 41/04-22-007-03W2 plot spans the upper part of Alida interval (it was eroded on the top of Alida interval); Well (D) 01/01-11-006-33W1 occupies the upper Tilston and lower Alida Beds. The well (E) 01/16-10-005-32W1 plot spans the Alida and Kisbey interval (it was eroded on the top). Well (F) 01/12-29-001-05W2 spans the lower Tilston Beds.

There are 34 meter scale cycles in the Frobisher, Kisbey and Alida intervals

(Figure 4.5). The Tilston Beds preserve 28 cycles (Figure 4.5). The cycle numbers were used to construct the plots. Cumulative departure from mean cycle thickness was plotted against cycle number. Mean cycle thickness is calculated by total thickness of strata divided by cycle numbers of each section. The mean cycle thickness of well A, B, C, D, E and F are 2.99m, 2.99m, 1.853m, 2.15m, 1.845m, and 1.62m (Figure 4.5).

These 62 shallowing-upward cycles of the Mission Canyon Formation were plotted using Fischer Plot (Fischer 1964; Read & Goldhammer, 1988). The plot allows grouping of the cycles into six longer range, possibly 3rd-order cycles of which one corresponds to the lower Tilston Beds, three to upper Tilston and Alida Beds, one to the top Alida and Kisbey interval and one to the Frobisher Beds (Figure 4.6). The amplitudes of these large scale order events were from 0 to 12m based on the Fischer Plots. The amplitudes of these relative sea level changes in Frobisher interval are larger than those in Tilston, Alida and Kisbey intervals (Figure 4.6). Periods of relative sea level rise are defined by higher amplitudes of the Milankovitch cycles and positive departure from the average thickness of the cycles (i.e., higher accommodation spaces) whereas periods of relative sea level drop are indicated by thinner cycles. The sandstone-dominated Kisbey interval formed during a descending stage (sea level dropping) of cycle #5 (Figure 4.6).

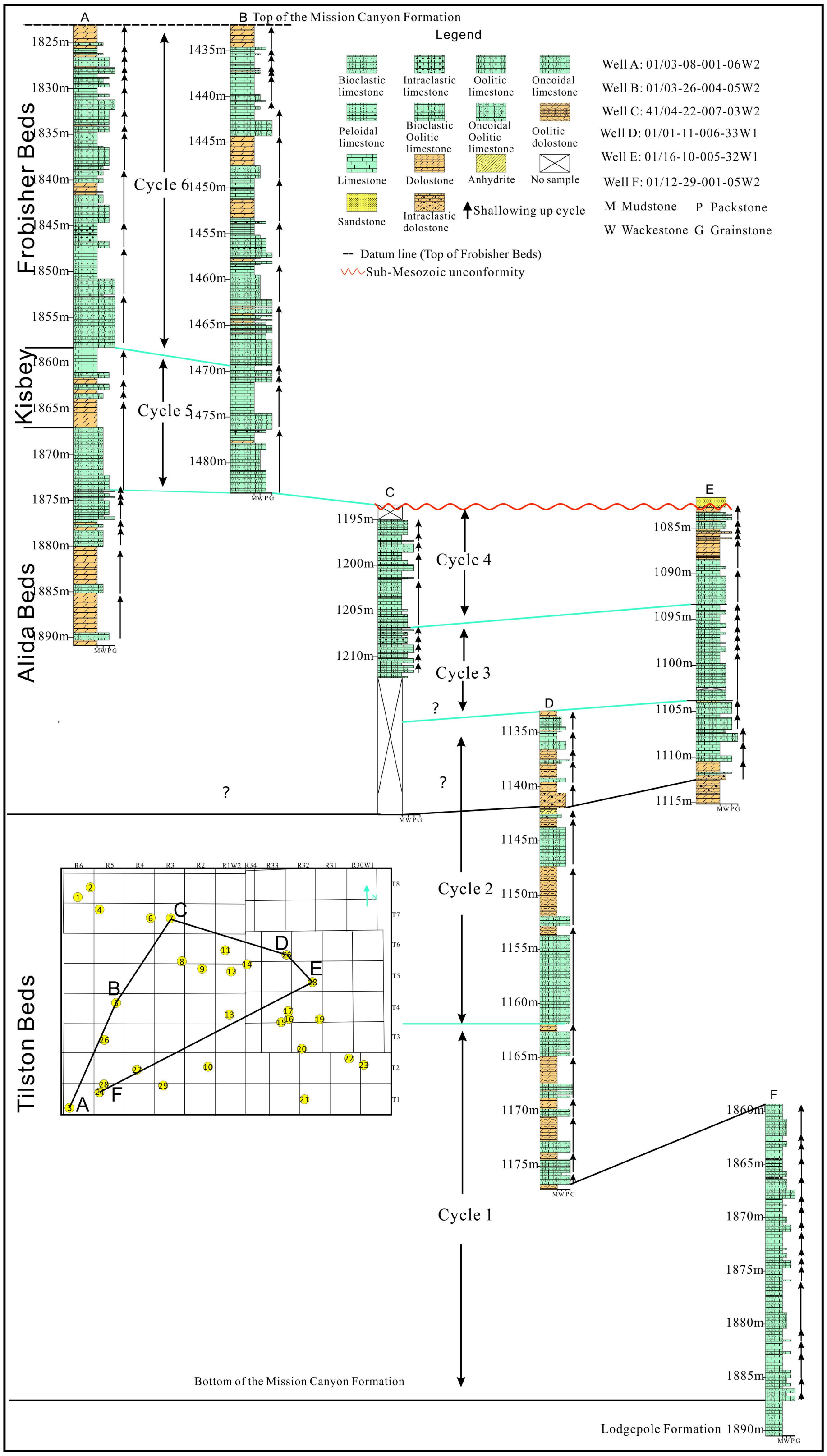

Figure 4.5 Cross section showing the cycles and correlation of the measure section in Mission Canyon Formation.

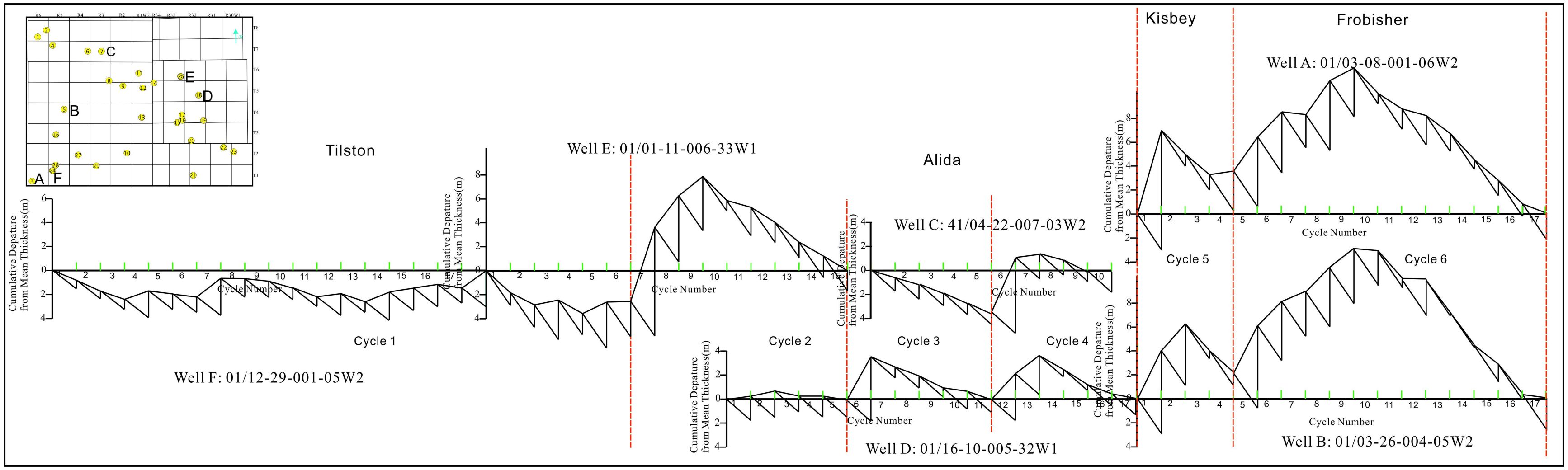

Figure 4.6 Fischer plots of the Mission Canyon Formation, from well 01/03-08-001-06W2, 01/03-26-004-05W2, 01/16-10-005-32W1, 41/04-22-007-03W2, well 01/01-11-006-33W1 and 01/12-29-001-05W2 in the southeast Saskatchewan; inset map shows location of measured sections. A = 01/03-08-001-06W2; B = 01/03-26-004-05W2; C = 01/16-10-005-32W1; D = 41/04-22-007-03W2; E=01/01-11-006-33W1; F=01/12-29-001-05W2. On Fischer plots, third order rises in sea level are indicated by rise in curve toward right; third order falls shown by fall in curve toward right.

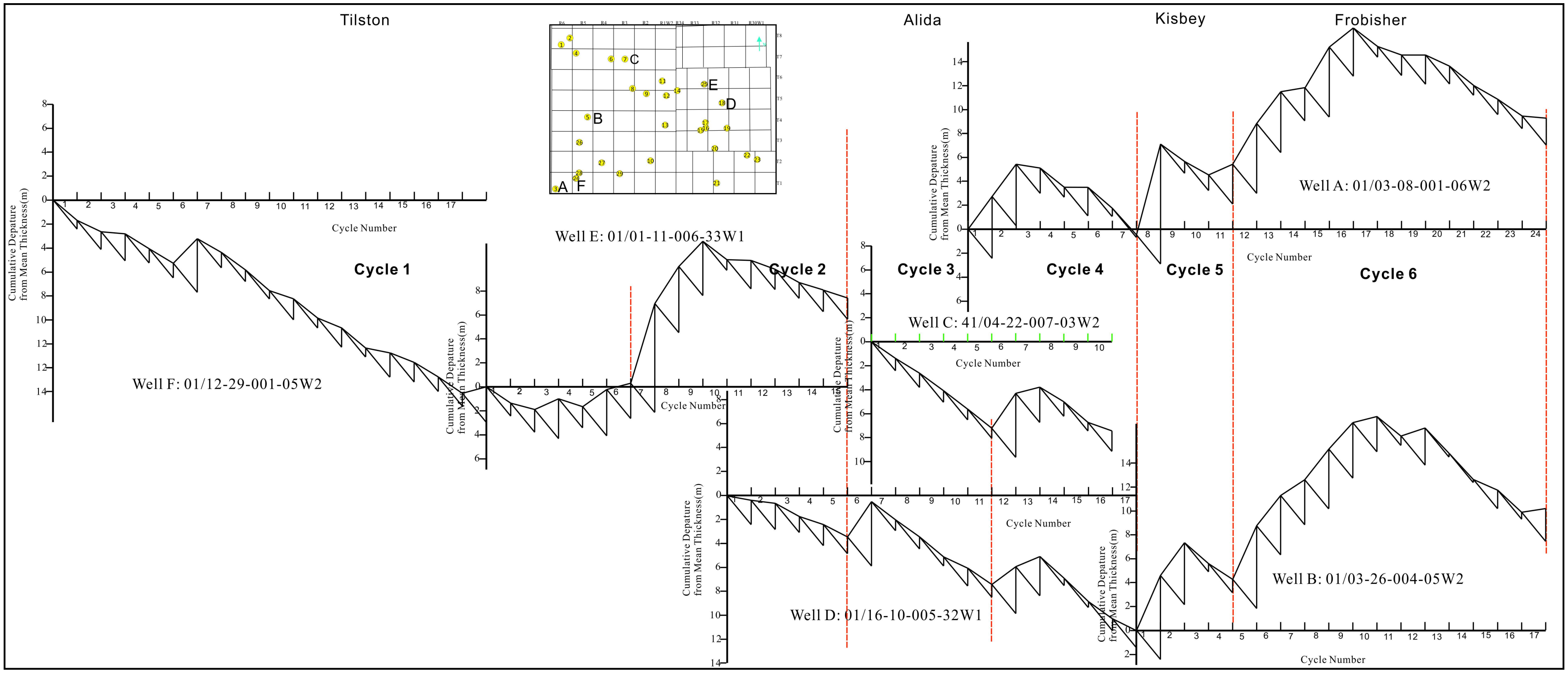

Figure 4.7 Fischer plots of the Mission Canyon Formation (average thickness of all measured interval), from well 01/03-08-001-06W2, 01/03-26-004-05W2, 01/16-10-005-32W1, 41/04-22-007-03W2, well 01/01-11-006-33W1 and 01/12-29-001-05W2 in the southeast Saskatchewan; inset map shows location of measured sections. A = 01/03-08-001-06W2; B = 01/03-26-004-05W2; C = 01/16-10-005-32W1; D = 41/04-22-007-03W2; E=01/01-11-006-33W1; F=01/12-29-001-05W2. On Fischer plots, third order rises in sea level are indicated by rise in curve toward right; third order falls shown by fall in curve toward right.

Another calculation of the mean cycle thickness was used to plot the graph (Figure 4.7). Mean cycle thickness is calculated by total thickness of the six measured sections divided by total cycle number. The plot also shows six megacycles, which corresponds to the previous one (Figure 4.7).

4.4 Discussion

There are four possible explanations for the relative sea level changes in the Fischer Plots: compaction difference, cycle duration changes, subsidence rate changes and eustatic sea level changes (Fischer, 1964; Sadler et al., 1993; Read and Goldhammer, 1988; Koerschner and Read, 1989). The Mission Canyon Formation typically lacks significant shale, and consists of dolomite or limestone throughout, which implys that they underwent relatively uniform compaction (Read and Goldhammer, 1988). If cycle thickness changes were only due to cycle duration changes, the curves would appear to be horizontal lines. In fact, the thick cycles appeared during long term rise which suggest the cycle durations were longer during the long term rise versus the fall. This is the opposite of what the modelling shows. As the comparatively short period of cycles relative to the total duration of plot, the using of average cycle period for the plot is valid (Koerschner and Read, 1989).

The Mission Canyon Formation and the Midale Beds of the Charles Formation were deposited during the Osagian Stage (334 to 351 Ma, Saskatchewan Ministry of Energy and Resources, 2011). During this time, the subsidence rate of the Williston Basin remained constant (Fowler and Nisbet, 1985, Figure 4.8) and therefore the accommodation space changes in the Fischer Plot were not caused by subsidence rate changes but can be envisaged as the result of eustatic changes. The Carboniferous Period is known for its glacial events prominent in the then southern hemisphere of the world. The Euramerican continent was located within the tropical to equatorial climatic zone where coal cyclothems and carbonate deposition was prominent (Stanley, 2009). The cyclothems were controlled by the glacio-eustatic changes (Figure 4.9). The six larger scale cycles identified from the Fischer plot of the studied stratigraphic interval are interpreted to have related to correlative third-order cyclothems recognized to form in the upper Tournaisian to lower Visean stages (Figure 4.9). These cyclothems range between 1.2 to 3.5 Ma, third order cycle ranges from 1 to 10 Ma (Boggs, Jr, 2006) and, thus define these cycles as third-order sea level fluctuations (Read and Goldhammer, 1988). The Kisbey interval was formed in the end of cycle 5, where fall from the previous highstand has major magnitude (Figure 4.9). During the largest sea level drop of all these six cycles, the detrital grain was transported into the basin and formed Kisbey interval.

The Fischer plots provide a valuable correlation tool that could prove useful in cyclic sequences of widely differing thicknesses of strata. As the Fischer plots are graphed against time, the positions of third-order sea level rise and drop provide a means of correlating between different sections.

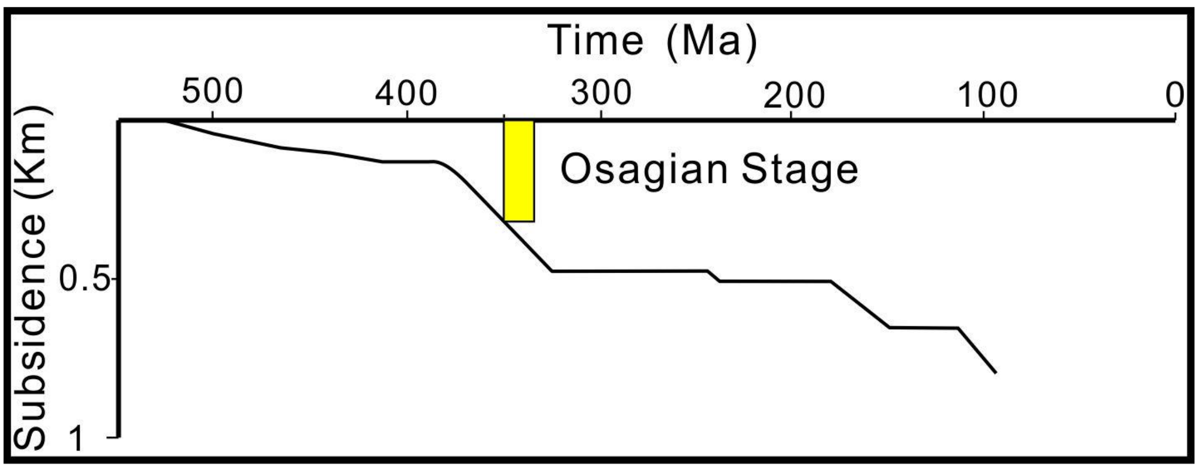

Figure 4.8 Figure shows subsidence after backstripping in the Williston Basin.
The Mission Canyon Formation (Osagian in age) was deposited during a period of constant subsidence rate suggesting that creation of accommodation space was due to eustatic changes (Modified after Fowler and Nisbet, 1985).

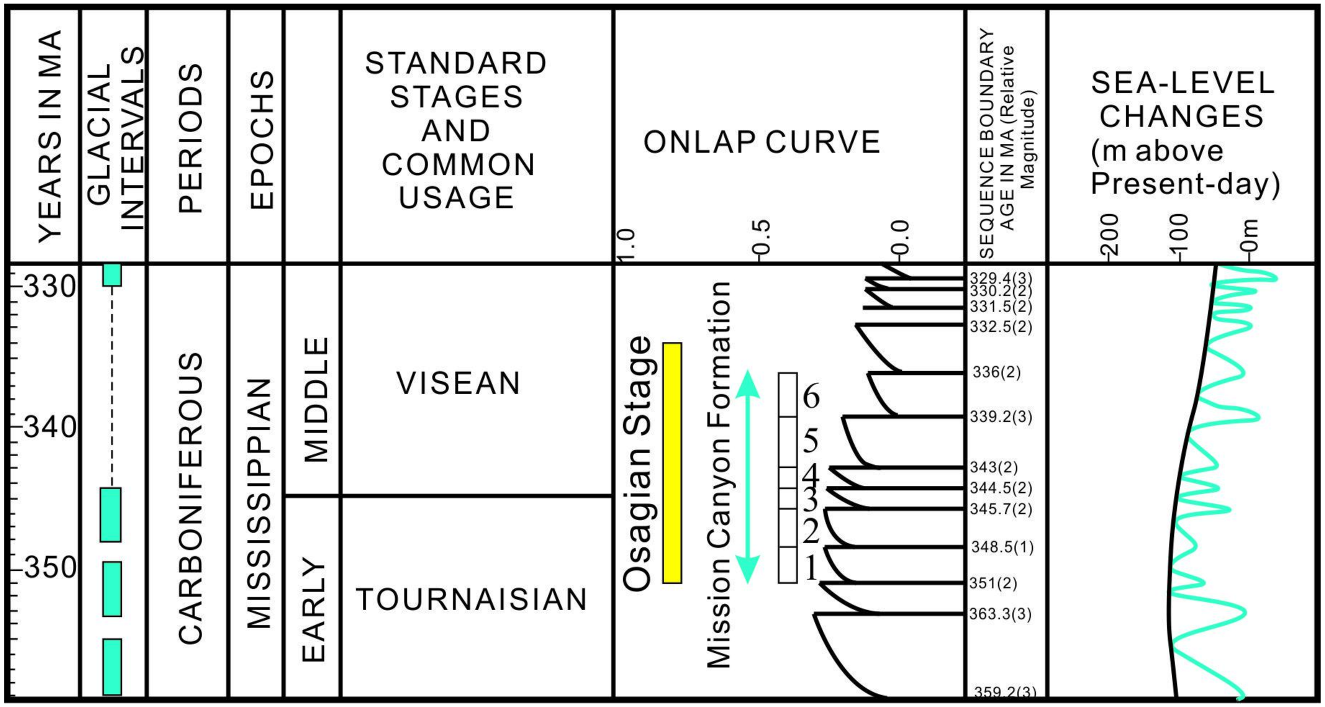

Figure 4.9 Early and Middle Mississippian sea-level changes, coastal onlap curves and periods of glaciation that caused the coal and carbonate cyclothems. Note the age range of the Mission Canyon Formation and the "bed" units that constitute it. The numbers 1 to 6 indicate the six cycles inferred from the stratigraphic interval studied in this project. Magnitude of fall from the previous highstand was classified as minor (1) <25m, medium (2) 25-75m, and major (3) >75m. Modified from Haq and Shutter, 2008. The yellow bar shows the Osagain time.

5.0 Diagenesis and Reservoir Characterization

5.1 Introduction

Several studies of the Mission Canyon Formation in the adjacent USA states have emphasized the occurrence of solution-collapse breccias and its effect on porosity, permeability and hydrocarbon production (Roberts, 1966; Sando, 1974, 1988; Gargallo-Quinones, 1985). Studies of the depositional and diagenetic history of this formation include Vice (1988, 1993), Vice and Utgaard (1989, 1996), Lindsay (1982), Lindsay and Kendall (1980), Lindsay and Roth (1982), Smith (1991), and Smith and Dorobek (1993a, 1993b). Vice et al., (2000) established a paragenetic sequence for the Mission Canyon Formation in South-Central Montana and Northern Wyoming. The diagenesis and porosity development within the Alida Beds in southeastern Saskatchewan was studied (Mundy and Roulsten, 1998; Rott and Qing, 2006; 2013). Despite a sizable number of studies addressing the lithologic, stratigraphic and diagenetic aspects of the Mission Canyon Formation in northern Williston Basin, more detailed and thorough work on the diagenetic evolution of the formation and reservoir characterization within the context of these diagenetic alterations is required. The present study intends to decipher the diagenetic features preserved in the various beds/intervals of the formation, their paragenetic sequence, diagenetic realms and their effects on the reservoir qualities of the various lithofacies of the formation.

5.2 Diagenetic features

The Mission Canyon Formation has been affected by a complex and extensive diagenetic evolution. The recognized diagenetic products are as follows: micritization and micrite envelope, different events of calcite cementation, dolomitization, anhydrite cementation, dissolution, compaction and fracturing (Ji and Salad Hersi, 2015a; 2015b).

5.2.1 Micritization and micrite envelope

Micritization and micrite envelope belong to the earliest changes to the framework grains of the Mission Canyon Formation (Figure 5.1; Figure 5.2). Partial to total micritization (Figure 5.1), as well as formation of a thin micrite cover on certain grains, e.g., skeletal grains (Figure 5.1b, c), have been observed and micritization takes place centripetally.

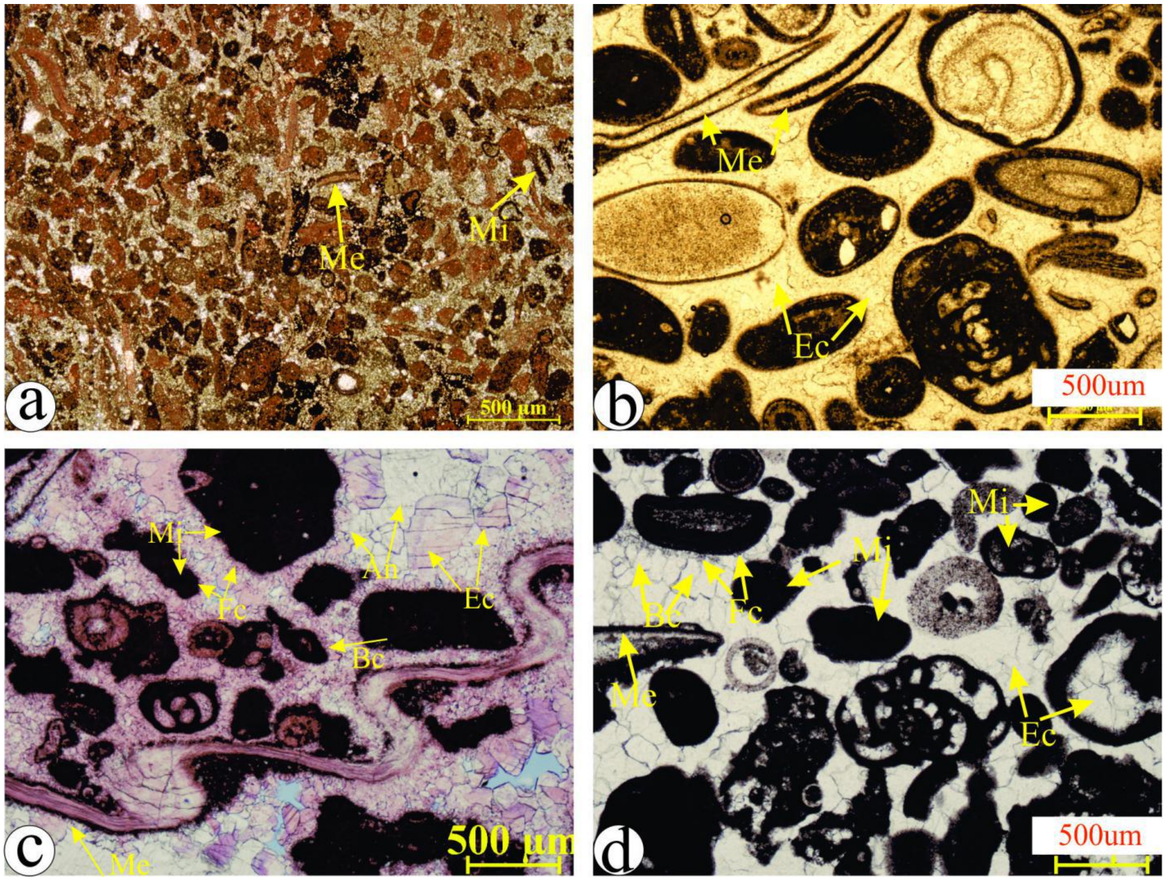

Figure 5.1 a) photomicrograph showing fine dolomite, micrite (Mi) and micrite envelope (Me). Alida Beds, 1270.4m, 01/05-20-001-32W1; 85K115; b) photomicrograph of oolitic bioclastic grainstone showing micrite envelope (Me) and equant calcite cement (Ec). Photo is taken under plane polarized light. Kisbey interval, 1195.5 m, 11/13-13-008-6W2; 87I040; c) photomicrograph showing fibrous calcite cement (Fc), blade calcite (Bc), equant calcite (Ec) and anhydrite (An); the thin section is stained with Alizarin Red. Photo is taken under single polarized light. Alida Beds, 1162.9 m, 01/16-04-005-33W1; 55C028; d) photomicrograph of bioclastic peloidal grainstone showing micrite (Mi), micrite envelope (Me), fibrous calcite cement (Fc), blade calcite cement (Bc) and equant calcite cement (Ec). Photo is taken under plane polarized light. Kisbey interval, 1191.0m, 01/04-12-004-33W1; 96I248.

Figure 5.2 Paragenetic sequence of the diagenetic features observed in the Mission Canyon Formation in southeastern Saskatchewan. The initial porosity of shallow marine carbonate sediment is about 40 percent (Enos and Sawatsky, 1979, 1981; Halley and Harris, 1979).

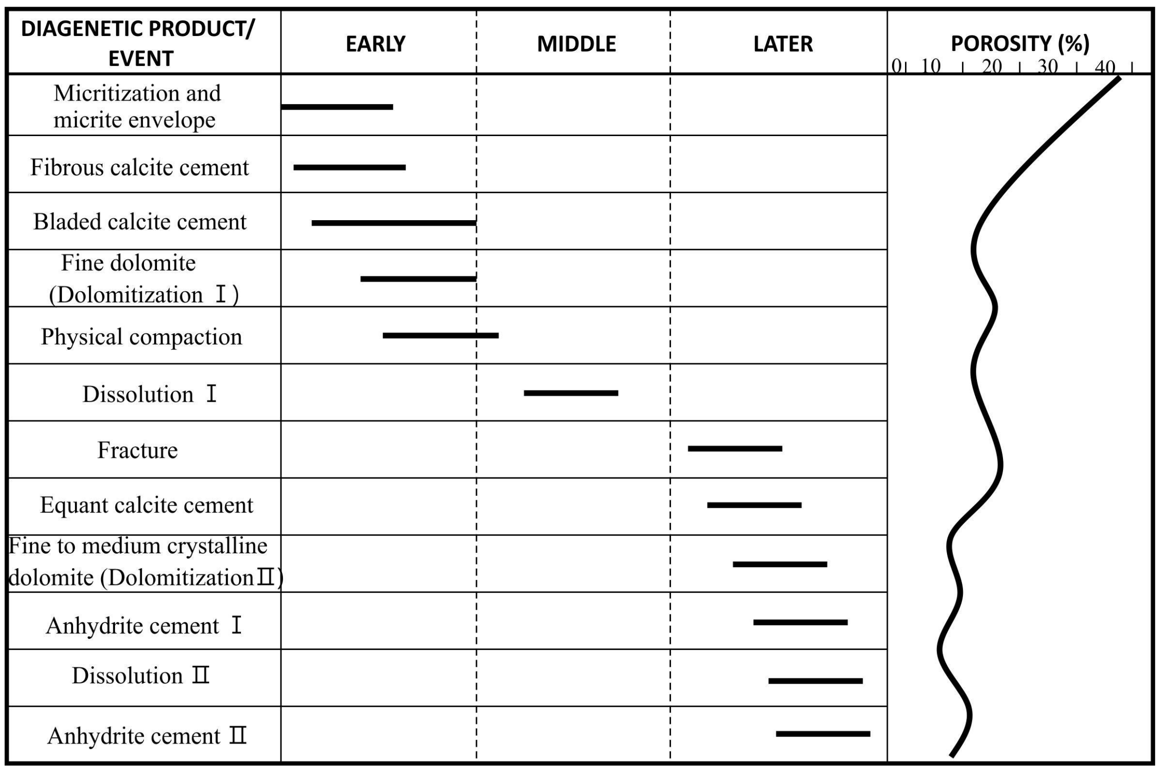

Micrite envelopes around the grains result from incomplete micritization (Bathurst, 1966), whereas completely micritized grains show no trace of original microstructure and may become rounded or subrounded to be called peloids (Swinchatt, 1965). The micritization and micrite envelope are diagenetic features that commonly form in the shallow marine phreatic zone (Longman, 1980, Tucker and Wright, 1990). They mainly develop in the bioclastic packstone to grainstone lithofacies which more often occur in the Kisbey interval and Alida Beds. The micritization and micrite envelopes are distributed across the study area. Production of micritic particles during micritization may have contributed to the overall matrix content at the depositional site and, therefore, reduced the original intergranular effective porosity of the sediments.

5.2.2 Calcite Cements

Calcite cements are the most common diagenetic products of the Mission Canyon Formation and contain three different types: isopachous fibrous calcite cement, bladed calcite cement and equant calcite cement (Figure 5.1c, d; Figure 5.2; Figure 5.3a). The isopachous fibrous calcite cement and bladed calcite cement appear as thin cement rims around the grains and occlude interparticle and intraparticle pore spaces. The crystal shape of the fibrous calcite cement is usually needle-like or columnar, and crystal size is micron-sized. The bladed calcite generally shows a gradual increase in width along their length. Both fibrous and bladed calcite cements are non-ferroan. The equant calcite is characterized by equant to elongate, anhedral to subhedral, non-ferroan crystals. The average crystal size is usually larger than 0.1mm. This cement occurs in primary (intergranular and intragranular) and secondary space. (Figure 5.1b, c, d; Figure 5.4a).

Fibrous calcite cement, which precipitated from marine water, represents an early-diagenetic feature (Tucker and Wright, 1990). The bladed calcite may indicate mixed marine and meteoric water (Folk, 1974; Tucker and Wright, 1990) whereas the equant calcite cement is interpreted as precipitates from meteoric phreatic water diagenetic realm (Folk, 1974; Flugel, 2004; James and Choquette, 1990; Tucker and Wright, 1990). The fibrous and bladed calcite cements are more common in the Kisbey interval and Alida Beds, while the equant calcite cement occurs in all intervals of the Mission Canyon Formation. The calcite cements are mainly distributed within the packstone to grainstone, sandy packstone to grainstone and rudstone lithofacies throughout the study area. The three types of calcite cements have filled the primary and secondary pore spaces and, therefore, reduce the primary effectiveness of the sediments and negatively effect the reservoir quality of the formation.

5.2.3 Dolomite cements

Dolomitization is an important diagenetic process in the Mission Canyon Formation. It includes two different types of dolomite cements: fine crystalline dolomite (dolomite event I, Figure 5.3a; Figure 5.2) and fine to medium crystalline replacive dolomite (dolomite event II, Figure 5.3b; Figure 5.2). The fine crystalline dolomite (dolomite event I) generally exhibits loosely packed, fine anhedral to subhedral crystals (Figure 5.3a). Dolomitization is commonly pervasive, obscuring most of the original textures and grains. However, outlines of bioclastic and peloidal fragments can still be observed in some samples. This dolomitization created intercrystalline microporosity and microvuggy porosity, potentially leading to an enhancement of the porosity and permeability. The second dolomite event (II) is a replacive dolomite characterized by fine to medium crystalline, subhedral to euhedral crystals (Figure 5.3b) that post-date compaction features (such as stylolites) and other diagenetic features (Figure 5.3). The replacive dolomite II tends to be fabric selective, commonly incomplete and preferentially replaces the micritic matrix rather than allochems and burrows. Intercrystalline porosity, genetically related to the dolomitization, is also well developed and associated with this dolomite II event. This dolomite also precipitates as cement that partially fills previously existing pore spaces (e.g., inter- and intra-granular pores). The degree of dolomitization ranges from rare floating dolomite rhombs to partial replacement of the micritc matrix, sometimes complete replacement of original rock constituents.

This fine crystalline dolomite (dolomite Ⅰ) is interpreted as the product of early, near-surface diagenetic process comparable to the penecontemporaneous dolomitization well documented in the literature (e.g., Landes, 1946; Friedman and Sanders, 1967; Butler, 1969; Hsu and Siegenthaler, 1969; Gregg and Sibley, 1984; Saller, 1984; Hardie, 1987; Moore, 1989; Tucker and Wright, 1990; Purser et al., 1994; Morrow, 1998; Flugel, 2004). The fine to medium euhedral dolomite (dolomite Ⅱ) is suggestive of formation at a shallow-medium burial environment (Sibley & Gregg, 1987; Amthor & Friedman, 1991). The two stages of dolomite are recognized in most of the carbonate lithofacies (including dolomudstone and lime mudstone to grainstone lithofacies) throughout the Mission Canyon Formation and study area. The dolomitization events have locally created porosity (Lavoie et al., 2005; Warren, 2000) and thus increased the overall reservoir quality of the various stratigraphic intervals they have affected.

5.2.4 Anhydrite cementation

Anhydrite cements are very common diagenetic products of the Mission Canyon Formation. It is commonly white in color in hand specimens. Anhydrite typically occurs as medium to coarse blocky or bladed crystal in thin sections (Figure 5.1, 5.3; Figure 5.2). There are two stages of anhydrite cement in the studied strata: coarse, blocky or bladed crystals that fill interparticle or intraparticle pores ((Figure 5.1c, d; Figure 5.3) and later stage medium blocky anhydrite crystals that fill in the vuggy porosity (Figure 5.3d) which is older than coarse anhydrite cement

The anhydrite cements are most common in the sandstones of the Kisbey interval and subordinate in the other units of the Mission Canyon Formation, and even more common along the erosional line. These cements destroy a good portion of the primary and secondary porosity, reducing the overall reservoir quality of the formation.

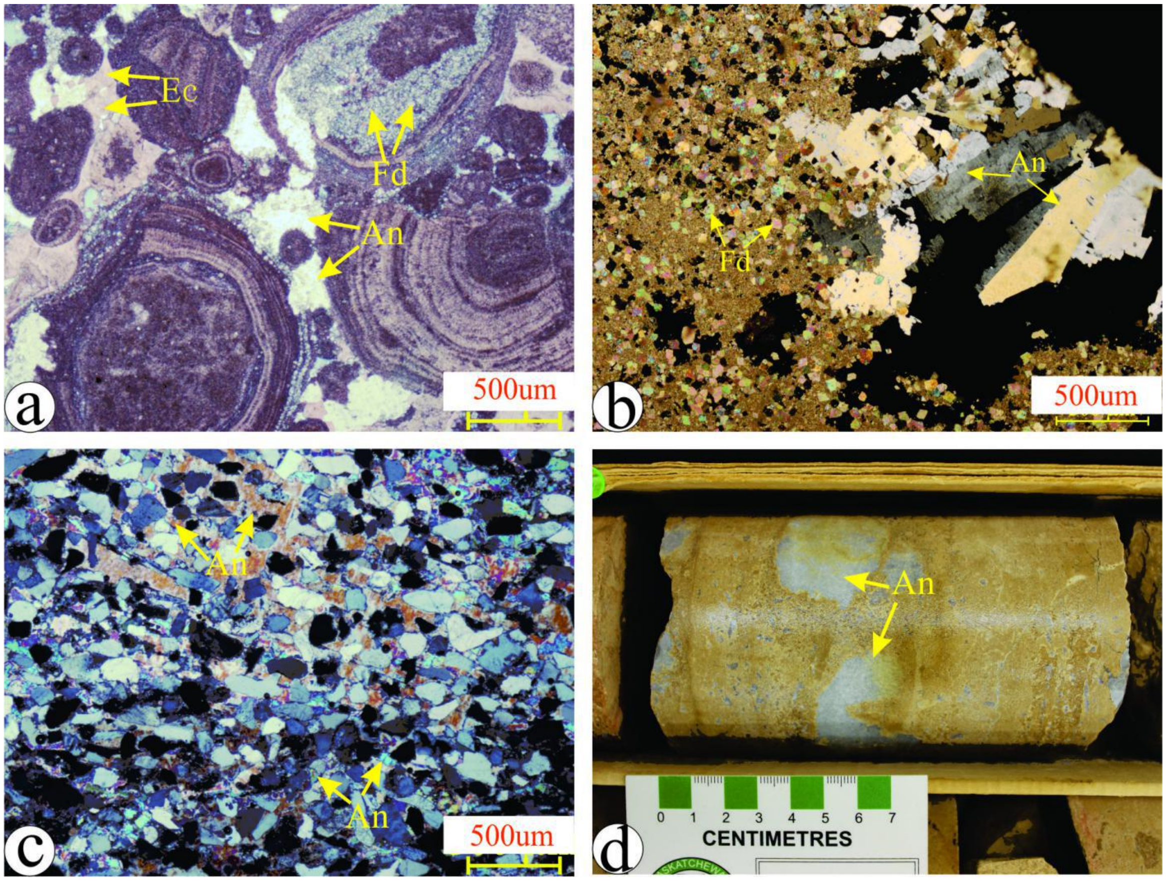

Figure 5.3 a) photomicrograph of oolitic grainstone showing equant calcite (Ec), anhydrite (An) and fine dolomite (Fd, dolomite 1); the thin section is stained with Alizarin Red. Photo is taken under plane polarized light. Alida Beds, 1185.5 m, 11/06-12-004-33W1; 96K245; b) photomicrograph showing fine dolomite (Fd, dolomite Ⅱ) and anhydrite cement (An 1). Alida Beds, 1083.9m, 01/10-10-005-32W1; 85K115; c) photomicrograph of sandstone showing anhydrite cement (An). Photo is taken under X-polarized light. Kisbey interval, 1223.1m, 01/04-12-004-33W1; 96I248; d) Core photograph showing vuggy porosity filled by anhydrite (An). Frobisher Beds, 1103.5m, 01/16-27-2-31W1; 56K022.

5.2.5 Dissolution

Dissolution occurs in two different stages (I and II). The earlier stage postdates calcite cements (etched outlines of calcite). Although porosity enhancement accompanied this initial dissolution stage, later events (e.g., precipitation of anhydrite cement, calcite cement and dolomite II, and compaction) had partially destroyed the pore spaces that were generated earlier. The second dissolution event II, during which relatively large moldic pores were formed, occurred at a later stage (Figure 5.3). Petrographic evidence (such as etched outlines of calcite and dolomite cements) shows that stage II dissolution postdates the calcite and dolomite precipitations.

The two stages dissolution occurs in all four stratigraphic units of the Mission Canyon Formation and is common in the mudstone to wackestone lithofacies in the northeast corner of the study area. Dissolution is one of the most important events to create porosity for the reservoir and increase the overall reservoir quality of the formation, especially in the Frobisher Beds.

5.2.6 Compaction

There are two types of compaction features recognized from core and thin-section studies of the formation: (i) mechanical compaction and (ii) chemical compaction. The mechanical compaction caused deformation and breakage of grains, (e.g., ooids, Figure 5.4b; Wanless, 1979; Ehrenberg, et al., 2006). Stylolites and microstylolites are common features in the Mission Canyon Formation, especially in the packstone / grainstone lithofacies (Figure 5.4). Compaction destroys a good portion of the porosity, reducing the overall reservoir quality of the formation.

5.2.7 Fracturing

Fractures in the studied rocks are typically vertical, and partially filled by white anhydrite cement (Anhydrite Ⅰ and Ⅱ). Fractures are more common in the fragile limestone lithofacies in the Mission Canyon Formation (e.g., mudstone and bioclastic wackestone). Although later partially plugged by the anhydrite cement (Anhydrite Ⅰ and Ⅱ), fracture generation has contributed to increasing the original effective secondary porosity of the sediments.

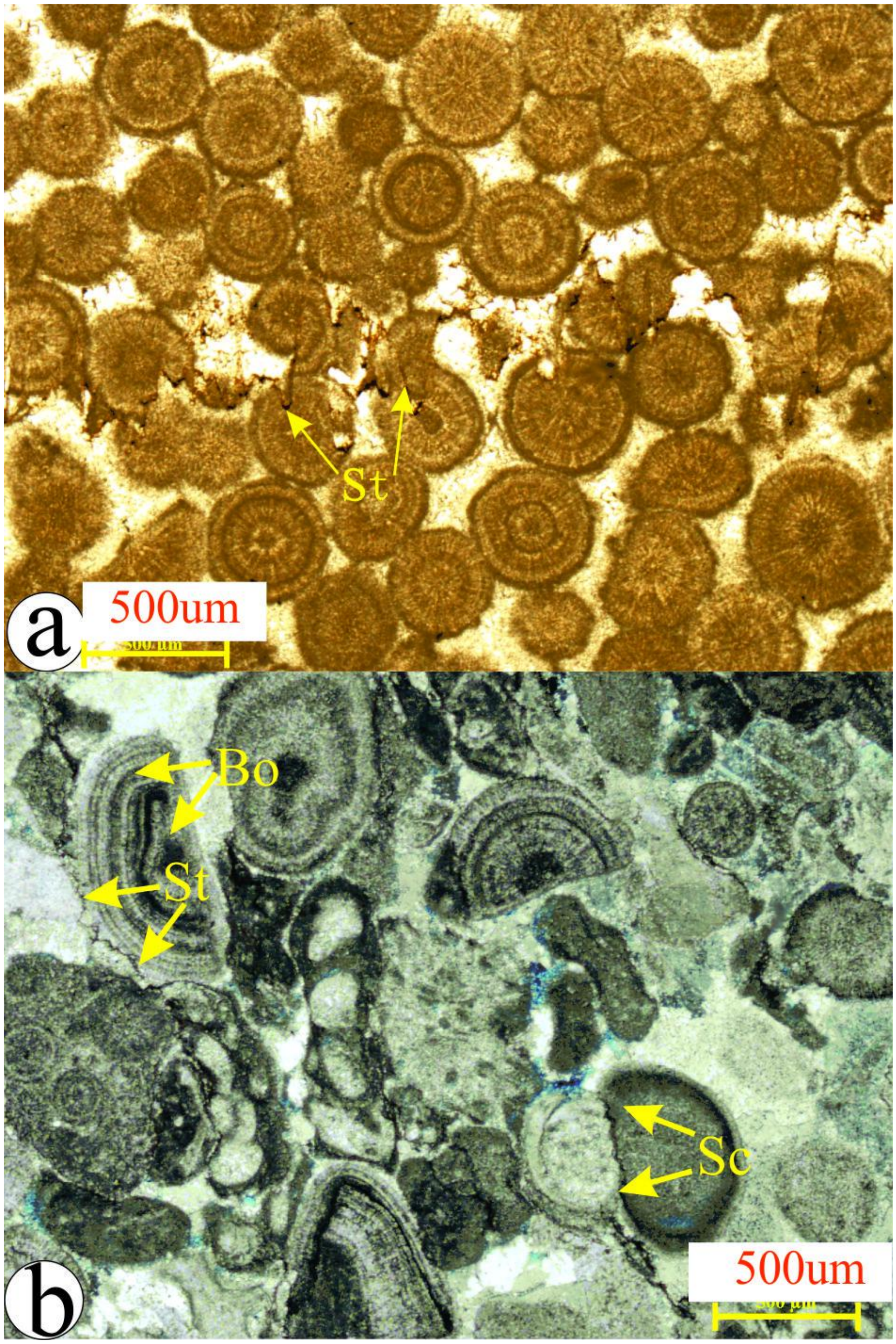

Figure 5.4 a) photomicrograph showing stylolite (St). Frobisher Beds, 1262.5m, 01/15-19-008-08W2; 85K115; b) photomicrograph of bioclastic oolitic grainstone showing broken ooid (Bo), stylolite (St) and suture contact (Sc). Photo is taken under plane polarized light. Tilston Beds, 1870.6m, 01/12-29-001-05W2; 54D007.

Based on the petrographic study of diagenetic products in Mission Canyon Formation, the recognized paragenetic sequence are as follows: micritization and micrite envelope; fibrous calcite cement; bladed calcite cement; fine crystalline dolomite (dolomite event 1); dissolution event 1; stylolites; fractures; equant calcite cement; fine to medium crystalline dolomite (dolomite event II); anhydrite cement 1; dissolution event II and anhydrite cement II (Figure 5.2).

Three major diagenetic processes profoundly affected porosity development of the Mission Canyon Formation. Cementation, dolomitization and dissolution were active throughout the evolution of the formation.

5.3 Porosity and Reservoir Quality

The porosity and reservoir quality study is based on integration of petrographic attributes from core samples and thin sections and porosity and permeability data obtained from GeoScout for a few select wells from the various strata of the Mission Canyon Formation. Porosity identified in the Mission Canyon Formation varies from 1% to 35%. Following the porosity scheme of Choquette and Pray (1970), seven types of porosity can be recognized: interparticle, intraparticle, intercrystalline, fenestral, fracture, vuggy and moldic (Figures 5.5; 5.6).

Primary interparticle porosity is one of the most common porosity types in the Mission Canyon Formation. Packstone/grainstone, rudstone and sandstone lithofacies exhibit good primary interparticle porosity (Figure 5.5a), although most of them are occluded by calcite, dolomite and anhydrite cement. Intraparticle pores are not uncommon in the studied area and usually develop in the bioclastic packstone/grainstone lithofacies (Figure 5.5b). Intercrystalline porosity is related to pervasive replacement of limestone by dolomite (Figure 5.5c). Moldic porosity is a minor contributor to porosity and mainly occurs in the bioclastic mudstone/wackestone (Figure 5.6a). Fenestral and fracture porosities are also present throughout the Mission Canyon Formation (Figure 5.6b). Vuggy and moldic porosities are mainly due to dissolution event II; the vuggy is the principle one of the two (Figure 5.6c), although both of them are partially filled by later anhydrite cement (anhydrite II).

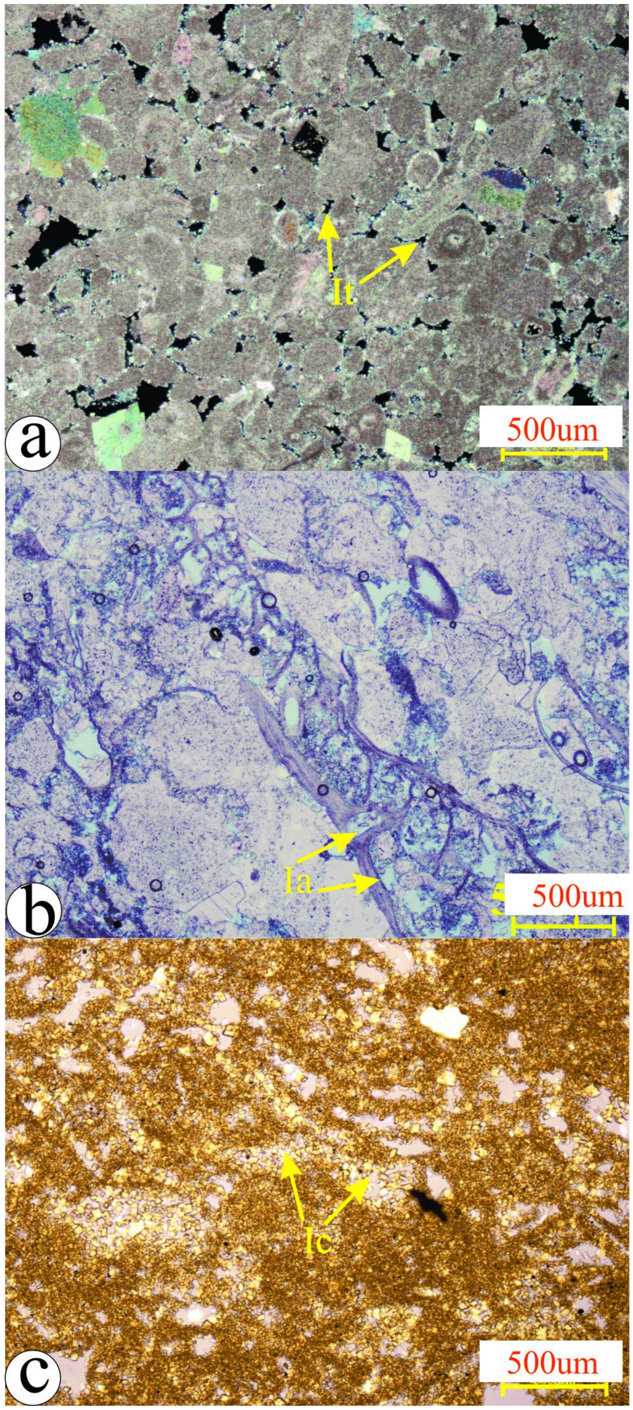

Figure 5.5 a) photomicrograph of peloidal, oolitic grainstone showing interparticle porosity (It). Photo is taken under X-polarized light. Tilston Beds, 1158.5m, 01/01-11-006-33W1; 86J054; b) photomicrograph of bioclastic grainstone showing intraparticle porosity (Ia *Brachipod*). Photo is taken under plane polarized light. Alida Beds, 1122.9 m, 01/01-11-006-33W1; 86J054; c) photomicrograph of dolomudstone showing intercrystalline porosity (Ic); Photo is taken under plane polarized light. Kisbey interval, 1222.7m, 01/03-24-007-4W2; 93H085.

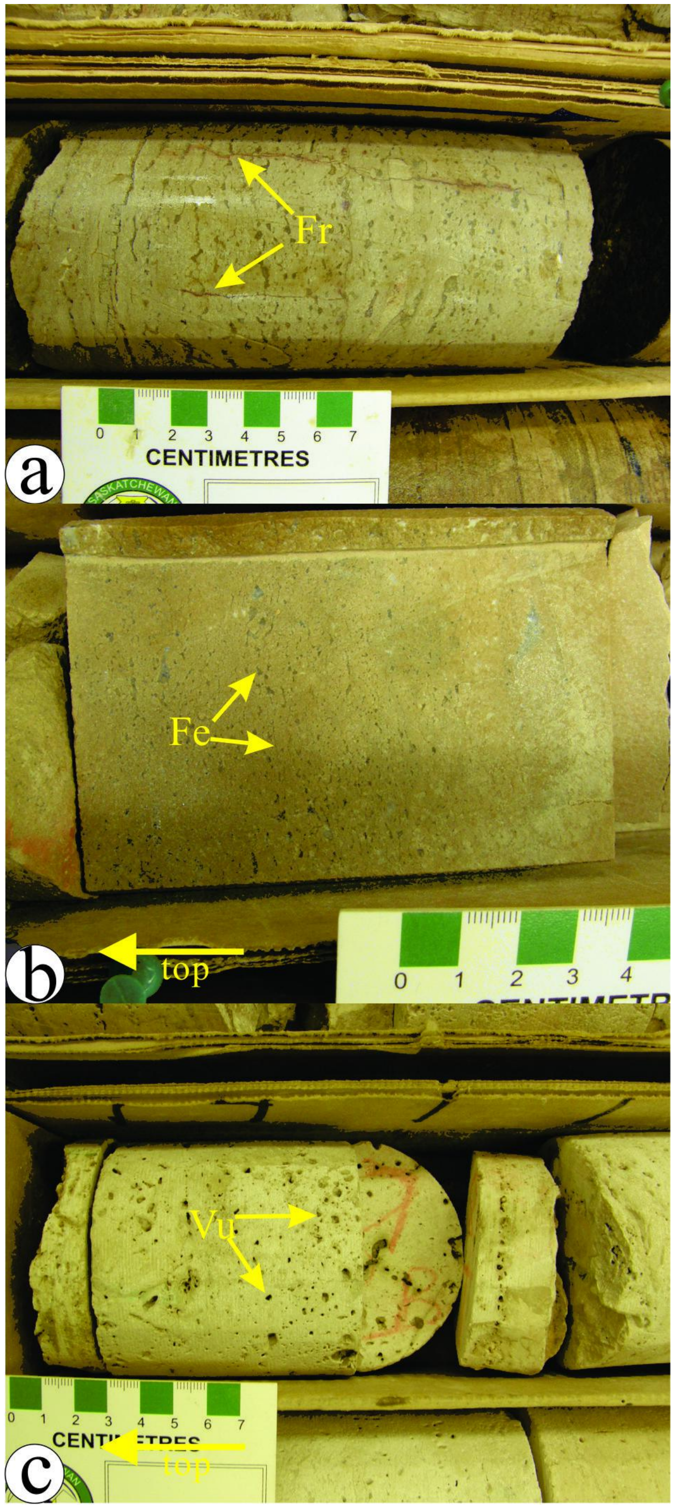

Figure 5.6 a) Core photograph of oncoidal grainstone showing fracture porosity (Fr). Frobisher Beds, 1232.1m, 01/04-09-008-06W2; 61J038; b) Core photograph showing fenestral porosity (Fe) filled by anhydrite. Frobisher Beds, 1157.1 m, 41/09-33-005-34W1; 87K208; c) Core photograph showing vuggy porosity (Vu) Frobisher Beds, 1185.5m, 01/02-27-005-01W2; 85K115.

5.3.1 Tilston Beds

The recognized paragenetic sequence and its effect on the porosity evolution of the Tilston Beds are summarized in Table 5.1. The paragenetic sequence of Tilston Beds are as follows: bladed calcite cement, dissolution event 1, stylolites, equant calcite cement, fine to medium crystalline dolomite (dolomite event II), anhydrite cement 1, dissolution event II and anhydrite cement II (Figure 5.1).

The porosity types of Tilston Beds are mainly interparticle and vuggy in nature (Figure 5.5a). Porosity is influenced by burial depth and calcite cement dissolution, which partially reinstates the original primary porosity. However, the highest values are associated with natural fractures. Higher values of permeability are also associated with natural fractures. Porosity within the Tilston Beds is generally very well-developed (Figure 5.7), however permeability is very low. Take well 101/01-11-006-33W1(86J054) as an example, porosity ranges from 8.7% to 28.7% (average 19.7%, n=25), while permeability varies from 0.19 to 76.2 millidarcies (MD) (average 33.7, n=25). The packstone/grainstone lithofacies shows relatively good porosity in the Tilston Beds while dolomudstone lithofacies appears dense with lower porosity (Figure 5.8a; 5.7).

Table 5.1 Paragenetic sequence of the diagenetic features observed in the Tilston Beds in southeastern Saskatchewan. (The porosity curve is based on the estimated average porosity)

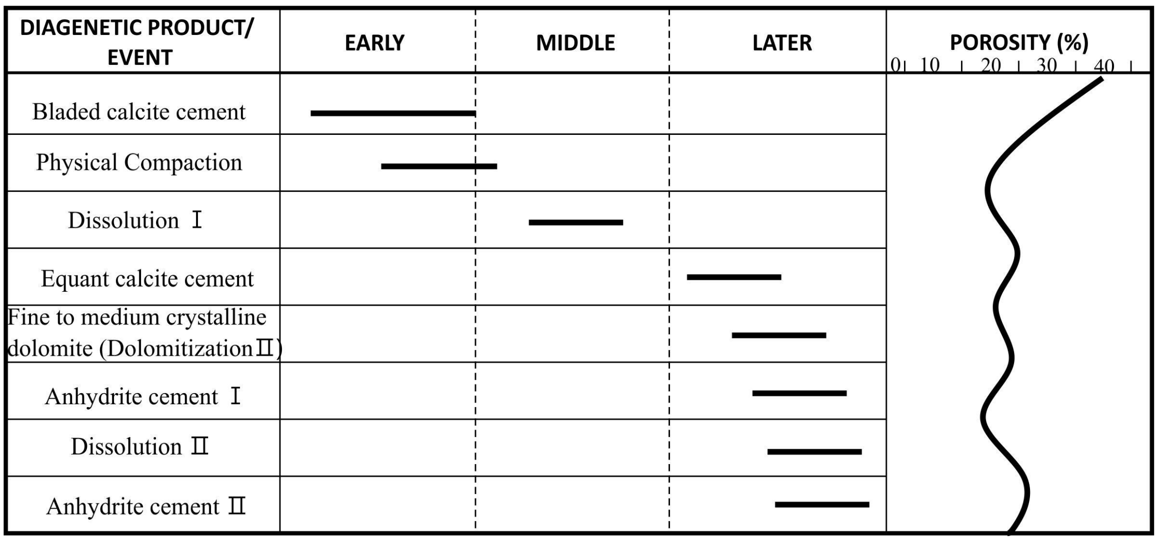

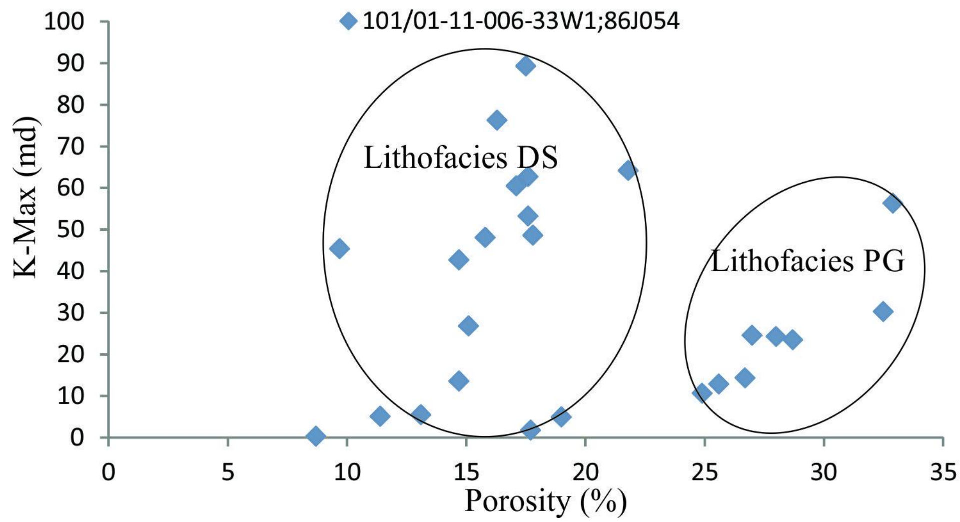

Figure 5.7 Crossplots of Tilston porosity and permeability.

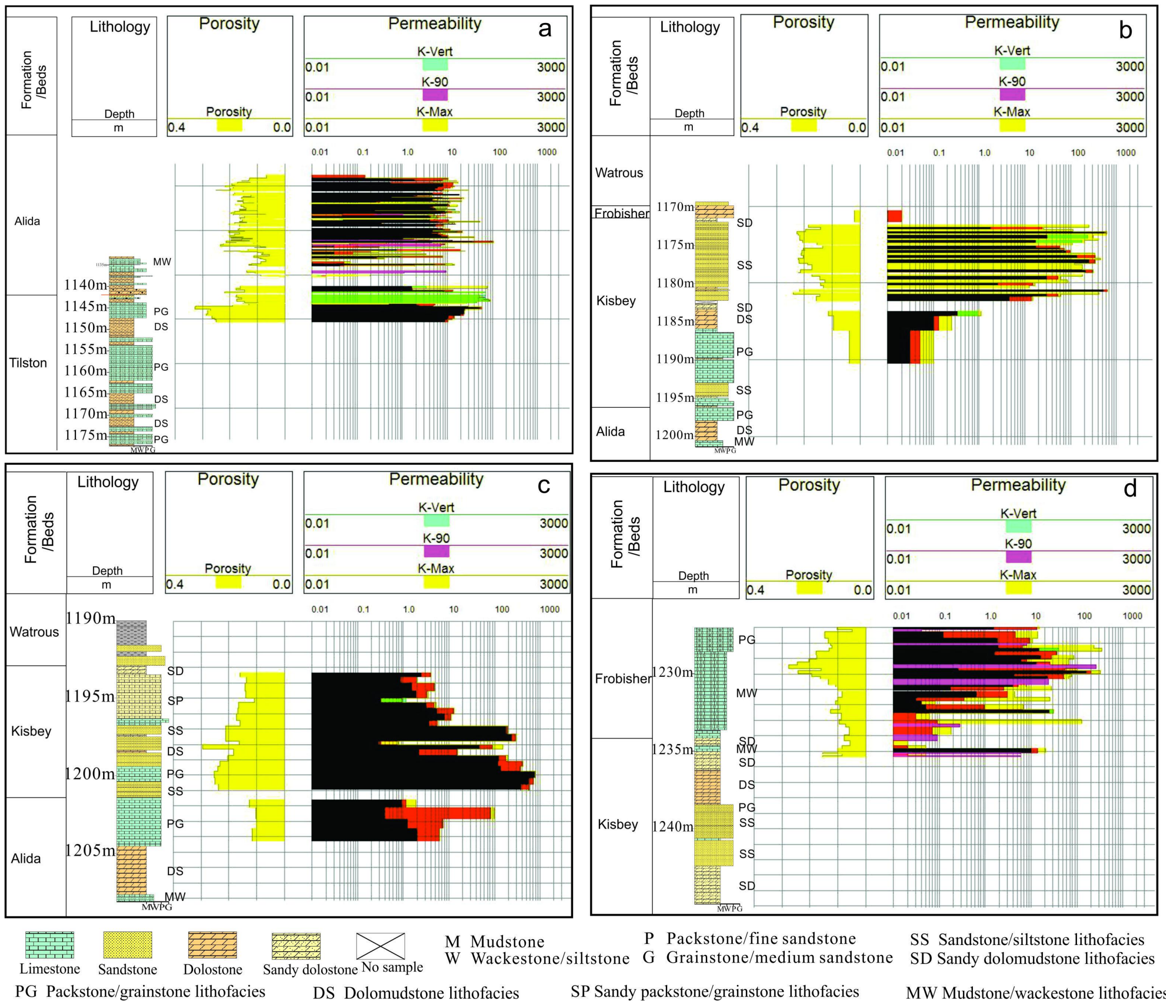

Figure 5.8 Porosity and permeability of Mission Canyon Formation in four different wells: a, well 01/01-11-006-33W1; b, 01/04-12-004-33W1; c, 01/05-20-006-01W2; d, 01/07-34-005-02W2. The black bar type is the green overlapping purple and yellow. The red is the purple overlapping yellow bar.

5.3.2 Alida Beds

The diagenetic features in the Alida Beds are micritization and micrite envelopes, fibrous calcite cement, bladed calcite cement, fine crystalline dolomite (dolomite event 1), dissolution event 1, stylolites, equant calcite cement, fine to medium crystalline dolomite (dolomite event II), anhydrite cement 1, dissolution event II and anhydrite cement II.

The representative porosity types of Alida Beds are interparticle, intraparticle, moldic, and vuggy (Figure 5.5; 5.6). In the northeast of study area, the Alida Beds show porosity changes from 6.6% to 25% (average 14.5%, n=90), while permeability varies from 0.01 to 96.7 millidarcies (average 11.0, n=90) and concentrate in the 0-40 millidarcies range (Figure 5.9). It can develop into excellent reservoirs with up to 25% of porosity (Figure 5.9). The the micritic coatings that formed on the bioclasts tend to suppress the syntaxial overgrowths of the calcite cement that normally destroy the interparticle porosity in crinoid-rich grainstone/packstone lithofacies (Figure 5.8c; 5.9).

Table 5.2 Paragenetic sequence of the diagenetic features observed in the Alida Beds in southeastern Saskatchewan.

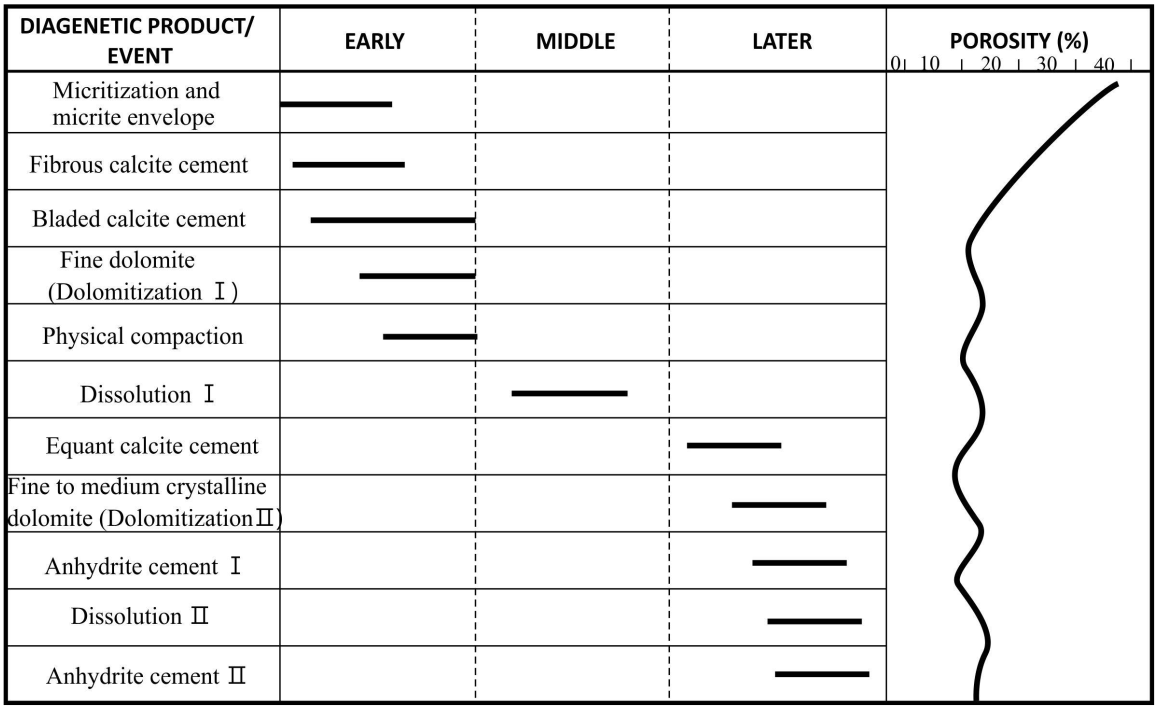

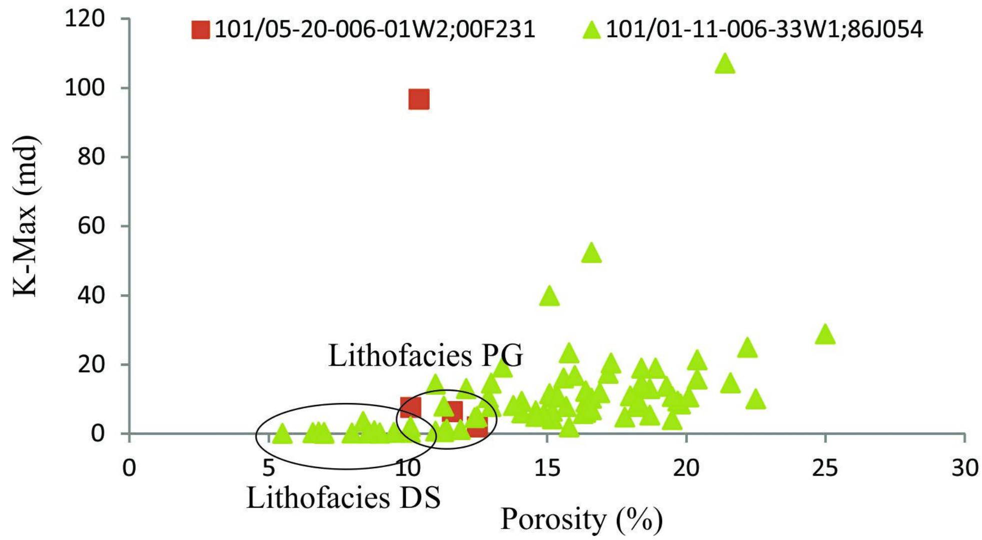

Figure 5.9 Crossplots of Alida porosity and permeability.

5.3.3 Kisbey Interval

The Kisbey interval has gone through a complex diagenetic evolution. The recognized paragenetic sequence is as follows: micritization and micrite envelope, fibrous calcite cement, bladed calcite cement, fine crystalline dolomite (dolomite event 1), equant calcite cement, dissolution event 1, stylolites, anhydrite cement 1, dissolution event II and anhydrite cement II.

Interparticle and intercrystalline pore types are dominant in the Kisbey interval. Moreover, dark-colored, dolomitized mudstone intraclasts, that are often dissolved, contribute microporosity to the Kisbey interval. Near the eastern end of the Kisbey erosional line (e.g., well 101/04-12-004-33W1; 101/05-20-006-01W2; 141/10-09-004-01W2), the Kisbey interval exhibits porosities of up to 29.5% (average 18.2%, n=68) and permeabilities from 0.02 to 780 millidarcies (average 199.3, n=68; Figure 5.10). The porosity increases with permeability in the Kisbey interval. The sandstone/siltstone lithofacies shows the best porosity and permeability of all kinds of lithofacies in the Mission Canyon Formation (Figure 5.8b, c; 5.10). The main reservoir lithology in the Kisbey sandstone is a clean, well-sorted, and fine to medium-grained quartz arenite (lithofacies v) with anhydrite, calcite and dolomite cement. The primary interparticle porosity is well interconnected.

Table 5.3 Paragenetic sequence of the diagenetic features observed in the Kisbey interval in southeastern Saskatchewan.

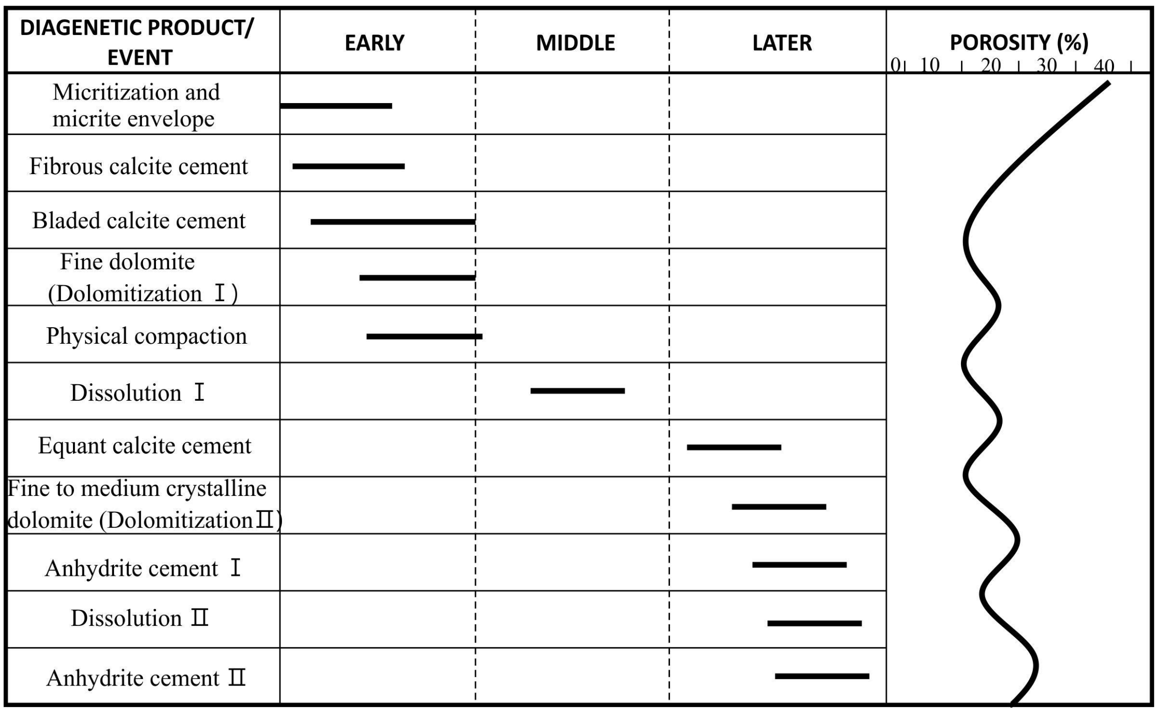

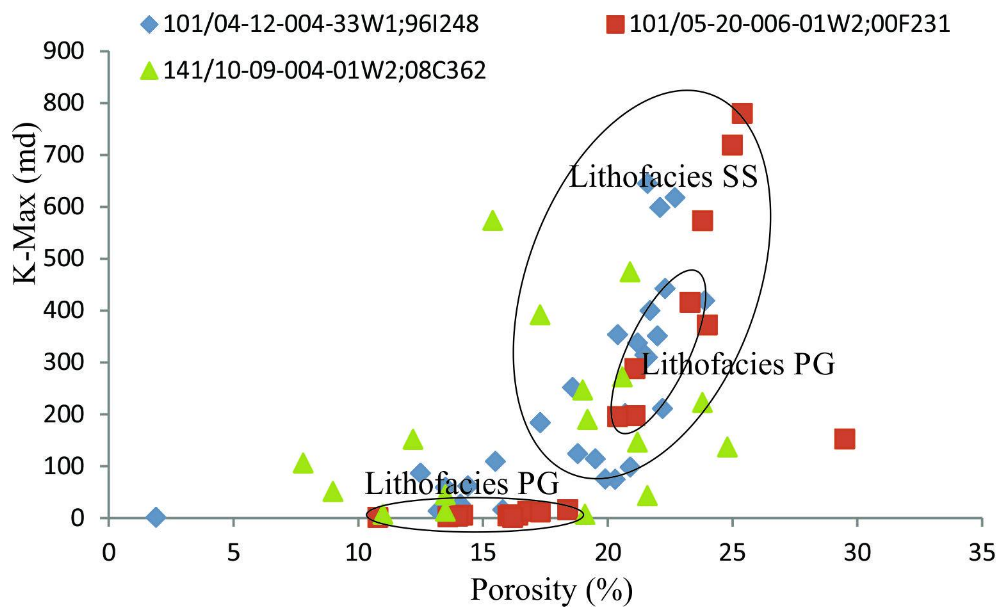

Figure 5.10 Crossplots of Kisbey interval porosity and permeability.

5.3.4 Frobisher Beds

The Frobisher Beds have a number of diagenetic events: fibrous calcite cement, bladed calcite cement, fine crystalline dolomite (dolomite event 1), dissolution event 1, stylolites, fractures, equant calcite cement, fine to medium crystalline dolomite (dolomite event II), anhydrite cement 1, dissolution event II, and anhydrite cement II (Table 5.4).

The Frobisher Beds contain a good amount of leached particles that result in moldic, fenestral, vuggy and (reinstated) interparticle porosity within the packstone and grainstone lithofacies (Figure 5.6). Since Frobisher Beds are adjacent to the top of the Mississippian unconformity surface in most of the study area, anhydrite has cemented and occluded many of the interparticle, vuggy, and fenestral pores (Figure 5.8d; 5.11). The wackestone intervals exhibit scattered moldic porosity (e.g., bioclasts), but this porosity is not effective. In well 101/07-34-005-02W2, the porosities range from 5.7% to 24.2% (average 11.3%, n=18) and permeabilities from 0.02 to 127 millidarcies (average 45.5, n=18; Figure 5.11). The mudstone/wackestone lithofacies shows relative good vuggy porosity (Figure 5.8d; 5.11).

Table 5.4 Paragenetic sequence of the diagenetic features observed of the Frobisher Beds in southeastern Saskatchewan.

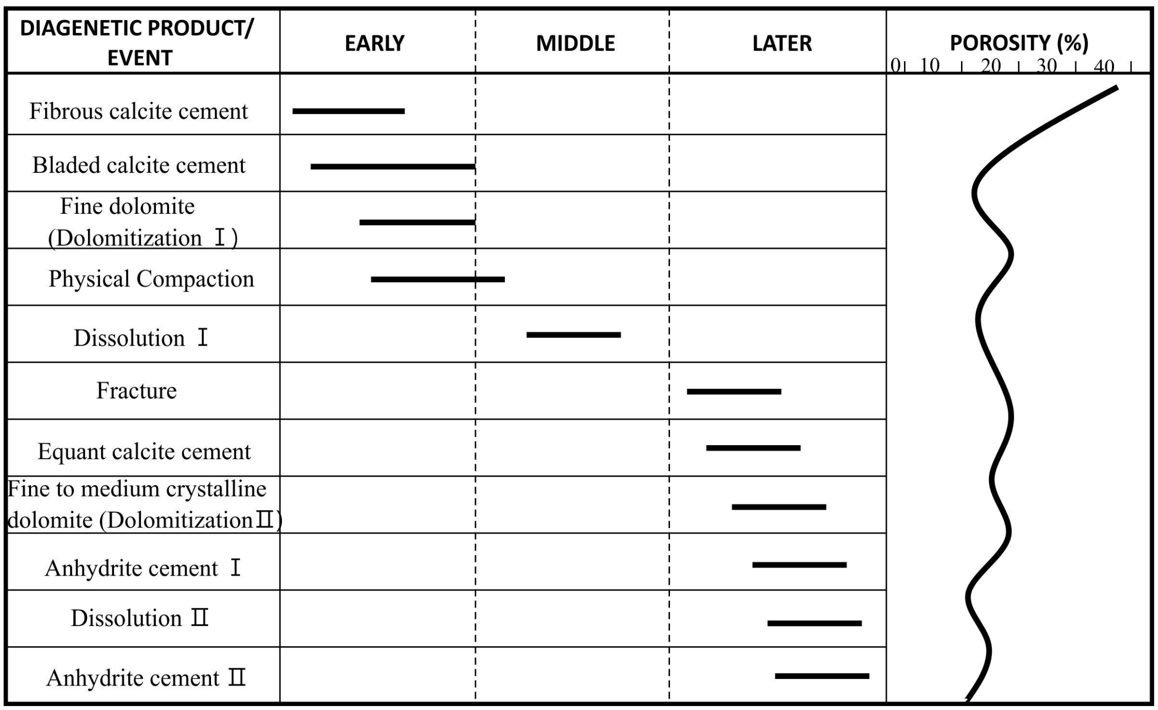

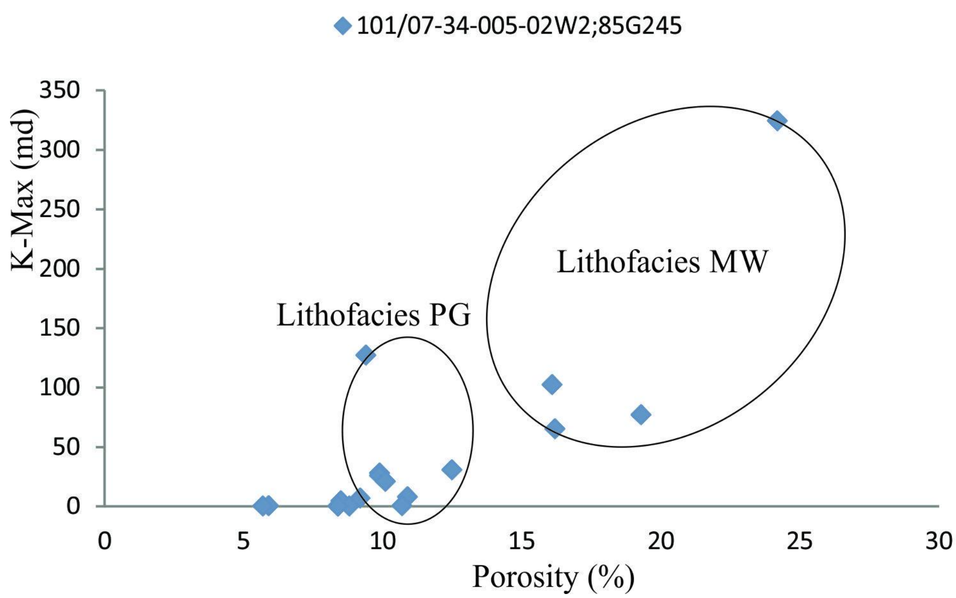

Figure 5.11 Crossplots of Frobisher porosity and permeability.

5.3.5 Summary of the Mission Canyon reservoir quality

Porosity and permeability in the Mission Canyon Formation is determined in part by depositional facies (Lindsay, 1988; Petty, 1988). The sandstone lithofacies shows very good porosity and permeability which represents relative clean tidal channel deposit (Figure 5.8). However, diagenetic signatures have a great effect on the present day reservoir conditions of the formation. The carbonate sand shoal (packstones/grainstones) exhibits good porosity and permeability, but in some part, pore was filled by anhydrite, calcite and dolomite which reduced porosity and permeability (Figure 5.8d). Fracture, dissolution and dolomitization events create porosity for the rock and thus have increased the overall reservoir quality of the formation. The best reservoir rocks are found where one or several of the following apply: low degree of cementation, good preservation and reinstating of primary pore space, presence of fenestral/vuggy porosity in oolitic grainstone units, low degree of compaction, and dolomitization of the matrix. Both diagenetic products and original textural attributes of the various lithofacies intervals of the formation must be taken into account for better hydrocarbon production.

6.0 Conclusions

In southeastern Saskatchewan, the Mission Canyon Formation includes, from bottom to top, Tilston Beds, Alida Beds, Kisbey interval and Frobisher Beds. The succession consists largely of carbonate rocks with subordinate sandstone and evaporite intervals. Oil accumulations occur primarily within the Mission Canyon Formation, stratigraphically just below the pre-Mesozoic unconformity where porous carbonate and sandstone units of the formation have been truncated and sealed.

Lithologic analysis of the Mission Canyon Formation allowed recognition of eight lithofacies units, which include: i) packstone/grainstone (Facies PG), ii) rudstone (Facies RD,) iii)mudstone/wackestone (Facies MW), iv) dolomudstone (Facies DS), v) sandstone (Facies SS), vi) sandy dolomudstone (Facies SD), vii) sandy packstone/grainstone (Facies SP) and viii) anhydrite (Facies AH). The sandstone and sandy carbonate units are confined within the Kisbey interval, but the cleaner carbonate units are present in different layers of the Tilston to Frobisher intervals. The overall depositional setting can be summarized as a peritidal environment characterized by carbonate subtidal sand shoals with a landward lagoonal to tidal mud-flat system. The sedimentary attributes and areal distribution of sandstone lithofacies of the Kisbey interval suggests a connection between tidal creeks that cut a carbonate-dominated shallow platform and a fluvial system that brought the clastic particles into the basin.

The temporal lithofacies arrangement of the studied stratigraphic interval shows clear vertically-stacked rhythmic units defined by shallowing-upward cycles of basal subtidal lithofacies (PG, RD,SP, MW) grading to restricted lagoonal/tidal mudflat deposits (MW, DS, SD SS & AH). Three types of shallowing-upward lithofacies associations are recognized:

A) packstone/grainstone to wackestone/mudstone cycle: have a basal subtidal packstone to grainstone lithofacies grading into intertidal/supratidal wackestone/mudstone.

B) wackestone to mudstone cycle: the lower part is intertidal wackestone grading up into upper supratidal mudstone.

C) packstone/grainstone - wackestone - mudstone cycle: the lower subtidal packestone/grainstone grading up into intertidal wackestone and the supratidal mudstone on the top.

Fischer Plot analysis of these rhythmic units suggests higher (?4th and ?5th) order Milankovitch cycles that can be amalgamated into six, possibly 3rd-order depositional cycles of which one corresponds to lower Tilston Beds, three to upper Tilston and Alida Beds, one to the top Alida and Kisbey interval and one to the Frobisher Beds. These 3rd-order cycles appear to correlate well with the Mississippian cyclothems, and thus attributable to eustatic sea level changes. The amplitudes of these large scale order events were from 0 to 12m based on the Fischer Plots. The ampitudes of these relative sea level changes in Frobisher interval are larger than those in Tilston, Alida and Kisbey intervals. Periods of relative sea level rise are defined by higher amplitudes of the Milankovitch cycles and positive departure from the average thickness of the cycles (i.e., higher accommodation spaces) whereas periods of relative sea level drop are indicated by thinner cycles. The Kisbey interval appears to form in large scale cycles during the sea level drop period.

The recognized diagenetic products and their paragenetic sequence are as follows: micritization and micrite envelope; fibrous calcite cement; bladed calcite cement; fine crystalline dolomite, dissolution event 1; stylolite; fracture; equant calcite cement; fine-crystalline dolomite (dolomite event II); anhydrite cement 1; dissolution event II and anhydrite cement II. Fracture, dissolution and dolomitization events create porosity for the rock and thus have increased the overall reservoir quality of the formation.

Seven types of porosity are recognized: interparticle, intraparticle, intercrystalline, fenestral, fracture, vuggy and moldic. The porosity types of Tilston Beds are mainly interparticle and vuggy in nature. The representative porosity types of Alida Beds are interparticle, intraparticle, moldic, and vuggy. Interparticle and intercrystalline pore types are dominant in the Kisbey interval. The Frobisher Beds contain a good fair amount of leached particles that produce moldic, fenestral, vuggy and (re-instated) interparticle porosity within the packstone and grainstone lithofacies.

Porosity and permeability in the Mission Canyon Formation is quite variable, the Tilston Beds and Kisbey interval show good porosity and permeability, while the Alida Beds and Frobisher Beds exhibit relatively poor porosity. Overall, as the porosity increases, the permeability increases.

References

Allen, J.R.L. (1982): Sedimentary Structures: Their Character and Physical Basis; Elsevier, Amsterdam, v2, 664p.

Angulo, S. and Buatois, L. (2011): Petrophysical characterization of sedimentary facies from the Upper Devonian–Lower Mississippian Bakken Formation in the Williston Basin, southeastern Saskatchewan; in Summary of Investigations 2011, Volume 1, Saskatchewan Geological Survey, Sask. Ministry of Energy and Resources, Misc. Rep. 2011-4.1, Paper A-6, 16p.

Amthor, J. E. and Friedman, G. M. (1991): Dolomite – Rocks Textures and Secondary Porosity Development in Ellenburger Group Carbonates (Lower Ordovician), West Texas and Southeastern New Mexico; Sedimentology, v38, 343-362.

Bathurst, R.G.C. (1966): Boring algae, micite envelopes, and lithification of molluscan biosparites; Geol. Jour., v5, p5-32.

Bitney, M. (1983): Winnipeg Formation (Middle Ordovician), Williston Basin; AAPG Bulletin, v67 (8), p1330.

Bjorlie, P.F. and Anderson, S.B. (1978): Stratigraphic and depositional setting of the Carrington shale facies (Mississippian) of the Williston Basin; Montana Geological Society, Williston Basin Symposium, p165-176.

Butler. G P. (1969): Modern evaporate deposition and geochemisty of coexisting brines, the Sabkha, Trucial coast, Arabian gulf; Jurnal of sedimentary petrology, 39(1):70-80.

Carlson, C.G. and LeFever, J.A. (1987): The Madison, a nomenclatural review with a look to the future; in Carlson, C.G. and Christopher, J.E. (eds.), Fifth International Williston Basin Symposium, Sask. Geol. Soc., Spec. Publ. No. 9, p77-82.

Carlson, T.N. and Prospero, J.M. (1972): The large-scale movement of Saharan air outbreaks over the northern equatorial Atlantic; J. Appl. Meteor., v11, p283-297.

Campbell, C.V. (1967): Lamina, laminaset, bed and bedset; Sedimentology, v8, p7-26.

Choquette, P. W., and Pray, L. C. (1970): Geologic nomenclature and classification of porosity in sedimentary carbonates; AAPG Bulletin, v54, no. 2, p. 207 – 250.

De Boer, R.B. (1974): Thermodynamical and experimental aspects of pressure solution. In: Proceeding of International symposium on Water-Rock Interactions; (Eds Cadek, J.& Paces, T.), Geological Survey, Prague, 381-387.

De Souza, R.S. and De Assis Silva C. M. (1998): Origin and timing of carbonate cementation of the Namorado sandstone (Cretaceous), Albacora Field, Brazil: implication for oil recovery; Publs int. Ass. Sediment, 26, 309-325.

Edie, R.W. (1958): Mississippian sedimentation and oil fields in southeastern Saskatchewan; AAPG Bull., v42, p94-126.

Elliot, T.L. (1982): Carbonate facies, depositional cycles, and the development of secondary porosity during burial diagenesis: Mission Canyon Formation, Haas Field, North Dakota; in Christopher, J.E. and Kaldi, J. (eds.), Fourth International Williston Basin Symposium, Sask. Geol. Soc., Spec. Publ. No. 6, p131-151.

Ehrenberg, S.N., Eberli, G.P., Keramati, M., and Moallemi, A. (2006): Permeability-porosity relationships in interbedded limestone-dolostone reservoirs; AAPG Bulletin, 90, 91–114
.
Enos, Paul, and L. H. Sawatsky, (1979): Pore space in Holocene carbonate sediments (abs.): AAPG Bull., v. 63, p. 445.

Enos, Paul, and L. H. Sawatsky, (1981): Pore networks in Holocene carbonate sediments: Jour. Sed. Petrology, v. 51, p. 961-985.

Fischer, A.G., 1964, The Lofer cyclothems of the Alpine Triassic, in Merriam, D.F., ed., Symposium on cyclic sedimentation: Geological Survey of Kansas Bulletin 169, p. 107-149.

Flugel, E. (2004): Microfacies of carbonate rocks; Anlysis, Interpretation and Application, NewYork , springerverlag, 976 pp.

Fowler C. M. R and Nisbet E. G., (1985): The subsidence of the Williston basin, Can. J. Earth Sci., 22, 408-415.

Folk, R.L. (1974): The natural history of crystalline calcium carbonate: Effect of magnesium content and salinity; Journal of Sedimentary Petrology, 44, 40–53.

Fuzesy, L.M. (1960): Correlation and Subcrops of the Mississippian Strata in Southeastern and South- Central Saskatchewan; Sask. Dep. Miner. Resour., Rep. 51, 63p.

Fuller, J.G.C.M. (1956): Mississippian Rocks and Oilfields of Southeastern Saskatchewan; Sask. Dep. Miner. Resour., Rep. 19, 72p.

Friedman, G.M., and Sanders, J.E. (1967): Origin and occurrence of dolostones; In: Chilingar, G.V., Gasparrini, M., Bakker, R.J.,and Bechsta dt, T., 2006. Characterization of dolomitizing fluids in the Carboniferous of the Cantabrian Zone (NW Spain): a fluid-inclusion study with cryo-Raman spectroscopy; Journal of Sedimentary Research, 76: 1304–1322.

Gargallo-Quinones, M. (1985): Study of the ancient karstification and brecciation in the Madison Limestone (Mississippian) in Wyoming: unpublished M.S. thesis, State University of New York at Stony Brook, 208 p.

Gerhard, L.C., Anderson, S.B., and Fischer, D.W. (1991): Petroleum geology of the Williston Basin; in Leighton, M.W., Kolata, D.R., Oltz, D.F., and Eidel, J.J. (eds.), Interior Cratonic Basins, AAPG, Mem. 51, p507-560.

Goodwin, P. W., and Anderson, E. J. (1985): The Journal of Geology, Vol. 93, No. 5 (Sep., 1985), pp. 515-533.

Goodwin, P.W., Anderson, E.J., Goodman W.M., Saraka, L. J., (1986): Punctuated aggradational cycles: implications for stratigraphic analysis 1, 417-429.

Goldhammer, R.K., Dunn, P. A., and Hardie, L. A., (1987): High frequency glacio-eustatic sea-level oscillation with Milankovitch characteristics recorded in Middle Triassic platform carbonates in N. Italy: Am. Jour. Science, v. 287, p. 853-892.

Goldhammer, R.K., Dunn, P.A., Hardie, L.A., (1990): Depositional cycles, composite sea-level changes, cycle stacking patterns, and the hierarchy of stratigraphic forcing: examples from alpine Triassic platform carbonates. Geological Society of America Bulletin 102, 535–56.

Gregg, J.M., and Sibley, D.F. (1984): Epigenetic dolomitization the origin of xenotopic dolomite texture. J. Sediment. Petrol, 54: 907–931.

Hardie, L.A. (1987): Dolomitization: a critical view of some current views; Journal of Sedimentary Petrology, 57: 166–183.

Haq, B.U. and S.R. Shutter, (2008): A chronology of Paleozoic sea-level changes: Science, v. 322, October 2008, p. 64-68.

Halley, R. B., and Harris, P. M. (1979): Fresh-water cementation of a 1000-year-old oolite; Journal of Sedimentary Petrology, v. 49, p. 969-988.

Harris, S.H., Land, C.B., and McKeever, J.H. (1966): Relation of Mission Canyon stratigraphy to oil production in north-central North Dakota; AAPG, Bull. V. 50, p2269-2276.

Hasan Ferdous, (2001): Regional sedimentology and diagenesis of the Middle Bakken Formation Member: implications for reservoir rock distribution in southern Saskatchewan, PhD thesis.

Halabura, S.P. and Costa, A.L.L. (2005): Regional sequence stratigraphy of the Kisbey

Lowstand systems tract: implications for oil exploration; in Saskatchewan Geological Society, Core Workshop Volume, held in conjunction with the 13th Williston Basin Petroleum Conference, April 27, 2005, Sask. Geol. Soc., Spec. Publ. No. 17, p67-76.

Halabura, S.P. (2006): The Mississippian of southeastern Saskatchewan: regional considerations; in Gilboy, C.F. and Whittaker, S.G. (eds.), Saskatchewan and Northern Plains Oil & Gas Symposium 2006, Sask. Geol. Soc., Spec. Publ. 19, p146-164.

Halabura, S., Buatois, L., Angulo, S., and Piché, L. (2007): From source to trap—a review of the Bakken petroleum system, Upper Devonian–Mississippian, southeastern Saskatchewan; in Summary of Investigations 2007, Volume 1, Saskatchewan Geological Survey, Sask. Industry Resources, Misc. Rep. 2007-4.1, Paper A-4, 8p.

Hoff, J.L. (1987): Cyclicity in the Mission Canyon and Lower Charles Formations of the central Williston Basin; in Carlson, C.G. and Christopher, J.E. (eds.), Fifth International Williston Basin Symposium, Sask. Geol. Soc., Spec. Publ. No. 9, p117-122.

Howard, P. (2000): Mississippian sedimentology, depositional and diagenetic control on the Kisbey Sandstone petroleum reservoir development, Williston Basin; unpubl. MSc thesis, University of British Columbia, Vancouver, 250p.

Hsu, K.J. and Siegenthaler, C. (1969): Preliminary experiments on hydrodynamic movement induced by evaporation and their bearing on the dolomite problem; Sedimentology,12, 11-25.

Imam, B., Qing, H., and Chi, G. (2011): Petrographic study of the Middle Bakken Member, Viewfield area, southeastern Saskatchewan; in Summary of Investigations 2011, Volume 1, Saskatchewan Geological Survey, Sask. Energy and Resources, Misc. Rep. 2011-4.1, Paper A-5, 9p.

Janet K. Pitman, Leigh C. Price, and Julie A. LeFever, (2001): Diagenesis and Fracture Development in the Bakken Formation, Williston Basin: Implications for Reservoir Quality in the Middle Member. U.S. Geological Survey Professional Paper 1653, p.7-13.

James, N.P. and Choquette P.W. (1990): Limestones – the meteoric diagenetic environment; in McIlreath I.A. and Morrow D.W. (eds.), Diagenesis, Geological Association of Canada, Reprint Series 4. Ottawa, p35-74.

Ji, C. and Salad Hersi, O. (2013a): Sedimentary and facies description of Mississippian Alida-Kisbey-Frobisher stratigraphic interval, Mission Canyon Fm., SE Saskatchewan; Twenty-first Williston Basin Petroleum Conference; Regina, Saskatchewan Geological Society (abstract).

Ji, C. and Salad Hersi, O. (2013b): Lithofacies distribution of the Mississippian Alida-Kisbey-Frobisher stratigraphic interval, southeastern Saskatchewan; in Summary of Investigations 2013, Volume 1, Saskatchewan Geological Survey, Sask. Ministry of the

Economy, Misc. Rep. 2013-4.1, Paper A-6, 15p.

Ji, C. and Salad Hersi, O. (2014): Lithofacies and cyclicity of Mississippian Alida-Kisbey-Frobisher interval, southeastern Saskatchewan; Canadian Society of Petroleum Geologists; URL <http://geoconvention.org/archives/2014abstracts/075_GC2014_Lithofacies_and_cyclicity_of_Mississippian_Alida-Kisbey-Frobisher.pdf>, accessed 20 Jan 2015.

Ji, C. and Salad Hersi, O. (2015): Lithofacies, Cyclicity and Diagenetic Charcteristics of Mississippian Mission Canyon Formation, Southeast Saskachewan; Twenty-third Williston Basin Petroleum Conference; Regina, Saskatchewan Geological Society (abstract).

Ji, C. and Salad Hersi, O. (2015b): Diagenesis and Petrographic Reservoir Characterization of the Mission Canyon Formation, southeastern Saskatchewan; in Summary of Investigations 2015, submission.

Kent, D.M. (1984): Depositional setting of Mississippian strata in southeastern Saskatchewan: a conceptual model for hydrocarbon accumulation; in Lorsong, J.A. and Wilson, M.A. (eds.), Oil and Gas in Saskatchewan, Sask. Geol. Soc., Spec. Publ. No. 7, p19-30.

Kent, D.M. and Christopher, J.E. (1994): Geological atlas of the Western Canada Sedimentary Basin; Canadian Society of Petroleum Geologists and Alberta Research Council, URL <http://www.ags.gov.ab.ca/publications/wcsb_atlas/atlas.html>, accessed on May 17, 2013.

Kent, D.M. (1987): Mississippian facies, depositional history, and oil occurrences in the Williston Basin, Manitoba and Saskatchewan; in Mark, W.L. (ed.), Williston Basin, Anatomy of a Cratonic Basin, Rocky Mount Association of Geologist, p157-170.

Kent, D.M., Haidl, F.M., and MacEachern, J.A. (1988): Mississippian oilfields in the northern Williston Basin; in Goolsby, S.M. and Longman, M.W. (eds.), Occurrence and Petrophysical Properties of Carbonate Reservoirs in the Rocky Mountains Region, Rocky Mountain Association of Geologists, Denver, p381-418.

Kent, D.M. (2004): Quartz sandstone bodies in the Mississippian Frobisher, Kisbey, and Alida Beds of the Silverton – East-Silverton area, southeast Saskatchewan: remnants of an arid coastal setting; in Summary of Investigations 2004, Volume 1, Saskatchewan Geological Survey, Sask. Industry Resources, Misc. Rep. 2004-4.1, Paper A-8, 8p.

Kent, D.M. (2007): An enigmatic interval rich in sand-size quartz particles in the Mississippian of southeastern Saskatchewan: a possible solution to its origin based on sequence stratigraphy principles; in Summary of Investigations 2007, Volume 1, Saskatchewan Geological Survey, Sask. Industry Resources, Misc. Rep. 2007-4.1, Paper A-5, 16p.

Koerschner, W.F., and Read J.F., (1989): Field and Modelling studies of Cambrian Carbonate cycles, Virginia Applachians. Journal of Sedimentary Petrology 59, 654-687.

Lake, J.H. (1991): Transgressive cycles in an overall shallowing upwards sequence, Mississippian, Mission Canyon, Nottingham Unit, Williston Basin, southeast Saskatchewan; in Christopher, J.E. and Haidl, F.M. (eds.), Sixth International Williston Basin Symposium, Sask. Geol. Soc., Spec. Publ. No. 11, p136-141.

Landes, K.K. (1946): Porosity through dolomitization; Am. Assoc.Petrol. Geol. Bull, 30: 305–318.

Lavoie, D., Chi, G., Brennan-Alpert, P., Desrochers, A., and Bertrand, R. (2005): Hydrothermal dolomitization in the Lower Ordovician Romaine Formation of the Anticosti Basin: significance for hydrocarbon exploration; Bulletin of Canadian Petroleum Geology, v. 53, No. 4 (DECEMBER, 2005), P. 454-472.

Legault, A.R. (1999): A depositional model for the Frobisher-Alida K-2 and K-3 marker beds, Williston Basin, southeastern Saskatchewan; in Summary of Investigations 1999, Volume 1, Saskatchewan Geological Survey, Sask. Energy Mines, Misc. Rep. 99-4.1, p27-32.

LeFever, J.A., Martiniuk, C.D., Dancsok, E.F.R., and Mahnic, P.A. (1991): Petroleum potential of the middle member, Bakken Formation, Williston Basin; in Christopher, J.E. and Haidl, F.M. (eds.), Sixth International Williston Basin Symposium, Sask. Geol. Soc., Spec. Publ. No. 11, p74-94.

Lindsay, R.F., and Roth, M.S. (1982): Carbonate and evaporite facies, dolomitization and reservoir distribution of the Mission Canyon Formation, Little Knife Field, North Dakota: Fourth Internat. Williston Basin Symp., p. 153–179.

Lindsay, R.F., and Kendall, C.G.ST.C. (1980): Depositional facies, diagenesis and reservoir character of the Mission Canyon Formation (Mississippian) of the Williston Basin at Little Knife Field, North Dakota; Soc. Econ. Paleontologists and Mineralogists, Core Workshop No. 1, p. 79–104.

Lindsay, R.F., and Roth, M.S. (1982): Carbonate and evaporite facies, dolomitization and reservoir distribution of the Mission Canyon Formation, Little Knife Field, North Dakota: Fourth Internat. Williston Basin Symp., p. 153–179.

Lindsay, R.F. (1988): Mission Canyon Formation reservoir characteristics in North Dakota, in Goolsby, S.M., and Longman, M.W., eds., Occurrence and petrophysical properties of carbonate reservoirs in the Rocky Mountain region: Rocky Mountain Association of Geologists, Denver, Colorado, p. 317–346.

Longman, M.W. (1980): carbonate diagenesis as a control on stratigraphic traps (with example from the Willston Basin); AAPG Bull., V. 64, p.461-487.

Mack, G. H., and James, W.C., (1986): Cyclic sedimentation in the mixed siliciclastic-carbonate Abo-Hueco transitional zone (Lower Permian), SW New Mexico. Journal of Sedimentary Petrology. v 56. N.5. p 635-647.

Martin-Chivelet, J., Osleger, D.A., Montafiez, LP., (2000): Modified Fischer plots as graphical tools for evaluating thickness patterns in stratigraphic successions. J. Geosci. Educ. 48, 179-183.

Marsh, A.K.A. (2006): Sedimentology and diagenesis of the Frobishier succession in the Steelman field in southeast Saskatchewan; unpubl. MSc thesis, University of Regina, Regina, 10p.

McCartney, (1928): A Petrographic study of various sand horizons of Manitoba and eastern Saskatchewan; MSc thesis, University of Manitoba, Winnipeg.

Montafiez, I.P., Osleger, D. A., (1993): Parasequence stacking patterns, third-order accommodation events, and sequence stratigraphy of Middle to Upper Cambrian platform carbonates, Bonanza King Formation, Southern Great Basin. In: Loucks, R., Sarg, R. (Eds.), Carbonate Sequence Stratigraphy. American Association of Petroleum Geologists Memoir 57, Tulsa, OK, pp. 305- 326.

Mundy, D.J.C. and Roulston, P.E. (1998): Diagenesis and porosity development of subcropped Mississippian carbonate oil reservoir, an example from the Alida beds of the Pheasant Rump Pool, southeast Saskatchewan, Eighth International Williston Basin Symposium, Saskatchewan Geological Society Special Publication No. 13, p. 86-102.

Morrow, D. (1998): Regional subsurface dolomitization: models and constraints; Geoscience Canada, 25(2): 57–70.

Moore, C.H. (1989): Carbonate Diagenesis and Porosity, Developments in Sedimentology, New York: Elsevier, 338pp.

Nimegeers, A.R. (2006): Stratigraphic relationships and depositional model of Mississippian Midale beds in the Steelman-Bienfait area, southeastern Saskatchewan; unpubl. MSc thesis, University of Regina, Regina, 132p.

Nickel, E. and Yang, C. (comps.) (2011): Mississippian subcrop map and selected oil-production data, southeastern Saskatchewan; Sask. Ministry of Energy and Resources, Open File 2011-56, URL http://www.economy.gov.sk.ca/adx/aspx/adxGetMedia.aspx?DocID=12181,11586,11512,11455,11228,3385,5460,2936,Documents&MediaID=38699&Filename=OF2011-56_Mississippian_subcrop.pdf, accessed on August 17, 2013.

Perras, G.L. (1990): Sedimentological and reservoir characteristics of the Frobisher-Alida Beds, Lost Horse Hill Field, southeastern Saskatchewan; unpubl. MSc thesis, University of Regina, 182p.

Petty, D.M. (1988): Depositional facies, textural characteristics, and reservoir properties of dolomites in Frobisher–Alida interval in southwest NorthDakota: American Association of Petroleum Geologists Bulletin, v. 72, p. 1229–1253.

Pittman, E.D. (1979): Porosity, diagenesis and productive capability of sandstone reservoirs. In Aspects of diagenesis, edited by P. A. Scholle and P. R. Schluger, SEPM Special Publication no.26. pp. 159-173.

Porter, J.W. (1955): Madison complex of southeast Saskatchewan and southwest Manitoba; J. Alberta Soc. Petrol. Geol., v3 (August), p126-30.

Porter, J. W., Price, R. A., and McCrossan, R. G. (1982): The Western Canada Sedimentary Basin. Philosophical Transactions of the Royal Society of London, Series A, 305, pp. 169- 192.

Pratt, B.R. (2010): Peritidal carbonates; in James, N.P. and Dalyryple, R.W. (eds.), Facies Models 4, Geol. Assoc. Can., Geotext 6, p401-420.

Purser, B.H., Tucker, M.E., and Zenger, D.H. (1994): Problems, progress and future research concerning dolomites and dolomitization. IAS Special Publication, 21: 3–20.

Read, l.F., Goldhammer, R.K., (1988): Use of Fischer plots to define third-order sea-level curves in Ordovician peritidal cyclic carbonates, Appalachians. Geology 16, 895-899.

Read J.F., Grotzinger J.P., Bova J.A. and Koerschner W.F. (1986): Models for generation of carbonate cycles. Geology, v. 14, p. 107-110.

Reid, S.K. and Dorobek, S.L. (1993): Sequence stratigraphy and evolution of a progradational foreland carbonate ramp, Lower Mississippian Mission Canyon Formation and stratigraphic equivalents, Montana and Idaho; in Loucks, R.G. and Sarg, J.F. (eds.), Carbonate Sequence Stratigraphy, Recent Developments and Applications, AAPG, Mem. 57, p327-352.

Richards, B.C. (1989): Upper Kaskakia sequence: uppermost Devonian and Lower Carboniferous; in Ricketts, B.D. (ed.), Western Canada Sedimentary Basin: A Case History, Canadian Society of Petroleum Geologists, Calgary, Canada, p165-201.

Roberts, A.E. (1966): Stratigraphy of the Madison Group near Livingston, Montana, and discussion of karst and solutionbreccia features: U.S. Geological Survey Prof. Paper 526-B, 23p.

Rott, C.M. and Qing, H. (2005): Sedimentology and facies description of Mississippian Alida Beds, Williston Basin, southeastern Saskatchewan; in Summary of Investigations 2005, Volume 1, Saskatchewan Geological Survey, Sask. Industry Resources, Misc. Rep.

2005-4.1, Paper A-12, 10p.

Sadler, P.M., Osleger, D.A., Montan˜ ez, P., (1993): On the labeling, length, and objective basis of Fischer plots. Journal of Sedimentary Research 63, 360–368.

Saller, A.H. (1984): Petrologic and geochemical constraints on the origin of subsurface dolomite, Enewetak Atoll; an example of dolomitization by normal seawater. Geology, 12(4): 217–220.

Sando, W.J. (1974): Ancient solution phenomena in the Madison Limestone (Mississippian) of north-central Wyoming: U.S. Geological Survey Journal of Research, v. 2, n. 2, p. 133-141.

Sando, W.J. (1988): Madison Limestone (Mississippian) paleokarst: a geologic synthesis, in N.P. James and P.W. Choquette, eds., Paleokarst: Springer-Verlag, New York, p. 256-277.

Sibley, D. F. and Gregg, J. M. (1987): Classification of dolomite rock textures, Jour. Sedim. Petrol., 57, 967-975.

Smith, T.M. (1991): Diagenesis of shallow marine carbonate rocks: Isotopic and trace element constraints from the Mississippian Mission Canyon Formation, central and southwestern Montana: unpublished Ph.D. dissertation, Texas A&M University, 126p.

Smith, T.M. and Dorobek, S.L. (1993a): Alteration of early-formed dolomite during shallow to deep burial, Mississippian Mission Canyon Formation, central to southwestern Montana: Geological Society of America Bulletin, v. 105, n. 11, p. 1389-1399.

Smith, T.M. and Dorobek, S.L. (1993b): Stable isotopic composition of meteoric calcites, evidence for Early Mississippian climate change in the Mission Canyon Formation, Montana: Tectonophysics, v. 222, n. 3-4, p. 317-331.

Saskatchewan ministry of energy and resources, (2011): Stratigraphic correlation chart. www.er.gov.sk.ca/stratchart.

Shinn, E.A. (1983): Tidal flat environment; in Scholle, P.A., Bebout, D.G., and Moore, C.H. (eds.), Carbonate Depositional Environments, AAPG, Mem. 33, p172-210.

Schwarzacher, W., (2000): Repetitions and cycles in stratigraphy. Earth-Science Reviews 50,51-57.

Sloss, L.L. (1963): Sequences in the cratonic interior of North America; Geol. Soc. Amer., Bull., v74, p93-114.

Swinchatt, J. P. (1965): Significance of constituent composition, texture and skeletal breakdown in some recent carbonate sediments, Jour. Sed. Pet., V.42, P. 162-167.

Thomas, G.E. (1954): The Mississippian of the northeastern Williston Basin; Trans. Can. Inst. Min. Met., v57, p68-74.

Tucker M.E. and Wright, V.P. (1990): Carbonate Sedimentology. Oxford: Blackwell, 482 pp.

Ueno, K., Hayakawa, N., Nakazawa, T., Wang, Yand Wang, X (2012): Pennsylvanian-Early Permain cyclothemic succession on the Yangtze Carbonate Platform, South China. Palaeozoic Climate Cycles: Their Evolutionary and Sedimentological Impact. Geological Society. London, Special Publication, 376, 235-267.

Vice, M.A. (1988): Depositional environments and diagenesis in an interval of the Mission Canyon Limestone (Madison Group, Mississippian), south-central Montana and northern Wyoming: unpublished M.S. thesis, Southern Illinois University at Carbondale, 149p.

Vice, M.A. (1993): Deposition and diagenesis of the Mississippian Mission Canyon Limestone, northern Bighorn Basin region, southcentral Montana and northern Wyoming: unpublished Ph.D.dissertation, Southern Illinois University at Carbondale, 281p.

Vice, M.A. and Utgaard, J.E. (1989): Depositional environments in the Mississippian Mission Canyon Limestone (Madison Group, Mississippian), northern Bighorn Basin region, Montana and Wyoming, in D.E. French and R.F. Grabb, eds., Geological resources of Montana: Montana Geological Society Guidebook, v. 1, p. 55-64.

Vice, M.A. and Utgaard, J.E. (1996): Sedimentation and early diagenesis on the Mississippian Mission Canyon Platform in the Northern Bighorn Basin Region, in C.E. Bowen, T. Miller and S. Kirkwood, eds., Resources of the Bighorn Basin: Wyoming Geological Association Guidebook n. 47, p. 145-157.

Vice, M.A., Fifarek, R. H. and Utgaard, J.E. (2000): Diagenesis of the Mississippian Mission Canyon Formation, Montana Geological Society 2010 - Montana Geological Society: 50th Anniversary Symposium: Montana/Alberta Thrust Belt and Adjacent Foreland: Volume I.Northern Bighorn Basin Region, South-Central Montana and Northern Wyoming.

Warren, J. (2000): Dolomite: occurrence, evolution and economically important associations; Earth-Science Reviews, 52 2000 1–81.

Waters, D.L. and Sando, W.J. (1987): Depositional cycles in the Mississippian Mission Canyon Limestone Formation, Williston Basin, North Dakota; in Carlson, C.G. and Christopher, J.E. (eds.), Fifth International Williston Basin Symposium, Sask. Geol. Soc., Spec. Publ. No. 9, p123-133.

Wanless, H. (1979): Limestone response to stress: pressure solution and dolomitization;

Jour. Sed. Petrol, V.49, P.437-462.

Wilson, J. L. (1975): Carbonate facies in geologic history: New York, Springer-Verlag, 471 p.

Yurkowski, M. (2013): Saskatchewan oil and gas update; URL <http://www.estevaneconomicdevelopment.ca/energyexpo/PDF/Saskatchewan%20Ministry%20of%20the%20Economy.pdf>, accessed 1 December 2014.

Windom, H.L. (1975): Eolian contributions to marine sediments; J. Sed. Petrol., v45, p520-529.

Appendix

Well 1:01/04-09-008-06W2; 67B002

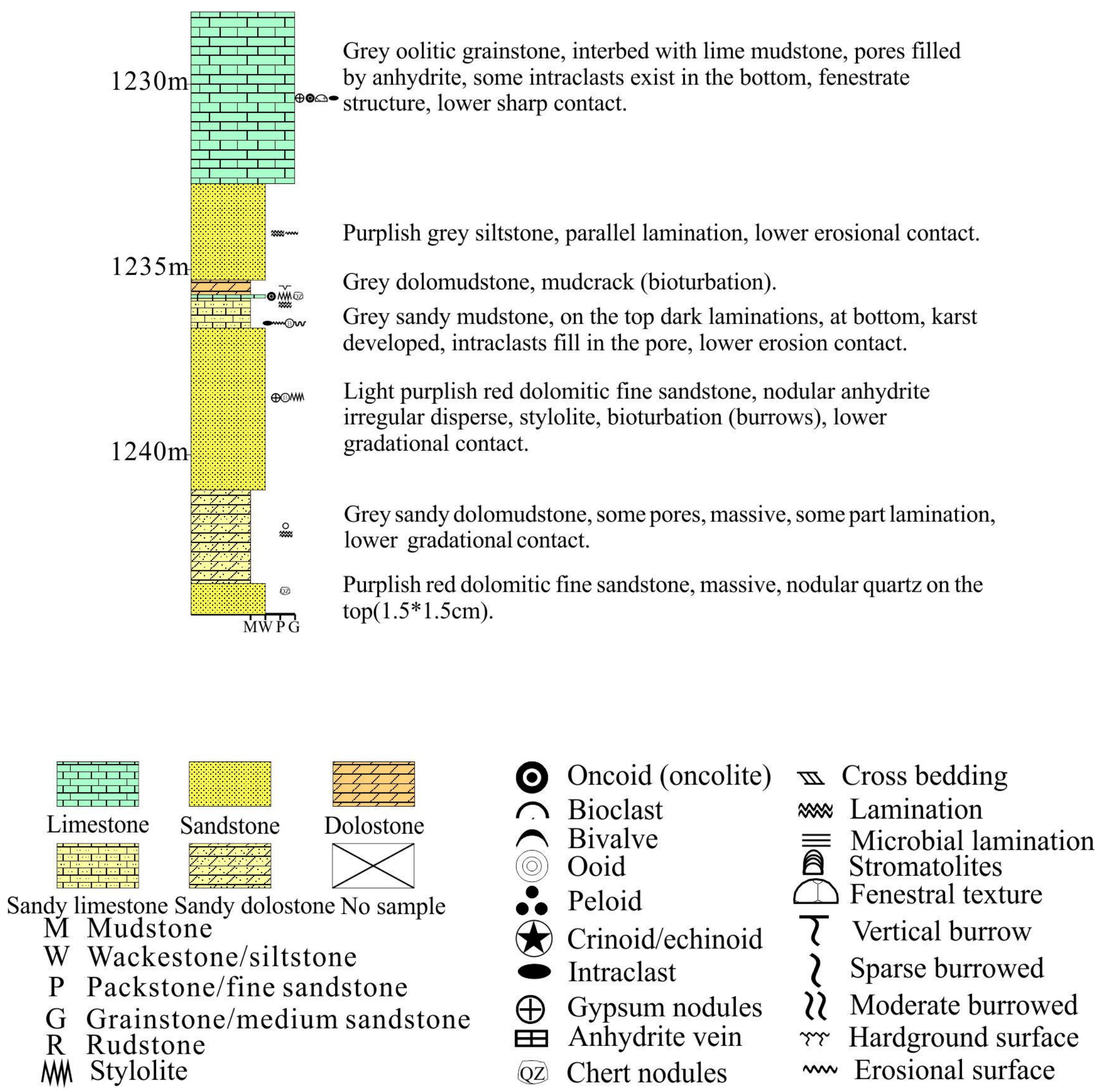

Well 2: 11/13-13-008-06W2; 87I040

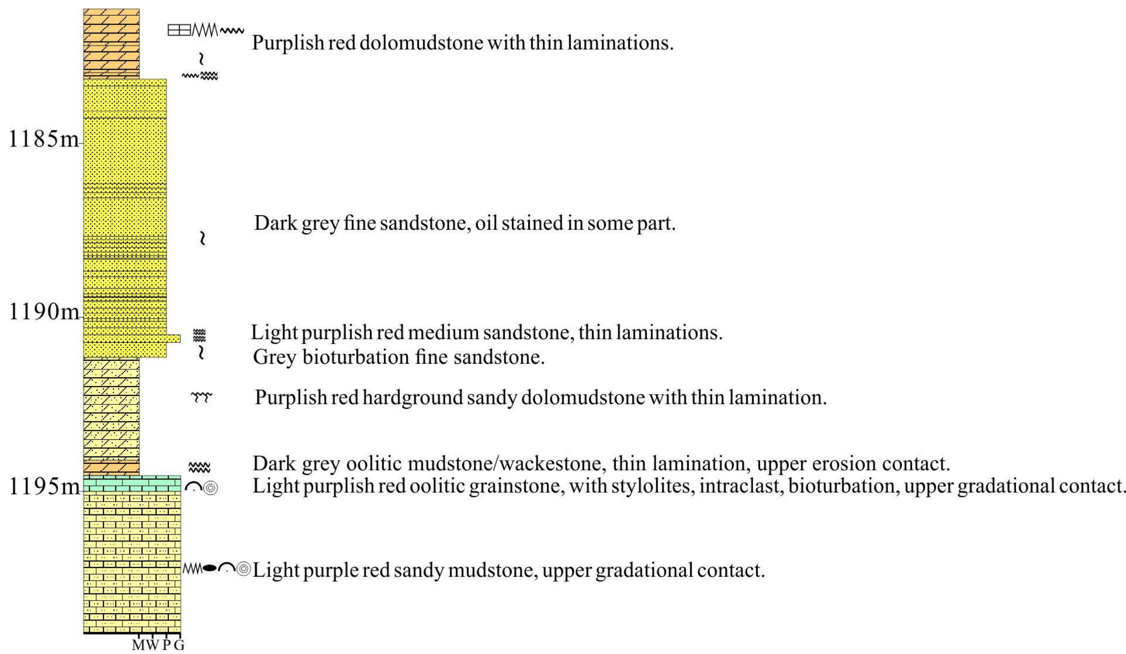

Well 3: 01/03-08-001-06W2;   57D025

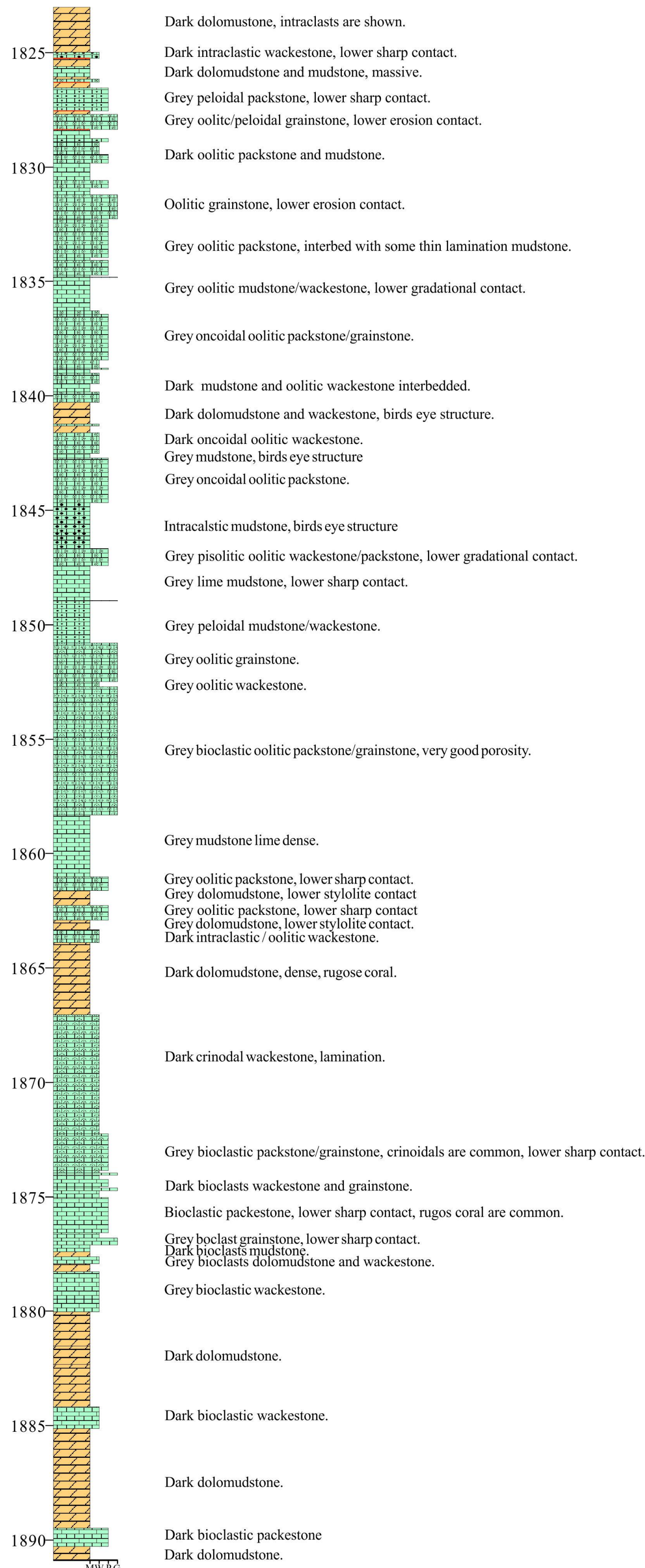

Well 4: 21/03-32-007-05W2; 84A107

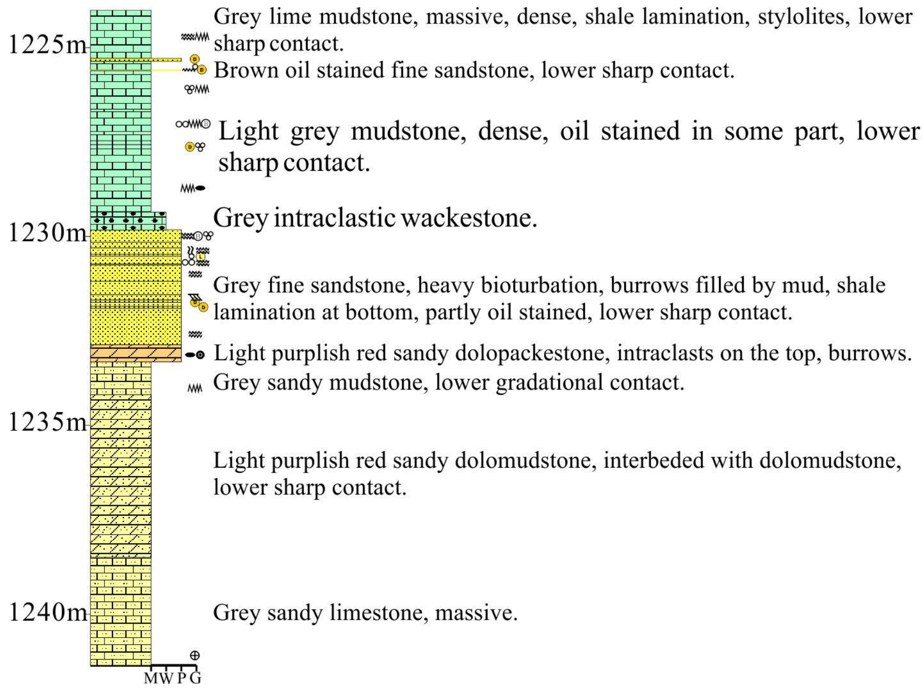

Well 5: 01/03-26-004-05W2; 55J092

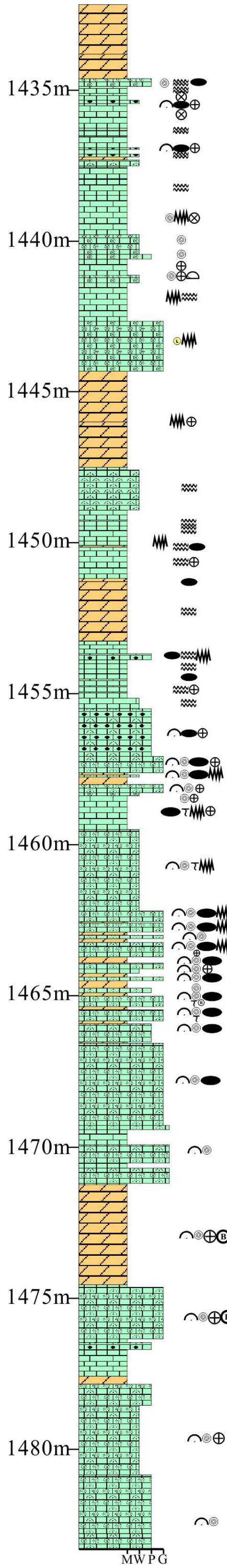

Pale grey dolomudstone, massive, lower gradational contact.

Dark grey oolitic packstone with black thin laminations, lower sharp contact.

Grey mudstone interbedded with wackstone, dense, lower sharp contact.

Grey oolitic wackestone, massive and dense, lower gradational contact.

Dark grey oolitic packstone, lower erosional contact.

Grey mudstone, lower sharp contact, anhydrite filling in the pore.

Grey oolitic lime wackestone, birds eye structure, anhydrite filling in the pore, lower sharp contact.

Pale grey mudstone, parallel laminations, dense, several stylolites are shown, lower gradational contact.

Light brown grainstone, dense, massive, oil stained, stylolites are shown, lower stylolite contact.

Grey dolomudstone.

Grey bioclastic wackestone, thin laminations, dense, no obvious pore, lower gradational contact.

Dark grey dolomudstone, thin laminations, nodular anhydrite, lower sharp contact.

Dark grey intraclastic packstone, laminations, lower stylolites contact.

Pale grey mudstone, massive and dense, lower gradational contact.

Yellowish grey bioclastic intraclastic packstone, nodular anhydrite, massive and dense. Lower erosion contact.

Blue grey mudstone, vertical burrow, intraclasts on the top, dense and massive, stylolites are common, nodular anhydrite, lower gradational contact.

Grey bioclastic oolitic wackestone, stylolites are very common, vertical burrows, lower gradational contact.

Grey grainstone interbedded with dolomudstone.

Grey bioclastic oolitic grainstone, dolomudstone intraclasts are common, lower gradational contact.

Grey oolitic bioclastic rudstone.

Grey mudstone.

Grey oolitic bioclastic rudstone.

Grey dolomudstone, lots of anhydrite nodular, anhydrite fill in the fracture, heavy bioturbation. Lower erosion contact.

Grey oolitic bioclastic grainstone, nodular anhydrite, bioturbation.

Oolitic intraclastic packstone.

Grey mudstone.

Yellowish grey bioclastic oolitic packstone, nodular anhydrite, some very big bivalve.

Yellowish grey bioclastic oolitic wackestone.

Pale grey bioclastic oolitic packestone.

Well 6:41/03-24-007-04W2; 93H085

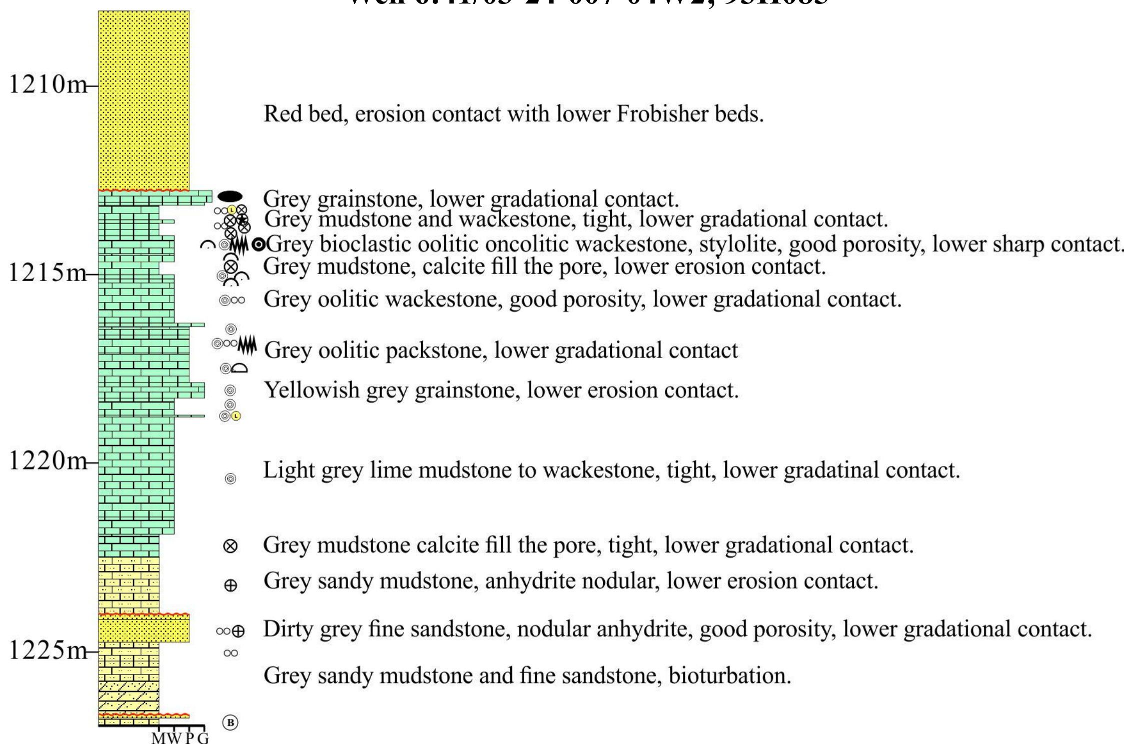

Well 7: 41/04-22-007-03W2; 08J43

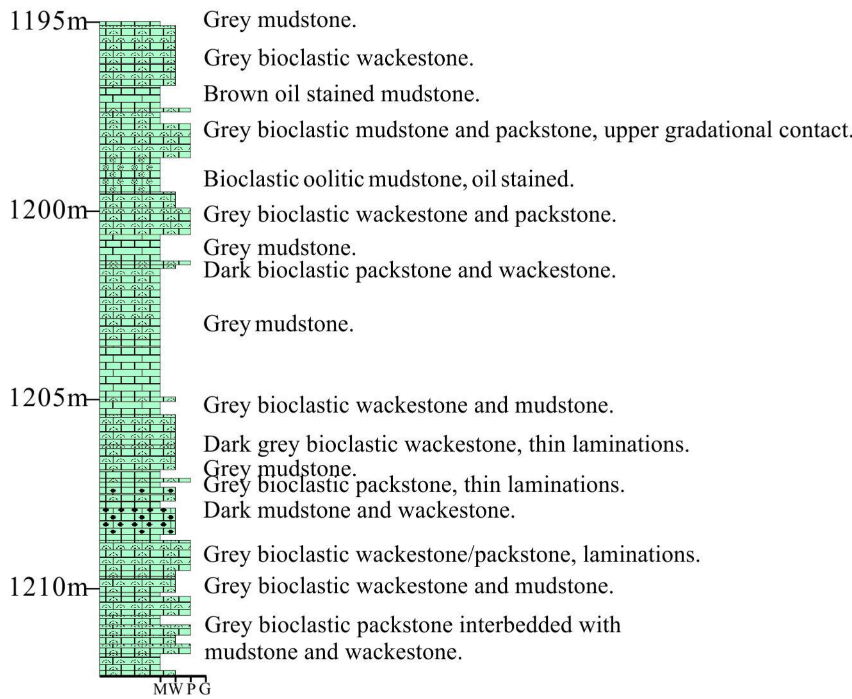

Well 8: 01/06-01-006-03W2; 62L012

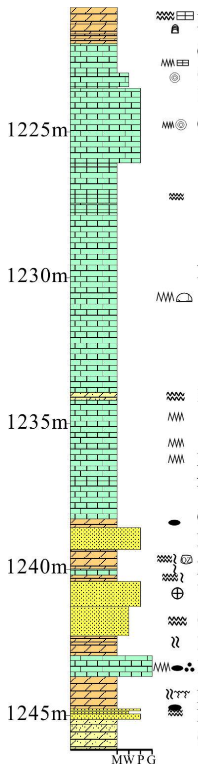

Purplish red dolomudstone, massive, dense, colorful stromatolite on the bottom, lower gradational contact.
Grey mudstone.
Grey oolitic wackestone/packstone, good porosity, pore filled by calcite, stylolites, fracture, anhydrite vein, lower sharp contact.
Grey oolitic packstone, well porosity, lower gradational contact, stylolite, oil stained.

Light grey mudstone, fracture, pores filled by calcite, stylolites, oil stained, birds eye structure.

Blue grey sandy dolomudstone, lamination, dense, lower gradational contact.

Light brown oil stained mudstone iterbedded with some thin peloidal wackestone, good porosity, half pores filled by calcite, stylolite.

Grey dolomudstone and anhydrite, gravel from underlying strata(3*5cm), angular, gradational contact, fracture zone.
Purplish red fine sandstone, fractures, irregular, filled by fine-medium sandstone.
Purplish red dolomudstone and anhydrite, parallel lamination, fracture, on the top nodular quartz and burrows.
Yellow grey fine sandstone with nodular anhydrite or quartz.
Grey siltstone, thin lamination.
Light purplish grey dolomudstone, burrows, bioturbation, lower gradational contact
Light purplish grey intraclastic grainstone, peloid, stylolite, lower sharp contact.
Purplish grey hardground, dolomudstone, burrows, lower sharp contact.
Purplish red fine sandstone, massive, lower sharp contact.
Grey sandy dolomudstone, massive.

Well 9: 01/07-34-005-02W2; 85G245

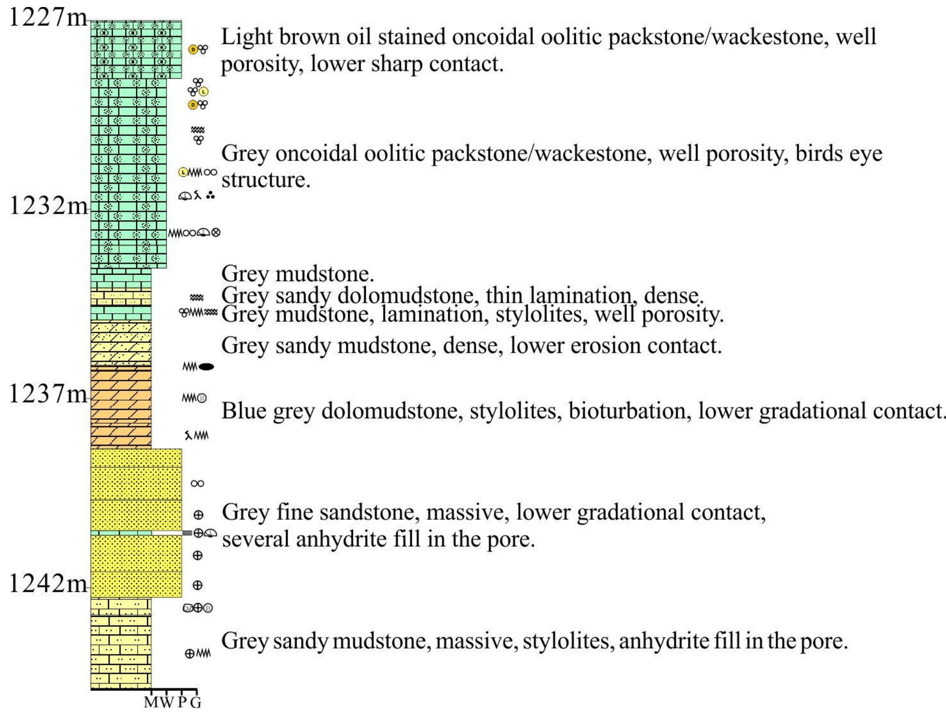

Well 10: 01/09-23-002-02W2; 56J006

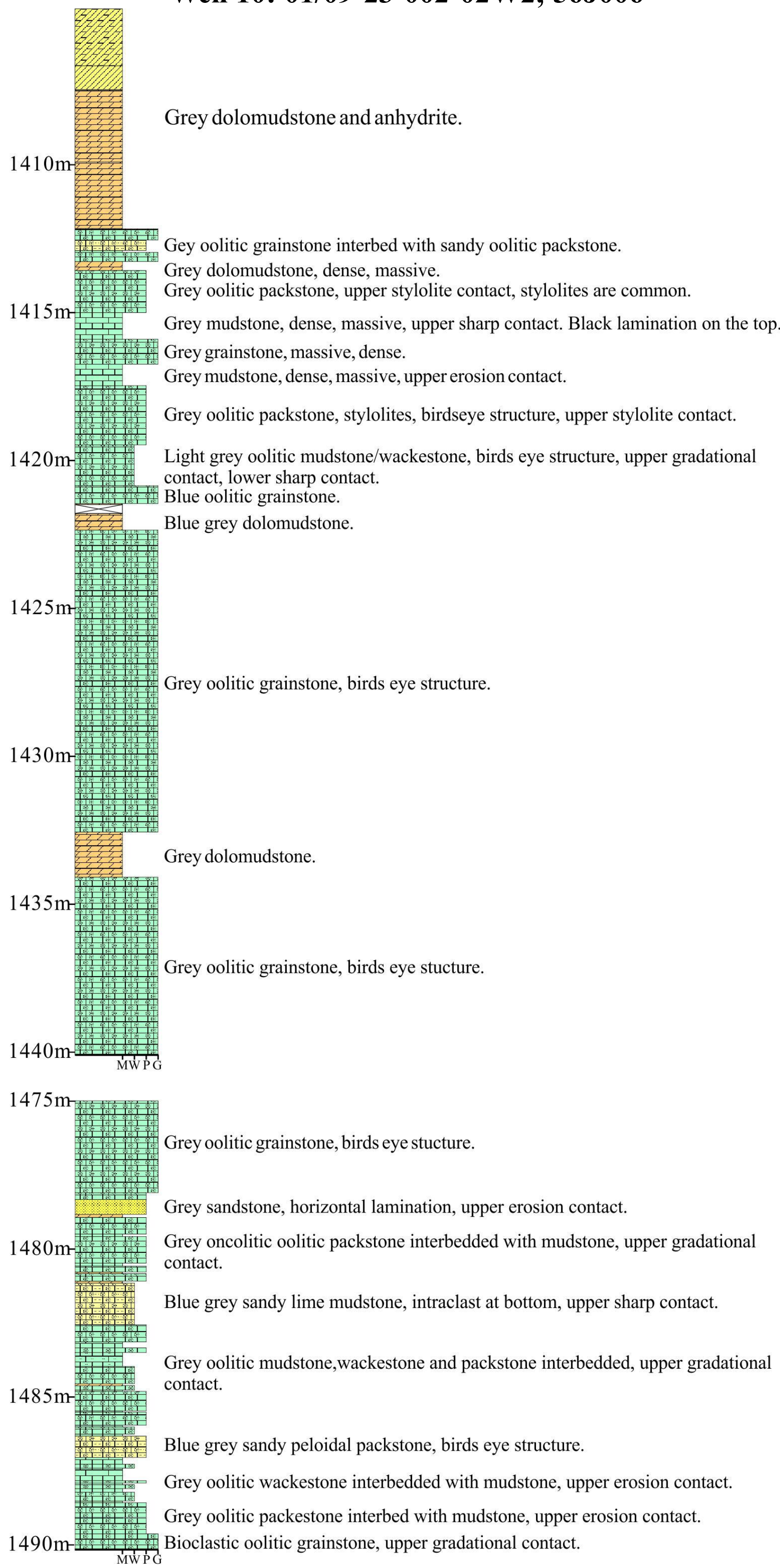

Well 11:01/05-20-006-01W2;00F231

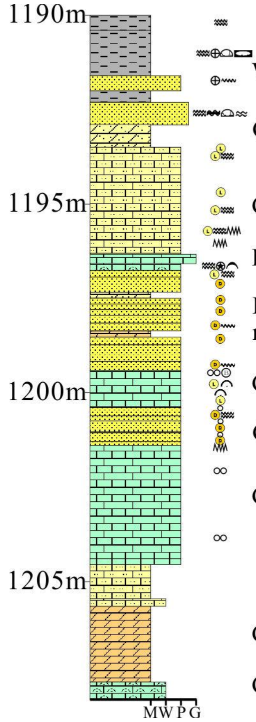

Watrous formation, red bed.

Grey sandy dolomudstone, massive, sharp contact.

Grey sandy bioclastic packstone.

Light brown oil stained grainstone and packstone, lower sharp contact.

Brown oil stained fine sandstone interbedded with dolomudstone,
massive, lower sharp contact.

Grey bioclastic packstone, crinoid, foraminifera. upper contact is not available.

Grey fine sandstone, partly oil stained.

Grey bioclastic packstone, crinoid, foraminifera. upper contact is not available.

Grey dolomudstone, upper sharp contact.

Grey bioclastic wackestone.

Well 12: 01/02-27-005-01W2; 85K115

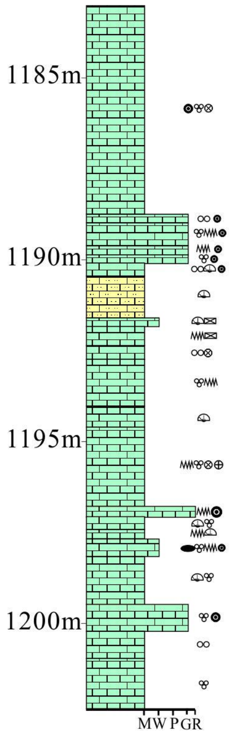

Grey mudstone, well porosity, oncoids partially develop, some pores filled by calcite, bird eye structure.

Grey oncolitic grainstone, with some tiny pores.

Grey sandy mudstone, quartz filling in the pore, good porosity, birds eye structure.
Grey wackestone, pores filling by calcite.

Light grey mudstone, anhydrite nodular (10cm), good porosity, pores filling by calcite or anhydrite.

Grey rudstone, 2 mm red oncoids, stylolite.
Grey mudstone, dense, stylolite, tiny pore filled by calcite, fenestrate stucture.
Light grey wackestone, well porosity, stylolite.
Grey mudstone.
Grey oncolitic grainstone, very well porosity.

Grey mudstone, good porosity.

Well 13: 41/10-09-004-01W2; 08C362

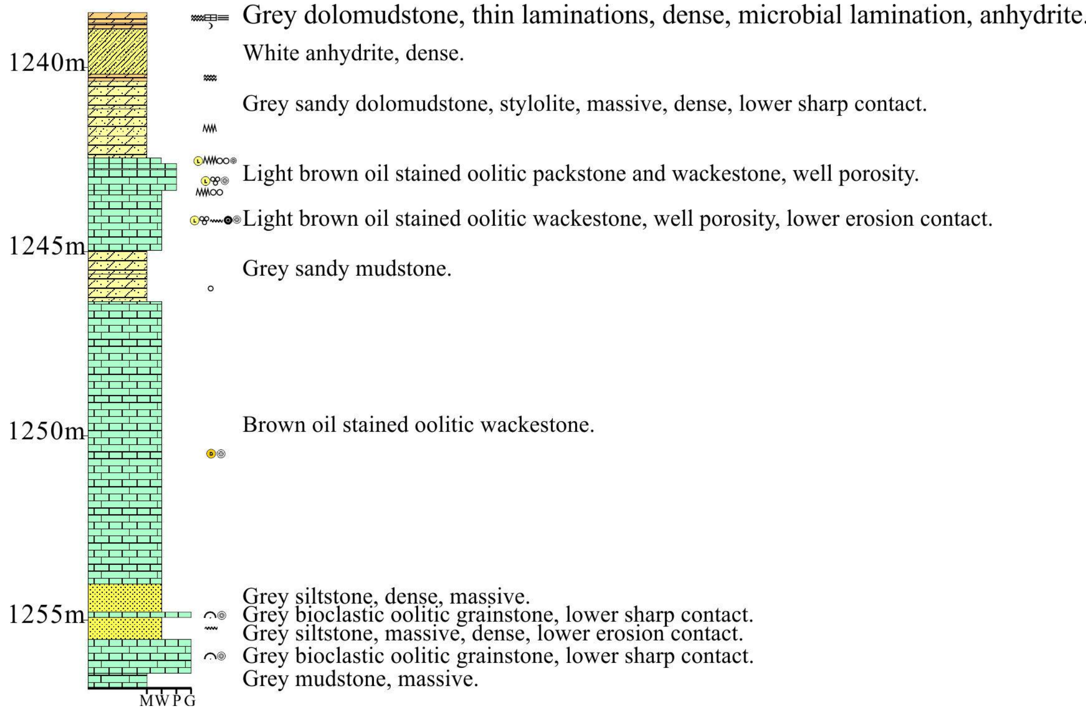

Well 14: 41/09-33-005-34W1; 87K208

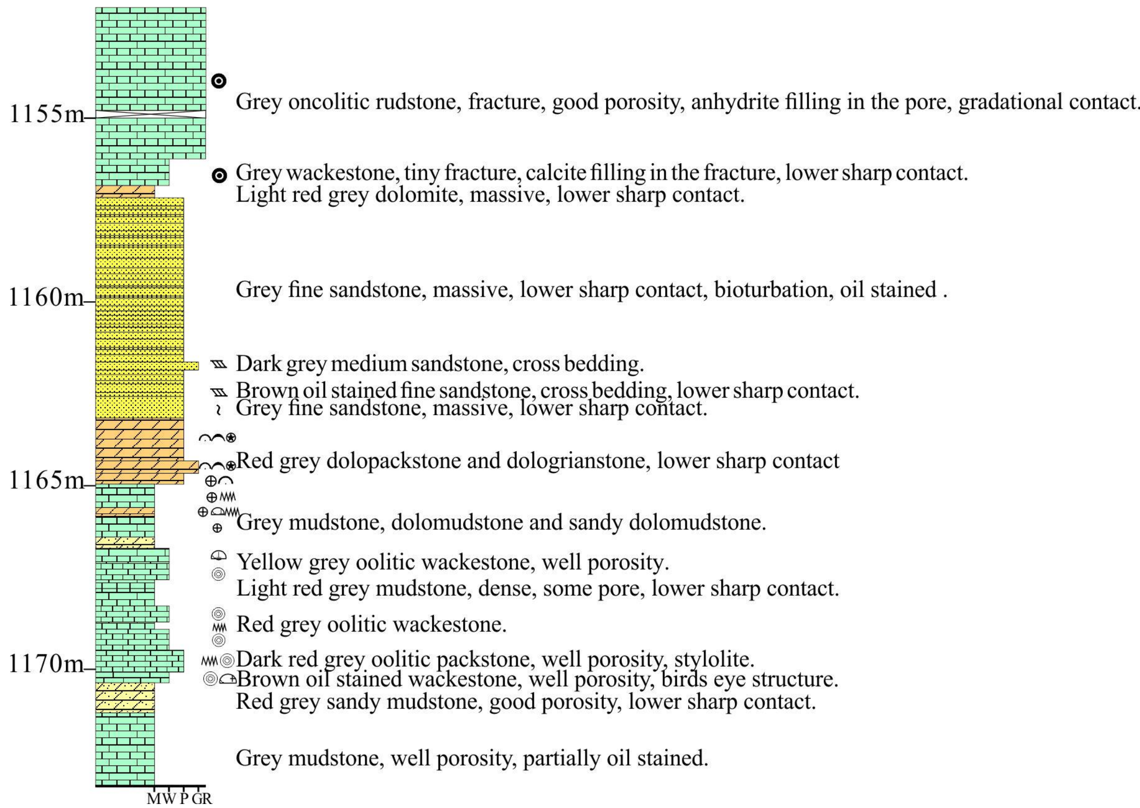

Well 15: 31/06-02-004-33W1; 97G141

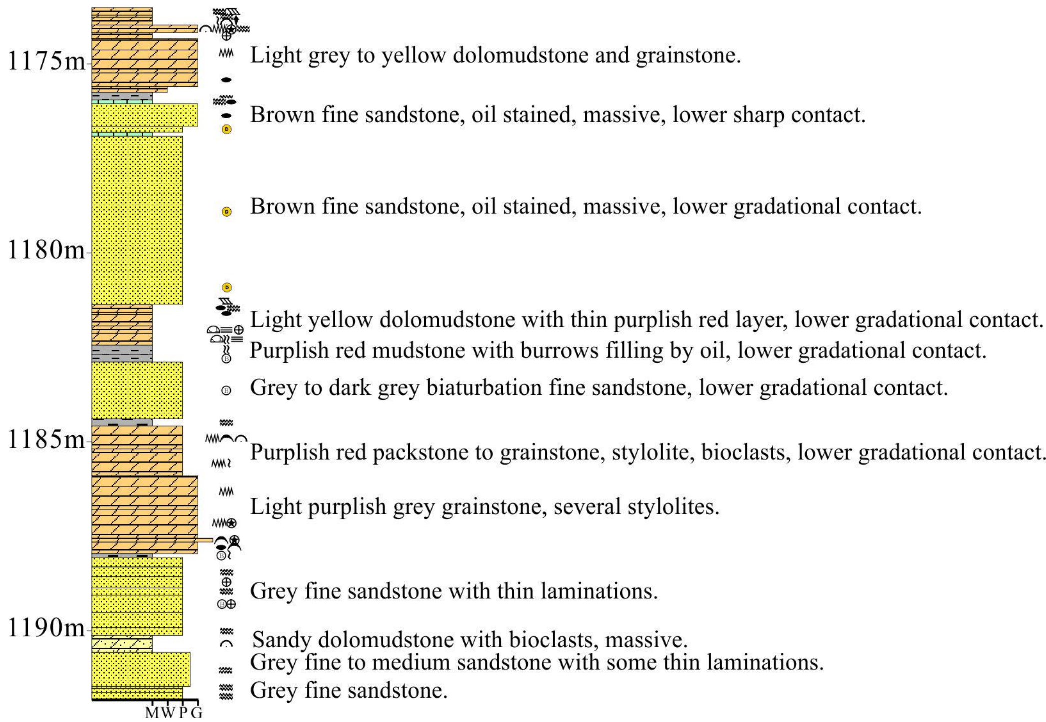

Well 16: 01/04-12-004-33W1; 96I248

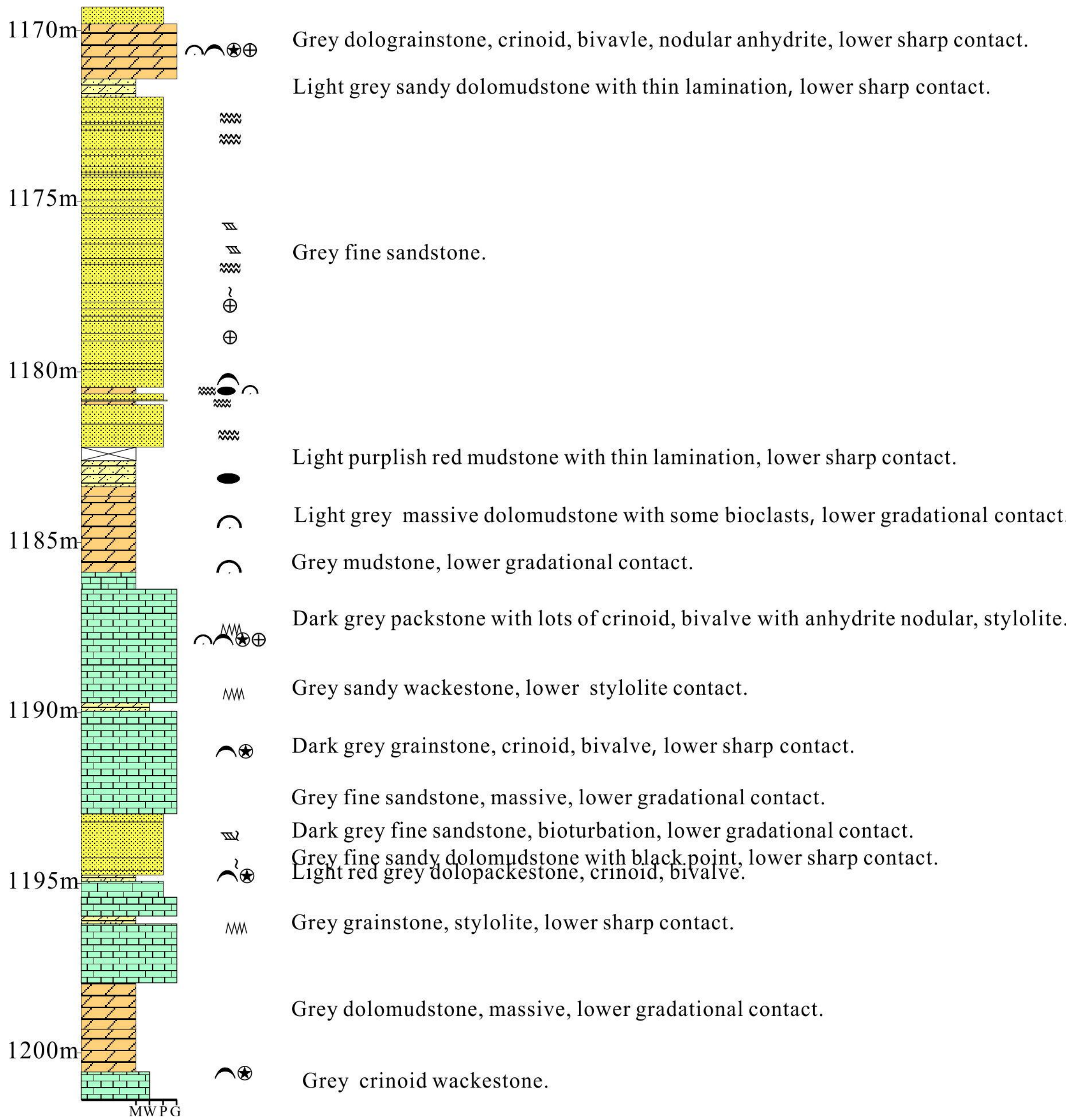

Well 17: 11/06-12-004-33W1; 96K245

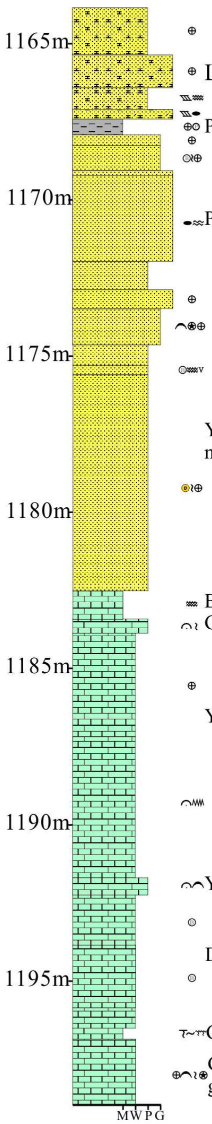

Light red fine to coarse sandstone with anhydrite.

Purplish mudstone, some grey nodular anhydrites exist on the top, lower gradational contact.

Purplish red fine to coarse sandstone with irregular anhydrite.

Yellow fine sandstone, oil stained, oil filled in burrows, there are some nodular anhydrite at bottom. Lower sharp contact.

Blue grey mudstone. thin lamination, upper gradational contact.

Grey packstone, bioclasts, burrows, upper gradational contact.

Yellow grey wackestone with nodular anhydrite. Upper sharp contact.

Yellow grey packestone, bioclast: bivalve, foraminferas, crinodal, upper gradational contact.

Dark grey wackestone, heavy bioturbation. Upper sharp contact.

Grey red hardground, vertical and horizontal burrows wackestone or mudstone, upper gradational contact.

Grey bioclastic wackstone, noudular anhydrite fill in burrows, bioclasts are crinodal, bivalve, gradational contact with overlying strata.

Well 18: 01/16-10-005-32W1; 55C028

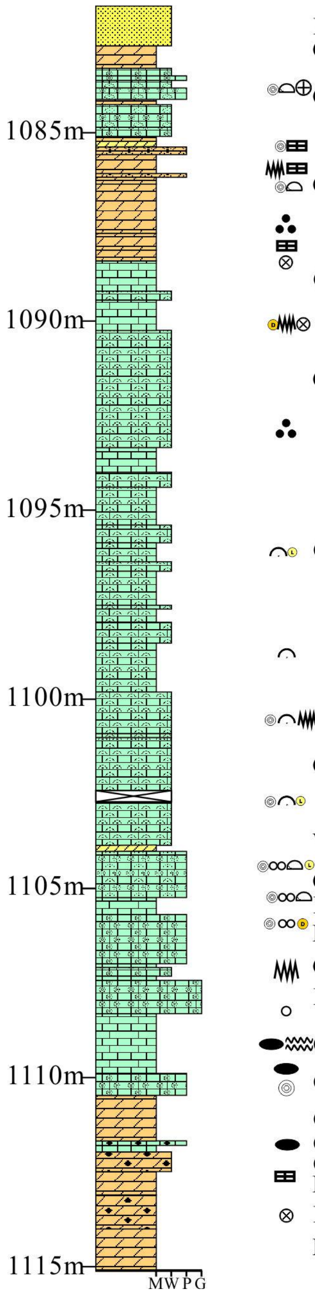

Red Watrous siltstone, lower erosion contact.
Grey oolitic dolomudstone.
Grey oncoidal oolitic wackestone and packstone, lower sharp contact.
Grey dolomudstone and dolopackstone.
Grey bioclastic mudstone and wackestone.
Grey bioclastic wackestone.
Grey bioclastic mudstone and wackestone.
Grey bioclastic wackstone.
White anhydrite.
Grey oolitic bioclastic packestone, oil stained.
Light grey mudstone, dense, no pore.
Light brown oil stained oolitic packstone, good porosity, birds eye structure.
Grey oolitic wackestone and mudstone, fenestral structure, good porosity.
Light grey ooilitic grainstone, good porosity, oil staining on the upper part.
Grey mudstone, dense, lower stylolites contact.
Grey oolitic packstone.
Grey mudstone, lamination, mudstone intraclasts.
Grey intraclastic packstone, lower erosion contact.
Grey oolitic intraclastic dolowackestone.
Blue grey dolomudstone, upper erosion contact.
Blue grey intraclastic dolomudstone.
Blue grey dolomudstone and anhydrite, lower sharp contact.

Well 19: 01/08-01-004-32W1; 67F004

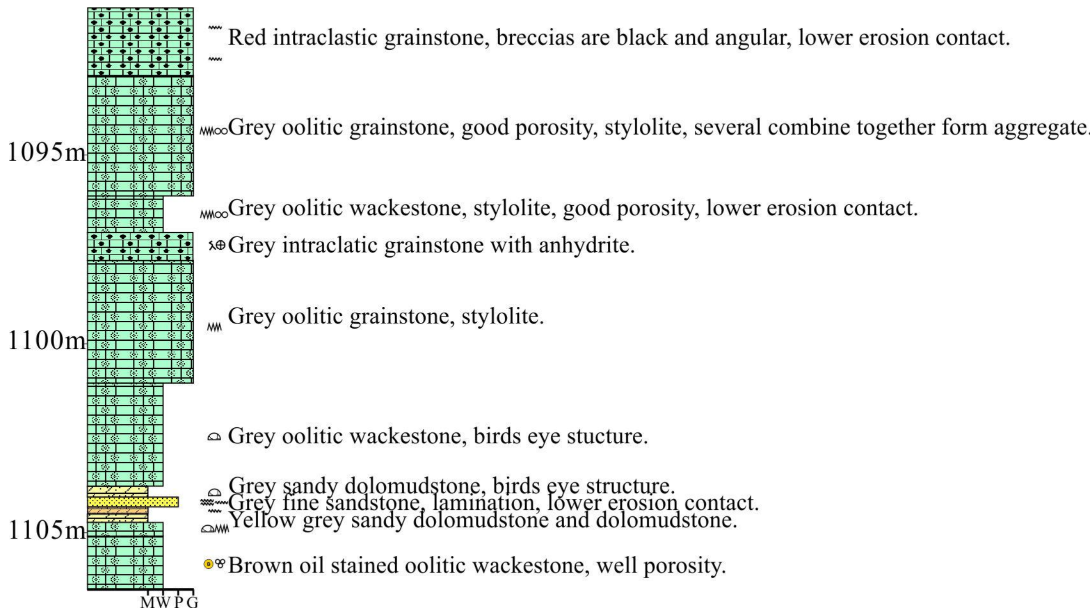

Well 21: 11/15-18-001-32W1; 90G125

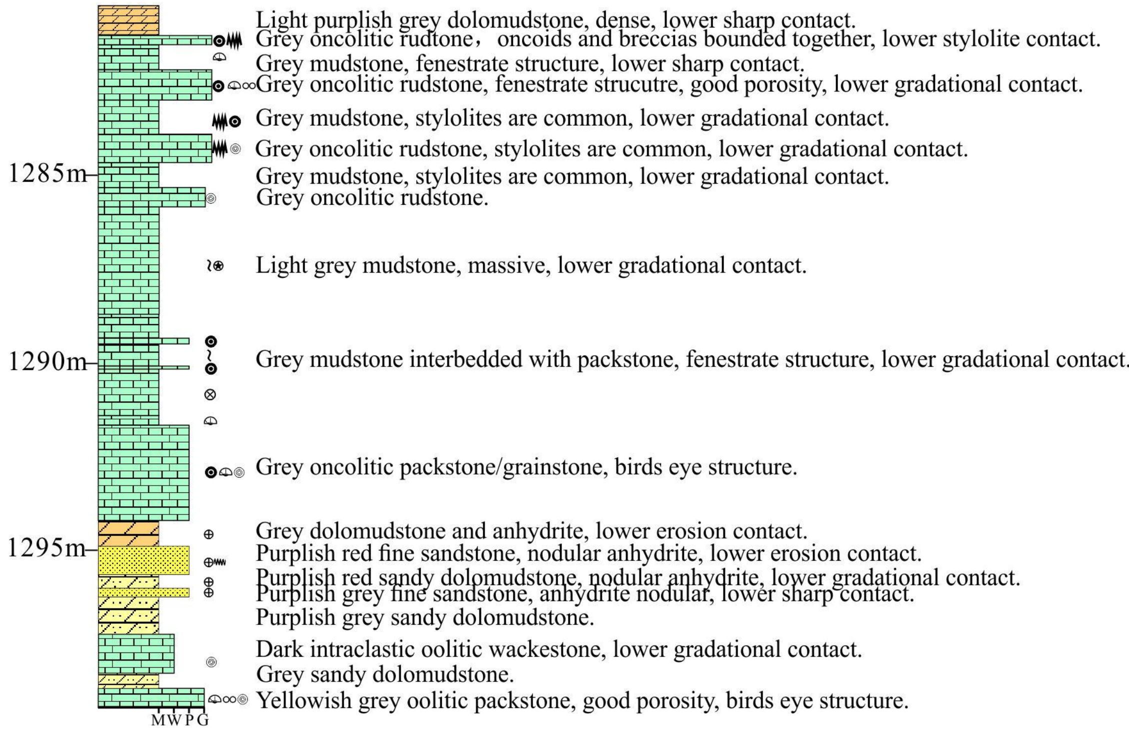

Well 22: 02/16-27-002-31W1; 56K120

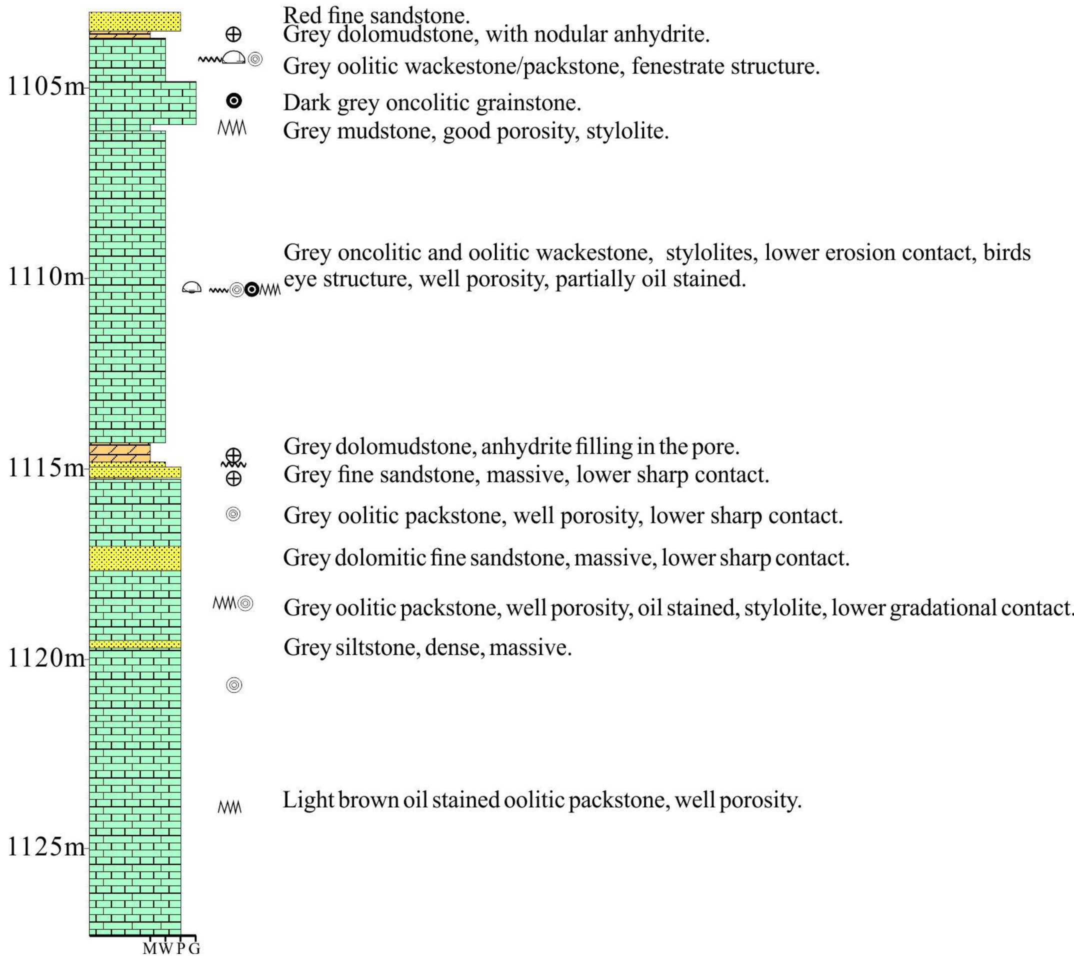

Well 23: 50/11-19-002-30W1; 72L015

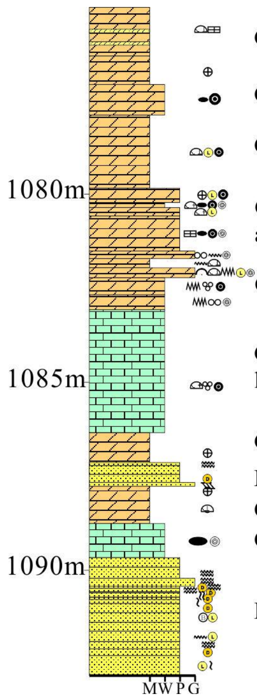

Grey dolowackestone, with several anhydrite layers, birds eye structure, dense.

Grey dolowackestone, intraclasts are from underlying strata, lower gradatinal contact.

Grey dolomudstone, birds eye structure, light oil stained.

Grey dolopackstone interbedded with dolowackestone. Ooids, oncoids, and intraclast float on it, anhydrite layer, light oil stained.

Grey dolomudstone, wackestone and grainstone, birds eye structure, lower erosion contact.

Grey oncolitic oolitic wackestone, dense, stylolite, some tiny pore, oncoids float in it, lower sharp contact.

Grey dolomudstone, anhydrite fill in the pore.

Blue grey fine sandstone and medium sandstone, massive.

Grey dolomudstone, birds eye structure, lower gradational contact.

Grey intraclastic oolitic packstone, oncoid float on it, lower sharp contact.

Dark grey fine and medium sandstone, partly oil stained.

Well 24: 01/01-11-006-33W1; 86J054

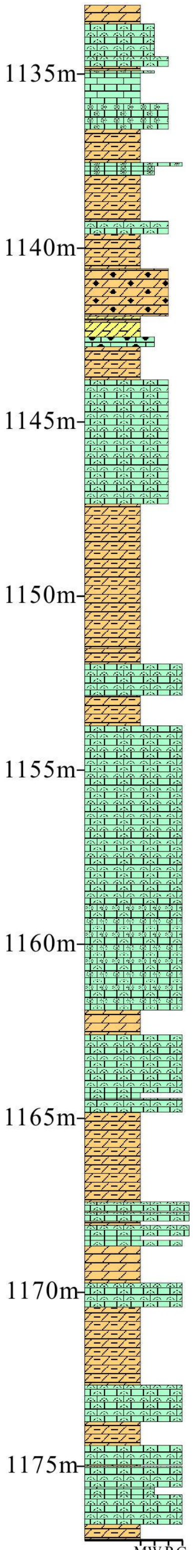

Grey dolomudstone, oil stained, lower gradational contact.
Grey wackestone, stylolites are common, lower contact is not available.
Grey bioclastic packstone, microbial lamination, lower gradational contact.
Grey lime mudstone to wackestone, microbial lamination, lower gradational contact.
Grey bioclastic oolitic packstone, lower sharp contact, stylolites.
Light grey dolomudstone, lower sharp contact, burrows, stylolites, horizontal lamination on the top.
Grey oolitic wackestone and grainstone, lower sharp contact.
Grey dolomudstone, cross bedding at bottom, burrows and microbial lamination, lower stylolite contact.
Dark grey bioclastic packstone.
Light grey dolomudstone, horizontal lamination, stylolites are common.
Light green intraclastic packstone, lower erosion contact.
Dark anhydrite, lower erosion contact.
Grey intraclastic wackestone, lower sharp contact.
Grey dolomudstone, lower sharp contact.
Grey bioclastic packstone, massive, cross bedding and burrows. Lower sharp contact.
Light grey dolomudstone, with nodular anhydrite, massive.
Grey bioclastic grainstone, lower sharp contact.
Light grey dolomudstone, massive, lower gradational contact.
Grey bioclastic packstone/grainstone, lower sharp contact. horizontal lamination, lower erosion contact.
Grey dolomudstone with anhydrite nodular, lower gradational contact.
Grey bioclastic grainstone interbedd with dolomudstone, lower erosion contact.
Grey bioclastic mudstone, lower gradational contact.
Grey bioclastic grainstone, lower erosion contact. several small cycle.
Grey calcarous dolomudstone, with anhydrite nodular
Grey bioclastic rudstone interbedded with dolomudstone
Grey dolomudstone, with anhydrite nodular, lower gradational contact.
Grey bioclastic grainstone, lower erosion contact. stylolites.
Grey calcarous dolomudstone, anhydrite, lower sharp contact.
Grey bioclastic grainstone, with some mudstone.
Grey dolomudstone, lower gradational contact.
Grey bioclastic grainstone interbedded with mudstone.
Grey bioclastic packstone/grainstone, lower sharp contact.
Grey dolomudstone.

Well 25: 01/12-29-001-05W2; 54D007